EEG Cortical Neuroimaging during Human Full-Body Movement

by
Julia E. Kline

A dissertation submitted in partial fulfillment
of the requirements for the degree of
Doctor of Philosophy
(Biomedical Engineering)
in the University of Michigan
2015

Doctoral Committee:

Professor Daniel P. Ferris, Chair
Associate Professor Victoria Booth
Assistant Professor Cynthia Chestek
Assistant Professor Sean Meehan

Acknowledgements

First and foremost, I would like to thank my committee. I am especially grateful to my advisor, Dan Ferris, for guiding me through six years of uncertainty and many failed experiments and never giving up on me. I would like to thank my wonderful lab mates for their help and patience throughout this process. Finally, I must acknowledge my closest and most supportive friends, Vanessa Prokuski, Barry Belmont, Beth Dalsing, and Layla Houshmand. Thanks for all your encouragement.

Table of Contents

List of Figures

List of Tables

Abstract

Studying how the human brain functions during full-body movement can increase our understanding of how to diagnose and treat neurological disorders. High-density electroencephalography (EEG) can record brain activity during body movement due to its portability and excellent time resolution. However, EEG is prone to movement artifact, and traditional EEG methods have poor spatial resolution. Combining EEG with independent component analysis (ICA) and inverse source modeling can improve spatial resolution. In my first study, I used EEG and ICA to investigate the biomechanical and neural interplay of performing a complicated cognitive task at different walking speeds. Young, healthy subjects stepped significantly wider when walking with the cognitive task compared to walking alone, but walking speed did not affect cognitive performance (i.e. reaction time and correct responses). EEG results mirrored cognitive performance, in that there were similar event-related desynchronizations in the somatosensory association cortex around encoding at all speeds. For my second study, I addressed the problem of movement artifact in EEG. I created an interface that blocked true electrocortical signals while recording only movement artifact. I quantified the spectral changes in the movement artifact EEG, tested various methods of removing the artifact, and compared their efficacies. Artifact spectral power varied across individuals, electrode locations, and walking speed. None of the cleaning methods removed all artifact. For my third study, I examined cortical spectral power fluctuations and effective connectivity during active and viewed full-body exercise with different combinations of arm and leg effort. Larger spectral fluctuations occurred in the cortex during rhythmic arm exercise compared to rhythmic leg exercise, which suggests that rhythmic arm movement is more cortically driven. The strength and direction of information flow was very similar between the active and viewed exercise conditions, with the right motor cortex being the hub of information flow. These studies provide insight into how the human brain functions during full-body movement and may have applications for rehabilitation after a brain injury or in brain monitoring for improving cognitive performance.

Chapter 1: Introduction

Human neuroimaging during activities such as walking can increase our understanding of how the brain coordinates full-body movement. Human full-body movement, and walking in particular, is controlled by a mixture of cortical (Suzuki et al., 2004;Harada et al., 2009;Gwin et al., 2011) and subcortical (Jahn et al., 2008) structures as well as spinal locomotor networks (Bussel et al. 1996; Lamb et al. 2000; Dietz et al. 2003). Understanding the cortical contribution to the control of human full-body movement is an important first step toward diagnosing and rehabilitating the brain after an injury or illness. In addition, the ability to monitor brain activity during real-world activities with walking could lead to the creation of brain-computer interfaces for gait assistance. Neuroimaging during full-body movement could also be used in healthy individuals for performance monitoring and enhancement. For instance, it could be employed to monitor cognitive fatigue in high-stress environments or to give real-time feedback on the performance of a cognitive task during walking.

Traditional neuroimaging with tools such as functional magnetic resonance imaging and positron emission tomography requires subjects to remain still during scanning. In the past, this significantly limited the tasks during which brain activity could be studied. Advances in neuroimaging technology, including the advent of functional near-infrared spectroscopy (fNIRS), have allowed human cortical activity to be measured during unconstrained movements,

such as walking. This has led to an increased estimation of the cortex's role in the control of walking. The primary motor cortex, premotor cortex and supplementary motor area are highly metabolically active during walking and running in young, healthy adults (Miyai et al. 2001; Suzuki et al. 2004). Studies with fNIRS have also indicated that cortical activity is positively correlated with walking speed. Harada and collegues showed increased oxygenated hemoglobin in the left prefrontal cortex and supplementary motor area during periods of higher walking intensity compared to periods of lower walking intensity in older adults (Harada et al. 2009). A drawback to fNIRS, however, is that is measures a slow metabolic signal rather than fast cortical potential changes. Therefore, it is not suitable for measuring cortical activity on the time scale of a stride during human walking.

Electroencephalography (EEG) is a possible alternative neuroimaging technique that does not suffer from the same limitations. Unlike functional magnetic resonance imaging and positron emission tomography, modern EEG hardware is light-weight and portable enough to be used during unconstrained full-body motion. Unlike fNIRS, EEG has temporal resolution on the order of a few milliseconds, which makes it suitable for measuring intra-stride cortical changes during walking and walking-like activities.

However, EEG has traditionally been thought of as having poor spatial resolution. Fortunately, the addition of advanced statistical techniques, such as independent component analysis (ICA), and inverse source modeling can provide spatial localization with a precision of approximately 1 cm (Mullen et al., 2011). ICA is a blind source separation technique that can separate mixed signals into their underlying independent component (IC) signals. EEG signals recorded at the

scalp represent a combination of true brain signals from many cortical areas, electromyographic signals, artifacts such as those arising from human movement, and other signals. ICA applied to EEG data makes the assumption that signals from functionally distinct cortical areas are temporally independent (Makeig et al., 1996). Once ICA has separated EEG signals into temporally independent component signals, highly stereotyped artifacts such as horizontal and vertical eye blinks, muscle signals, and electrocardiography signals can be easily removed based on their spectral properties and scalp maps (Jung et al., 2000a;Jung et al., 2000b). Electrocortical source signals arising from individual cortical domains are dipolar (Delorme et al., 2012). Inverse source modeling can represent each electrocortical independent component signal with a best-fit equivalent current dipole within a boundary element head model (Oostenveld and Oostendorp, 2002). Clustering these electrocortical dipoles across subjects allows for group level analysis of mobile EEG data (Gwin et al., 2011).

Recently, many studies have taken advantage of this improved EEG hardware and software to study the brain during walking (Gramann et al., 2010;Gwin et al., 2010;Gramann et al., 2011;Gwin et al., 2011;Presacco et al., 2011;Lau et al., 2012;Severens et al., 2012;Sipp et al., 2013;Seeber et al., 2014;Wagner et al., 2014;Seeber et al., 2015). These studies have all shown intra-stride cortical spectral fluctuations during human walking. This provides further evidence that the cortex is active during the control of human walking. However, the precise role the cortex plays in the control of human gait is still unknown. The answer will advance our fundamental knowledge of human motor control and may have many applications for rehabilitation and brain-computer interfaces.

Despite the successes of mobile brain imaging with EEG, the technique suffers from a substantial and previously unaddressed issue. EEG is very prone to movement artifact. This movement artifact can be an order of magnitude larger than true neural signals. During gait, spectral fluctuations induced by the foot hitting the ground can occur in the same frequency bands as true neural signal. Because gait artifact is time-locked to the stride cycle, tools such as ICA that rely on the temporal independence of the underlying signals of interest may not be able to fully separate brain activity and movement artifact. No previous studies have attempted to separate the relative contributions of movement artifact and brain signal during walking, therefore the results of previous EEG walking studies, particularly those conducted at fast walking speeds, need to be interpreted with caution.

The primary goals of this dissertation were two-fold: 1) to apply the tools of EEG, ICA, and spectral analysis to gain a deeper understanding of how the cortex functions during unconstrained full-body movements in humans and 2) to advance the field of mobile brain imaging by identifying issues in current methodologies and testing potential solutions. In chapter 1, I examined young, healthy subjects performing a challenging cognitive task across a range of speeds to tease out the effects of walking speed on both the performance of a spatial working memory task and the gait parameters associated with dual-tasking, such as step length, step width, and step length and width variability. In chapter 2, I tackled the problem of movement artifact in EEG signals. I designed a novel interface that blocked true electrocortical signals while retaining movement artifact signals. I characterized the spectral changes recorded by EEG electrodes at different walking speeds, tested various methods of artifact reduction, and quantified the results. In chapter 3, I investigated the cortical activity and effective connectivity

induced by active and viewed full-body exercise with varying combinations of arm and leg effort. The goal of all three of my dissertation projects was to increase our overall understanding of the human brain in motion. The following chapters (2-4) contain three complete manuscripts that can be read as individual studies. The first two chapters have been peer-reviewed and published. The third chapter will be submitted for publication shortly.

Chapter 2: Your brain on speed: cognitive performance of a spatial working memory task is not affected by walking speed

This chapter has been previously published:

Kline JE, Poggensee K, Ferris DP. Your brain on speed: cognitive performance of a spatial working memory task is not affected by walking speed. *Front Hum Neurosci* 8:288, 2014.

Abstract

When humans walk in everyday life, they typically perform a range of cognitive tasks while they are on the move. Past studies examining performance changes in dual cognitive-motor tasks during walking have produced a variety of results. These discrepancies may be related to the type of cognitive task chosen, differences in the walking speeds studied, or lack of controlling for walking speed. The goal of this study was to determine how young, healthy subjects performed a spatial working memory task over a range of walking speeds. We used high-density electroencephalography to determine if electrocortical activity mirrored changes in cognitive performance across speeds. Subjects stood (0.0 m/s) and walked (0.4, 0.8, 1.2, and 1.6 m/s) with and without performing a Brooks spatial working memory task. We hypothesized that performance of the spatial working memory task and the associated electrocortical activity would decrease significantly with walking speed. Across speeds, the spatial working memory task caused subjects to step more widely compared with walking without the task. This is typically a

sign that humans are adapting their gait dynamics to increase gait stability. Several cortical areas exhibited power fluctuations time-locked to memory encoding during the cognitive task. In the somatosensory association cortex, alpha power increased prior to stimulus presentation and decreased during memory encoding. There were small significant reductions in theta power in the right superior parietal lobule and the posterior cingulate cortex around memory encoding. However, the subjects did not show a significant change in cognitive task performance or electrocortical activity with walking speed. These findings indicate that in young, healthy subjects walking speed does not affect performance of a spatial working memory task. These subjects can devote adequate cortical resources to spatial cognition when needed, regardless of walking speed.

Introduction

In everyday life, people perform complex cognitive tasks while walking through various environments. This has led to a variety of studies on how humans dual-task cognitive and locomotor movements. However, the results from these studies are mixed. Recent reviews highlight the conflicting results in regard to cognitive and motor performance during dual-tasking (Al-Yahya et al., 2011;Schaefer and Schumacher, 2011;Kelly et al., 2012b). Elderly individuals (Lindenberger et al., 2000;Simoni et al., 2013;Venema et al., 2013) and individuals with neurological deficits (Sheridan et al., 2003;Camicioli et al., 2006;Panyakaew and Bhidayasiri, 2013) tend to exhibit increased gait variability and decreased mental performance when dual-tasking walking and a cognitive task. Data from young, healthy subjects do not follow such a clear pattern. Some studies have shown cognitive-motor dual task cost in young, healthy adults (Grabiner and Troy, 2005;Al-Yahya et al., 2009;Verrel et al., 2009;Szturm et al., 2013)

but other studies have found that young, healthy subjects either have no dual-task effect (Grubaugh and Rhea, 2014) or a reduced magnitude effect (Melzer and Oddsson, 2004;Siu et al., 2008;Srygley et al., 2009;Yogev-Seligmann et al., 2010b). Furthermore, the observed dual-task effect on kinematic or kinetic variables often differs across studies.

Some of the discrepancies in dual-tasking results across studies may be related to the type of cognitive task chosen. The cognitive tasks that have been used for gait dual-tasking studies include an N-back task (Verrel et al., 2009), Stroop tasks (Melzer and Oddsson, 2004;Grabiner and Troy, 2005;Siu et al., 2008;Kelly et al., 2012a), a serial subtraction and a phoneme-monitoring task (Al-Yahya et al., 2009;Srygley et al., 2009), an N-back task and a spatial attention task (Nadkarni et al., 2010), a verbal fluency task (Yogev-Seligmann et al., 2010a), and an automated operation span task (Grubaugh and Rhea, 2014). All of these tasks except the automated operation span task (Grubaugh and Rhea, 2014) had some effect on gait parameters. The N-back, Stroop, serial subtraction, verbal fluency, and automatic operation span tasks are all non-spatial working memory tasks. If walking is similar to upper limb motor tasks, it will engage cortical areas that are also involved in spatial working memory.

Work by Seidler and colleagues supports the idea that spatial working memory tasks overlap with sensorimotor brain areas (Anguera et al., 2010). Their subjects performed a visuomotor adaptation task that involved manipulating a joystick to hit a visual target, and they also separately performed a spatial working memory task that involved mental rotation. Activation in the dorsolateral prefrontal cortex and the bilateral inferior parietal lobule overlapped between the motor and mental tasks. Moreover, spatial working memory performance predicted the rate of visuomotor adaptation. This suggests that upper limb visuomotor adaptation and spatial working memory likely share mental resources (Anguera et al., 2010).

Another factor that may result in discrepancies in dual-task findings across studies is walking speed. Walking speed fundamentally changes the dynamics of human gait. At faster speeds there is less time to make changes in limb movement for each step, and the body's inertia is greater compared with slower speeds. These biomechanical changes are related to an increase in mechanical energy and passive dynamics at faster walking speeds compared with slower walking speeds (McGeer, 1993;Collins et al., 2005;Kuo, 2007). In addition, evidence from individuals with spinal cord injuries suggests that faster walking speeds rely more on spinal reflex pathways and spinal neural networks compared with slower walking speeds (Maegele et al., 2002;Beres-Jones and Harkema, 2004;Ferris et al., 2004;Behrman et al., 2005) Results from functional near-infrared spectroscopy indicates that humans have increased frontal brain activity at faster walking speeds compared with slower walking speeds (Harada et al., 2009). All of these data suggest that walking speed is likely to have an effect on brain activity during walking. By studying our subjects across a range of speeds, we could examine speed dependent differences in how the spatial working memory task affected brain activation and behavioral performance measures.

The purpose of this study was twofold. First, we wanted to determine if concurrent performance of a spatial working memory task affects human walking dynamics in young, healthy subjects across a range of walking speeds. Second, we wanted to determine if walking speed affects cognitive task performance and electrocortical activity during a working memory task across those same walking speeds. Reported differences between young and older subjects and across studies might be due to differences in the specific walking speeds studied or the fact that there was no control of walking speed across the cognitive task and no cognitive task conditions. We

studied young, healthy subjects because they generally use a wide range of walking speeds in everyday life, and they are more cognitively capable compared with older subjects. We chose a Brooks spatial working memory task, because a balance task during standing disrupted performance on the spatial but not the non-spatial Brooks task (Kerr et al., 1985), and because there seems to be an overlap in spatial working memory brain regions and sensorimotor brain regions (Anguera et al., 2010).

Specifically, we had two hypotheses about cognitive and motor dynamics. We hypothesized that walking kinematics would show signs of stability challenges when subjects performed the spatial working memory task compared with when they had no cognitive task. Increases in gait variability or wider step widths are both signs that humans are adapting to stability challenges. We also hypothesized that walking at higher speeds would decrease the performance of the spatial working memory task and decrease the related electrocortical activity. If faster walking speeds require greater cortical attention for control, then cognitive performance and the related electrocortical activity should both decrease with walking speed. In this study, we measured event-related spectral power synchronized to the presentation of a stimulus as our metric of electrocortical activity across conditions. To address these questions, our subjects stood (0.0 m/s) and walked at a range of speeds (0.4-1.6 m/s) on a treadmill, with and without performing the Brooks spatial working memory task.

Materials and methods

Data collection

Twenty healthy volunteers completed this study (18 males and 2 females, age range 18 to 39). All study procedures were approved by the University of Michigan Human Subjects Internal Review Board. All subjects provided written informed consent before participating.

Subjects stood (0.0 m/s) and walked (0.4, 0.8, 1.2, and 1.6 m/s) on a treadmill with and without performing the Brooks spatial working memory task (Brooks, 1967). We recorded electroencephalography (EEG), motion capture data, ground reaction forces, and response data from the Brooks task (Figure 1). We fit each subject with an appropriately sized EEG cap. Before recording EEG data, we marked the position of each electrode on the subject's head using a Zebris digitizer (Zebris, Germany). We ensured that all electrode offsets were <20 mV. We collected the EEG data at 512 Hz with a 264-channel active electrode array (ActiveTwo amplifier Biosemi, Amsterdam, The Netherlands). The EEG signals were initially referenced to a common reference. We placed reflective markers on the subjects' calcanei and recorded motion capture marker data at 100 Hz using 10 Vicon motion capture cameras (Vicon, Los Angeles, California) placed around the perimeter of the room. We created an automated version of the Brooks task using the Simulink toolbox (The MathWorks, Inc.) and collected response data in real-time using LabView (National Instruments, Austin, TX).

Figure 2-1. Experimental Setup. 20 subjects stood (0.0 m/s) and walked (0.4, 0.8, 1.2, and 1.6 m/s) on a treadmill while continuously performing the Brooks spatial working memory task. We recorded EEG, kinematics, ground reaction forces, and response data from the Brooks task.

Brooks task

The Brooks spatial working memory task uses visuospatial working memory (Brooks, 1967). In our version of the task, we asked the subject to imagine an empty 3-by-3 grid. Then, a screen one meter in front of the subject instructed him or her to visualize the digits one through nine in randomized positions in the grid. Digits and their associated positions were presented, one at a time. Each stimulus (a digit and its position) appeared on the screen and remained there for two

seconds, after which it vanished, and there was a two second pause before the next stimulus appeared. The subject had to maintain all the digits and their positions in working memory to successfully fill in the entire grid. It took 32 seconds for the subject to get all the information they needed to complete one grid. After all nine stimuli were presented, there was a four second pause, after which the screen prompted the subject to type the imagined grid, row-wise, into their hand-held keypad. Once the subject had pressed nine keys on their keypad the Brooks task began again (Figure 2). Subjects were not permitted to change any digits of their response once they had been entered. Subjects typically completed five or six runs of the Brooks task during each five-minute trial.

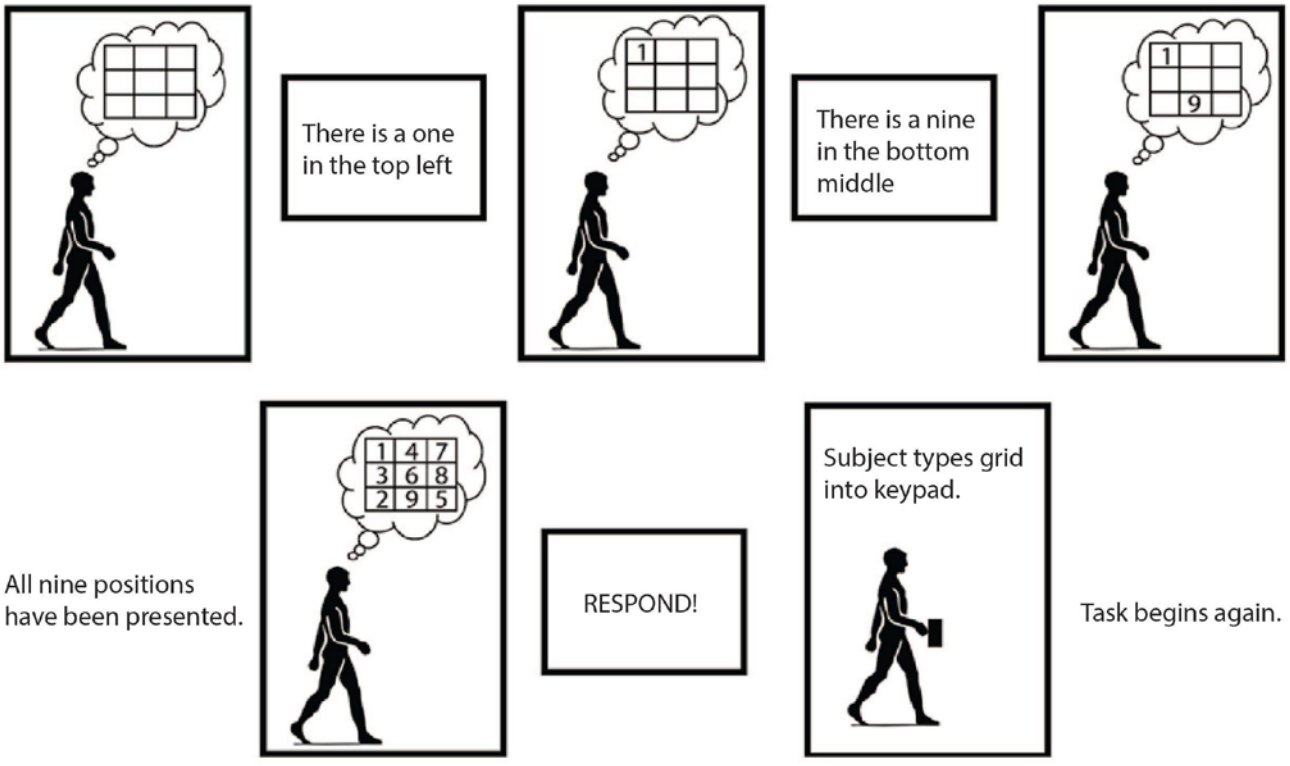

Figure 2-2. Brooks Task. Visual depiction of the Brooks spatial working memory task. Subjects performed the Brooks task continuously for five minute intervals.

Subjects performed the Brooks spatial working memory task continuously for five-minute intervals seven total times. Subjects began by performing the task while standing. Next, they alternated between walking with the cognitive task and walking without the cognitive task for four trials. Then, they performed a second cognitive task trial while standing. Next, they again alternated between walking with the cognitive task and walking without the cognitive task for four trials, and finally, they performed the cognitive task while standing for a third time. The order of the speeds for the walking trials was randomized across subjects to avoid order effects, but all subjects walked at all four speeds with and without the cognitive task. We instructed the subjects to respond to the cognitive task as quickly and accurately as possible, and we gave them no instructions about how to walk

Brooks task analysis

We gave the subjects two scores for each Brooks task trial, a percent correct score and a reaction time score. Percent correct was the number of digits placed correctly divided by the total number of presented digits. Reaction time was the average time that elapsed between the respond prompt and the ninth keystroke of the subject's response. We compared the results across walking speeds using a one-way repeated measures ANOVA and the Bonferroni correction post hoc test in SPSS version 21 (SPSS IBM, New York, U.S.A).

Gait kinematics analysis

To analyze the data with respect to the gait cycle, we used custom scripts in Visual3D (C-Motion, Germantown, MD) to identify gait events from the calcaneus marker motion capture

data. Specifically, we identified heel-strikes times by finding the minimum values for the position of the calcaneus marker in the z direction. The length for each step was the absolute value of the distance in the y direction between the right and left calcaneus markers at heel strike. The width for each step was the absolute value of the distance in the x direction between the right and left calcaneus markers at heel strike. We calculated the standard deviation of the step length and step width values to obtain step length variability and step width variability values. All values were divided by each subject's leg length to create unitless measures. We performed a two-way repeated measures ANOVA with speed and task (Brooks task versus no task) as factor levels for step length, step length variability, step width, and step width variability. We set the significance level at $p<0.05$ with a Bonferroni correction post hoc test.

We also performed a more finely-grained analysis of step variability between the encoding and retrieval periods of the Brooks task. We broke up the biomechanical data into periods of encoding, which is the time period between the start of a task trial (mental grid is empty) and the respond prompt (grid is filled), and retrieval, which is the time period between the respond prompt and the ninth keystroke of the subject's response. We calculated step length, step width, step length variability, and step width variability as above. We performed statistical analyses as above, with speed and task period (encoding period versus retrieval period) as factor levels.

EEG data analysis

We post-processed the EEG data using custom scripts in the open-source MATLAB toolbox, EEGLAB (Delorme and Makeig, 2004). We merged all EEG recordings from a single subject into one dataset and high-pass filtered the data above 1 Hz. We removed channels exhibiting

substantial artifact on the basis of: 1) magnitude, with channels exhibiting values <30 or >10000 μV removed, 2) kurtosis, with channels > 3 standard deviations from the mean removed, 3) correlation, with channels measuring voltages that are uncorrelated ($r \leq 0.4$) with the surrounding channel voltages for more than 0.01% of the time removed, and 4) standard deviation, with channels measuring voltages that are substantial more variability relative to other channel voltages as measured by standard deviation removed. These cutoffs were based on the work of Gwin and colleagues (Gwin et al., 2010). We identified and rejected noisy frames, or time periods of EEG data exhibiting high power across all channels (greater than 1.6 times the interquartile range of the channels). For some subjects, we made minor adjustments to these values to ensure that all the noisy channels and frames were removed. On average, we rejected 130.5 channels (range, 108–153; std. dev., 14.0). We re-referenced the remaining channels to an average reference.

To the cleaned data sets, we applied adaptive mixture independent component analysis (AMICA) (Palmer et al., 2006;Palmer et al., 2008) to transform the EEG channel data into temporally independent component signals (ICs) (Makeig and Jung, 1996). We used the DIPFIT function in EEGLAB (Oostenveld and Oostendorp, 2002) to model each IC as an equivalent current dipole within a boundary element head model based on the MNI brain (Montreal Neurological Institute, MNI, Quebec). We removed ICs from further analysis if the best-fit dipole accounted for less than 85% of the scalp map variance (Gwin et al., 2011), or if the scalp map or spectra were indicative of an eye or muscle artifact (Jung et al., 2000a;Jung et al., 2000b). We clustered ICs across all 20 subjects based on similarities in dipole location, scalp topography, and spectra using a k-means clustering algorithm that is available in EEGLAB. We made 20

clusters and retained clusters containing ICs from more than half of the subjects (>10) for further analysis.

For each cluster, we created an event-locked plot of spectral power change around each stimulus during the Brooks spatial working memory task, defined as the presentation of a digit and its position. We computed the power spectrum for each IC for every stimulus. We averaged the power spectrum over all stimuli for each IC and over all ICs for each cluster. To allow spectral changes over time to be easily visualized, we subtracted a baseline, which was the average spectrum over all time points, from the spectrum at each time point. These plots, showing spectral change from baseline, are referred to as event related spectral perturbations (ERSPs) (Makeig, 1993;Gwin et al., 2011). For the ERSP plots, time zero is stimulus onset. We used bootstrapping methods available in EEGLAB (Delorme and Makeig, 2004) to determine regions of significant difference from baseline ($p<0.05$).

We wanted to determine if the ERSP data from the cognitive task showed a significant trend across the five walking speeds (0.0 to 1.6 m/s). Each ERSP plot is made up of 507 frequency bins and 200 time bins, yielding a total of 101,400 TxF bins. For each TxF bin, we used the MATLAB nlmefit function to fit a group level slope that best represented the change in raw spectral power across walking speed (from 0.0 to 1.6 m/s) for all independent components in the cluster. The nlmefit function fits a model where each model parameter is the sum of a fixed and random effect (mixed effect). For our model, walking speed was a mixed effect. After fitting the model at each TxF bin, we computed a p-value representing the significance of the slope at that bin. Finally, we accounted for family-wise error rate by subjecting all 101,400 p-values for each cluster to a false discovery rate algorithm

(http://go.warwick.ac.uk/tenichols/software/fdr/FDR.m). False discovery rate (Genovese et al., 2002) controls the expected proportion of false positives. We set the accepted false discovery rate to 5%. Based on the assumption of positive dependence among observations, the false discovery rate algorithm generated a new p-value for significance.

Results

Cognitive task results

Subjects performed the Brooks spatial working memory task equally well at all walking speeds. Responses had an average percent correct around 50% regardless of walking speed (Table 1). Because each position had to be filled with one of nine digits, 11% accuracy reflects chance level performance. Subjects filled in all nine numbers in the grid after about 11-12 seconds, regardless of walking speed (Table 1). Statistically, there was no significant difference by speed for either parameter (Table 1).

Table 2-1. Average percent correct and average reaction time for the Brooks spatial memory task at all speeds. Data are the mean with the standard deviation in parentheses. The values for the Brooks task during standing is the average of the three standing Brooks task trials. The bottom two rows give the ANOVA results (F and p values) for percent correct and reaction time across speeds for the Brooks task. There were no significant changes with speed in these task parameters.

Speed	Average Percent Correct	Average Reaction Time (seconds)
stand (0.0 m/s)	48.3 (12.8)	11.1 (3.5)

0.4 m/s	51.3 (14.7)	11.5 (4.1)
0.8 m/s	49.8 (18.2)	11.9 (4.3)
1.2 m/s	53.3 (12.8)	11.8 (4.9)
1.6 m/s	46.0 (16.4)	10.9 (4.1)
p value	0.18	0.44
F value	1.798	1.000
df	4	4
Error (df)	76	76

Gait kinematics results

Brooks task vs. walking alone

The addition of the Brooks spatial working memory task had some limited effects on walking kinematics. At all walking speeds, step width increased significantly with the addition of the Brooks task compared with walking without the Brooks task (ANOVA, $F=22.62$, $p < 0.001$; Bonferroni, $p<0.05$) (Figure 3 (A), Table 2). There were no significant differences between cognitive task and no cognitive task for step length (ANOVA, $F=1.74$, $p=0.20$) (Figure 3 (B)). Step length variability and step width variability also were not significantly different between cognitive task and no cognitive task across speeds (ANOVA, $F=1.85$, $p=0.051$ and $F=1.16$, $p=0.30$, respectively) (Table 2). There was no interaction between speed and task condition for

each of the four outcomes: step length, step length variability, step width, or step width variability (Table 2).

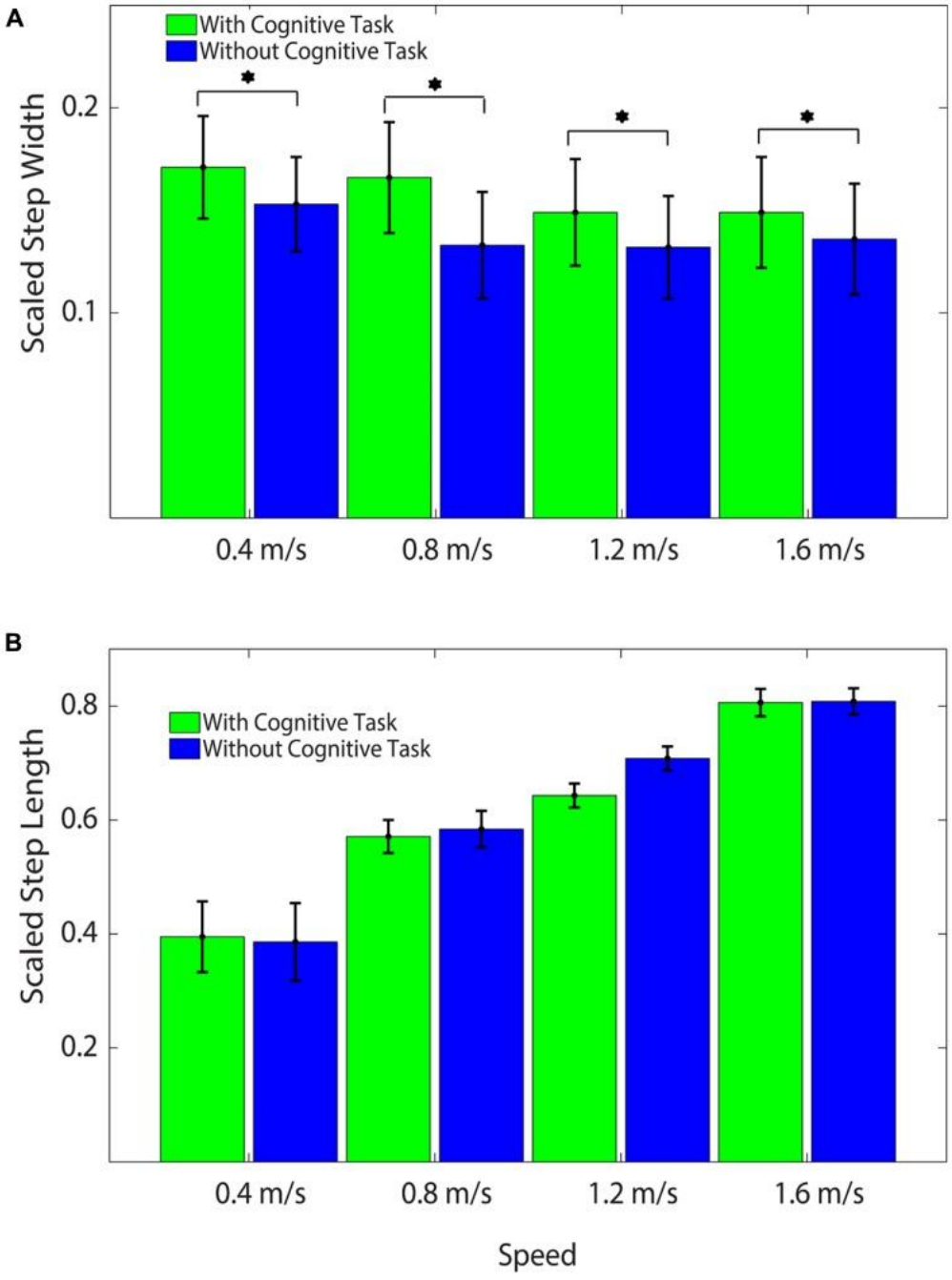

Figure 2-3. Average Step Lengths and Widths. (A) Average Scaled Step Widths at all speeds with and without the cognitive task. Subjects stepped significantly wider with the cognitive task than without the cognitive task at all speeds. Asterisks indicate significant differences between conditions. All values were scaled by each subject's leg length to create unitless measures. **(B)** Average Scaled Step Lengths at all speeds with and without the cognitive task. There were no significant differences by task across speed. All values were scaled by each subject's leg length to create unitless measures.

Some gait kinematic parameters varied with walking speed, as expected. When comparing the different speeds with each other, step length increased with speed (ANOVA, $F=499.08$, $p < 0.001$; Bonferroni, $p < 0.05$). Step width decreased at higher speeds (ANOVA, $F=6.93$, $p=0.003$; Bonferroni, $p < 0.05$). There were no significant differences in step length variability or step width variability between speeds (Table 2).

Table 2-2. ANOVA table showing F and p values for speed, task, and speed x task interaction. By speed, all but one crosswise comparison (0.8 m/s and 1.2 m/s) of step length values were significantly different from each other (ANOVA, $F=499.08$, $p<0.001$; Bonferroni, $p<0.05$), and step width values were significantly different between 0.4 m/s and 1.2 m/s and 0.4 m/s and 1.6 m/s (ANOVA, $F=6.93$, $p=0.003$; Bonferroni, $p < 0.05$). By task, step width was significantly greater with the cognitive task than without the cognitive task at all speeds (ANOVA, $F=22.62$, $p < 0.001$; Bonferroni, $p<0.05$).

	Speed (df=3)		**Task (df=1)**		**Speed x Task**		**Post-hoc Test**	
	F value	**p value**	**F value**	**p value**	**F value**	**p value**	**By speed p<0.05**	**By task p<0.05**
Step Length	499.08	< .001	1.74	0.20	0.90	0.46	All but 0.8 from 1.2	

Step Width	6.93	0.003	22.62	< .001	0.53	0.67	0.4 from 1.2, 1.6	ALL
Step Length Variability	3.18	0.051	1.85	0.19	0.81	0.50		
Step Width Variability	2.65	0.08	1.16	0.30	0.39	0.76		

Encoding period versus retrieval period for Brooks task

Walking kinematics during the Brooks task differed based on task period. Step length decreased during retrieval compared with encoding (ANOVA, $F=6.53$, $p=0.02$). There was also a significant interaction effect between speed and task period on step length (ANOVA, $F=6.63$, $p=0.004$). Both step width and step width variability increased during retrieval (ANOVA, $F=35.41$, $p < 0.001$ and $F=16.33$, $p=0.001$, respectively) compared with encoding. Step length variability did not show a statistically significant difference between encoding and retrieval (ANOVA, $F=3.07$, $p=0.097$).

Gait kinematic parameters again varied with walking speed. For steps taken in the encoding and retrieval periods, there was a significant increase in step length with speed (ANOVA, $F=988.22$, $p < 0.001$; Bonferroni, $p < 0.05$). Both step width and step length variability were significantly

lower at 1.2 m/s than at 0.4 m/s (ANOVA, F=3.49, p=0.04 and F=4.68, p=0.016, respectively; Bonferroni, $p < 0.05$). There were no other statistically significant differences in step width, step length variability, or step width variability at any other speeds.

Table 2-3. ANOVA table showing F and p values for speed, task period, and speed x task period interaction. Step length showed a statistically significant interaction between speed and task period (ANOVA, F=6.63, p=0.004) as well as an increase in step length at higher speeds and during encoding (ANOVA, F=988.22, $p < 0.001$; Bonferroni, $p < 0.05$ and F=6.53, p=0.02, respectively). Step width and step width variability increased during retrieval (ANOVA, F=35.41, $p < 0.001$ and F=16.33, p=0.001, respectively). Step width and step length variability were significantly lower at 1.2 m/s than at 0.4 m/s (ANOVA, F=3.49, p=0.04 and F=4.68, p=0.016, respectively; Bonferroni, $p < 0.05$).

	Speed (df=3)		**Task Period (df=1)**		**Speed x Task Period**		**Post-hoc Test**	
	F value	**p value**	**F value**	**p value**	**F value**	**p value**	**By speed p<0.05**	**By task period p<0.05**
Step Length	988.22	< 0.001	6.53	0.02	6.63	0.004	ALL	ALL
Step Width	3.49	0.04	35.41	< 0.001	2.42	0.10	0.4 from 1.2	ALL

Step Length Variability	4.68	0.016	3.07	0.097	0.64	0.60	0.4 from 1.2	
Step Width Variability	1.52	0.25	16.33	0.001	0.77	0.53		ALL

EEG results

Twelve independent component clusters met our criteria for further analysis (>10 subjects). Of the twelve clusters, six showed significant spectral power shifts temporally linked to stimulus presentation (Table 3).

Table 2-4. Centroid location for all clusters of electrocortical sources containing ICs from more than ten subjects with significant event-locked spectral power shifts. Brodmann area (BA) is listed as well as the number of independent components (ICs) in each cluster.

Functional area	**Brodmann area**	**# of Subjects**	**# of ICs**
Left Somatosensory Association Cortex	7	13	33
Central Somatosensory Association Cortex	7	12	35
Right Somatosensory Association Cortex	7	11	17

Central Posterior Cingulate Cortex	31	12	35
Right Superior Parietal Lobule	5	13	39
Central Premotor and Supplementary Motor Area	6	12	26

Three clusters in the somatosensory association cortex had large changes in spectral power that were temporally linked to stimulus presentation and were consistent for all walking speeds. These cluster centroids were located in left, central, and right somatosensory association cortex (Figure 4). In all three somatosensory association clusters, alpha (8-13 Hz) power increased prior to stimulus presentation and decreased following stimulus presentation (Figures 5-7). The increase in spectral power likely represented an anticipatory effect given that it preceded stimulus presentation.

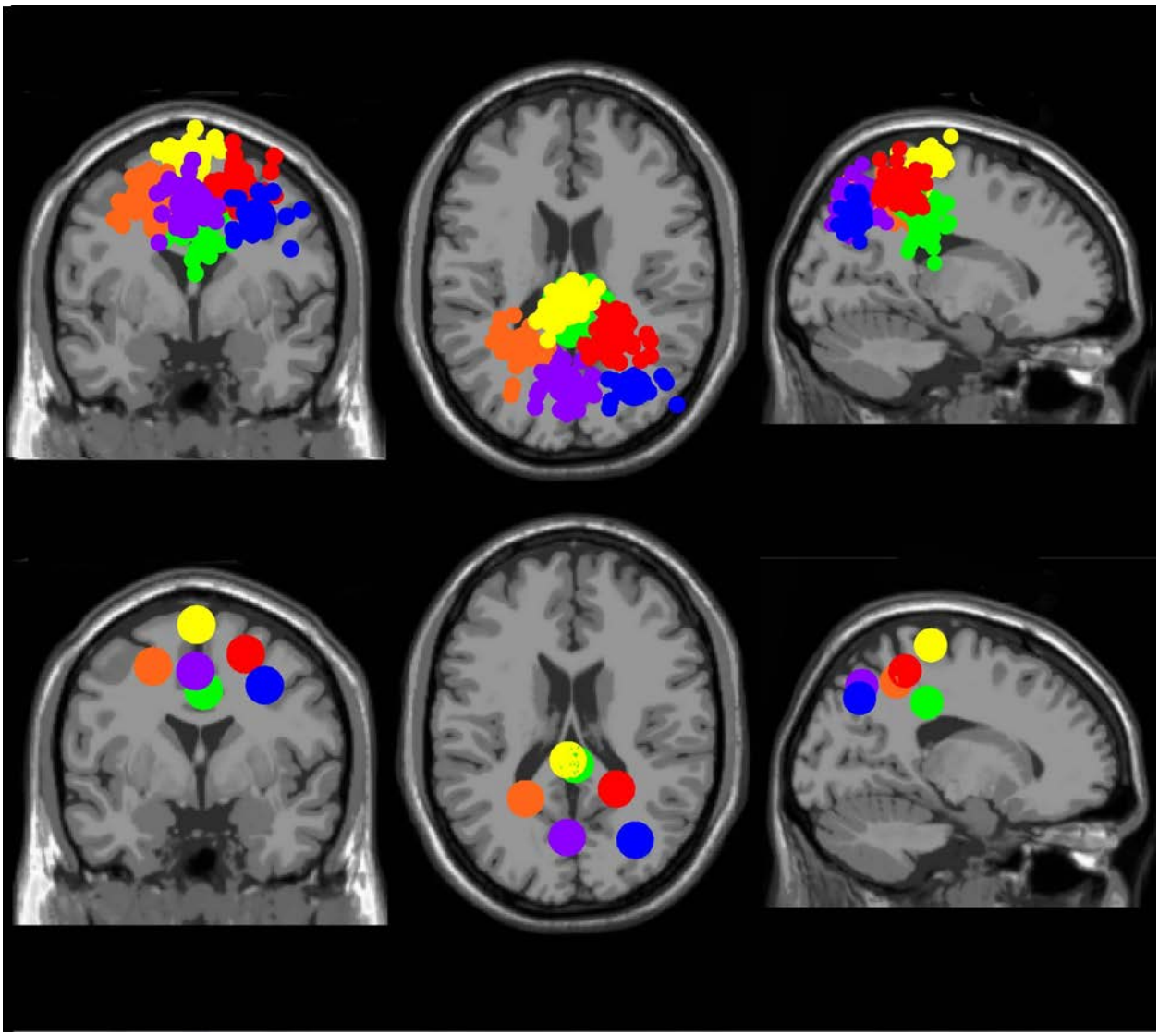

Figure 2-4. Electrocortical Clusters with event-locked spectral shifts. Clusters of electrocortical sources with significant spectral shifts time-locked to stimulus presentation during the Brooks spatial working memory task. Green is the central posterior cingulate (BA 31), blue is the right somatosensory association cortex (BA 7), orange is the left somatosensory association cortex (BA 7), purple is the middle somatosensory association cortex (BA 7), red is the right superior parietal lobule (BA 5), and yellow is the central premotor and supplementary motor cortex (BA 6). From left to right, the top three images show the centroid locations for each cluster from a horizontal, coronal, and sagittal view. The bottom three images show the independent component dipoles for each cluster from the same three perspectives.

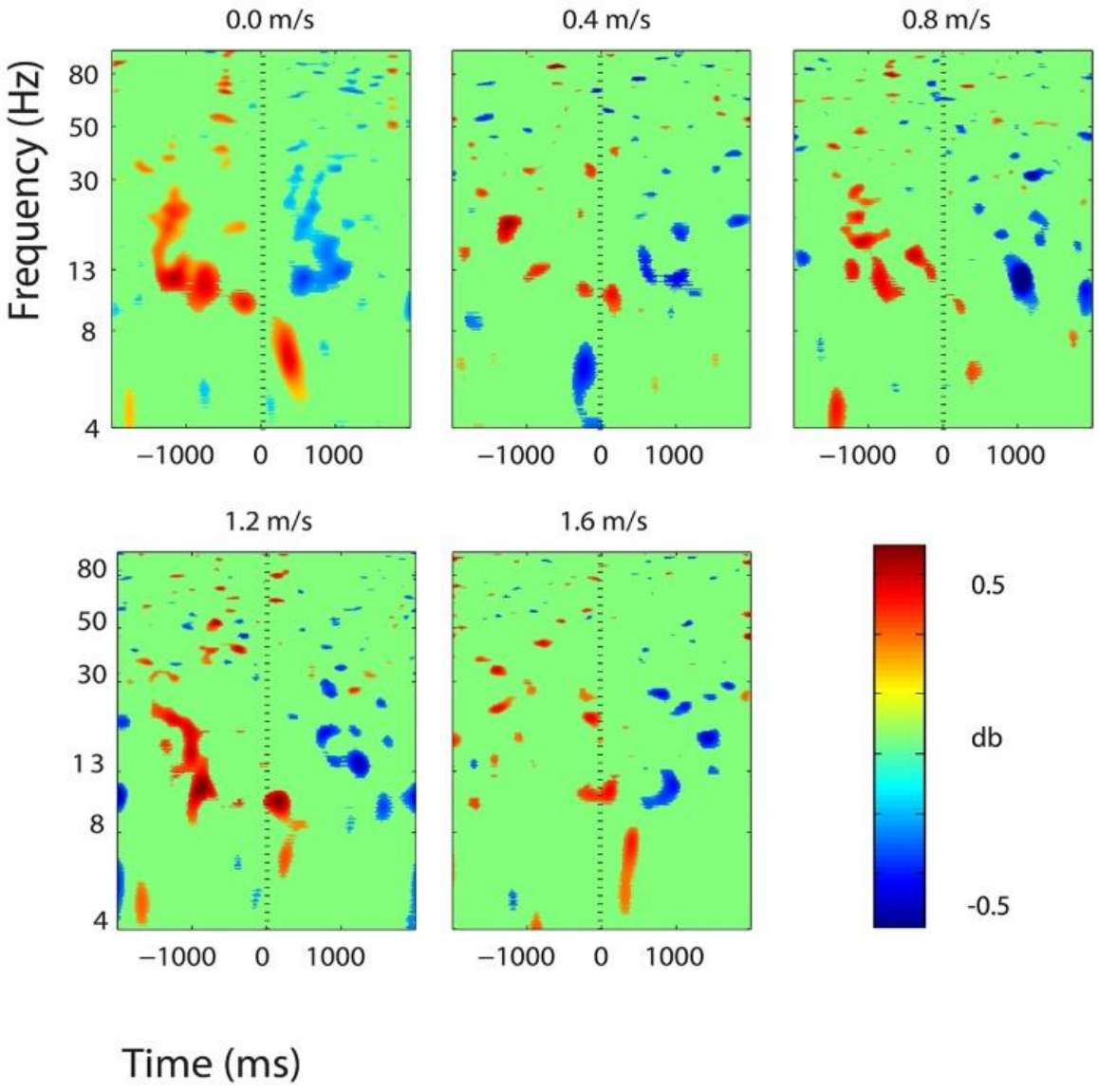

Figure 2-5. ERSPs Left BA7. Event Related Spectral Perturbation (ERSP) plots showing power change around the presentation of a stimulus (a digit and its position in an imagined grid) in the left somatosensory association cortex (BA 7). Red represents a power increase from baseline and blue represents a power decrease from baseline. We set non-significant differences to 0 dB (green). The stand condition ERSP is the average of all three standing Brooks spatial working memory task trials.

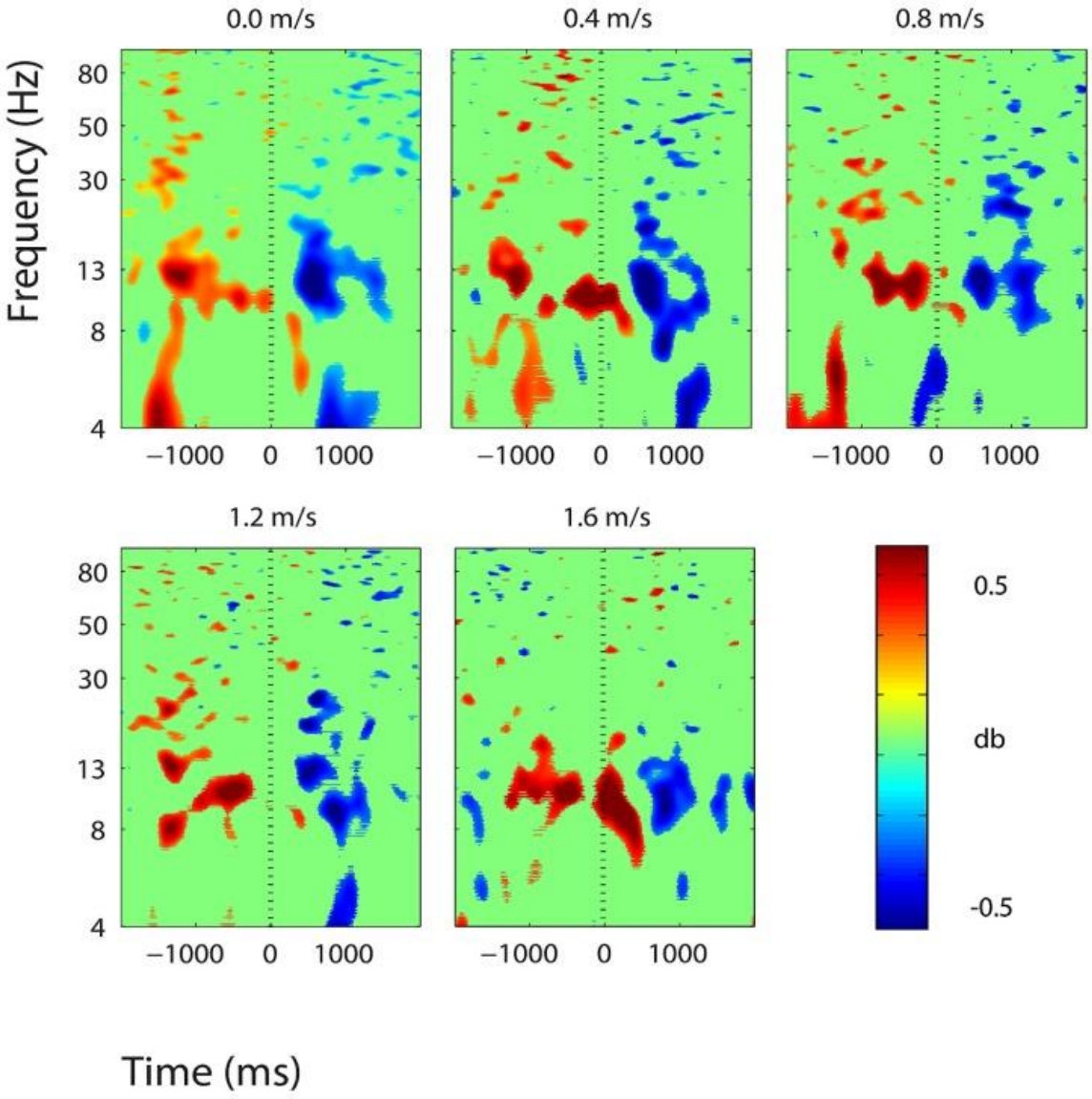

Figure 2-6. ERSPs central BA7. Event Related Spectral Perturbation (ERSP) plots showing power change around the presentation of a stimulus (a digit and its position in an imagined grid) in the central somatosensory association cortex (BA 7). Red represents a power increase from baseline and blue represents a power decrease from baseline. We set non-significant differences to 0 dB (green). The stand condition ERSP is the average of all three standing Brooks spatial working memory task trials.

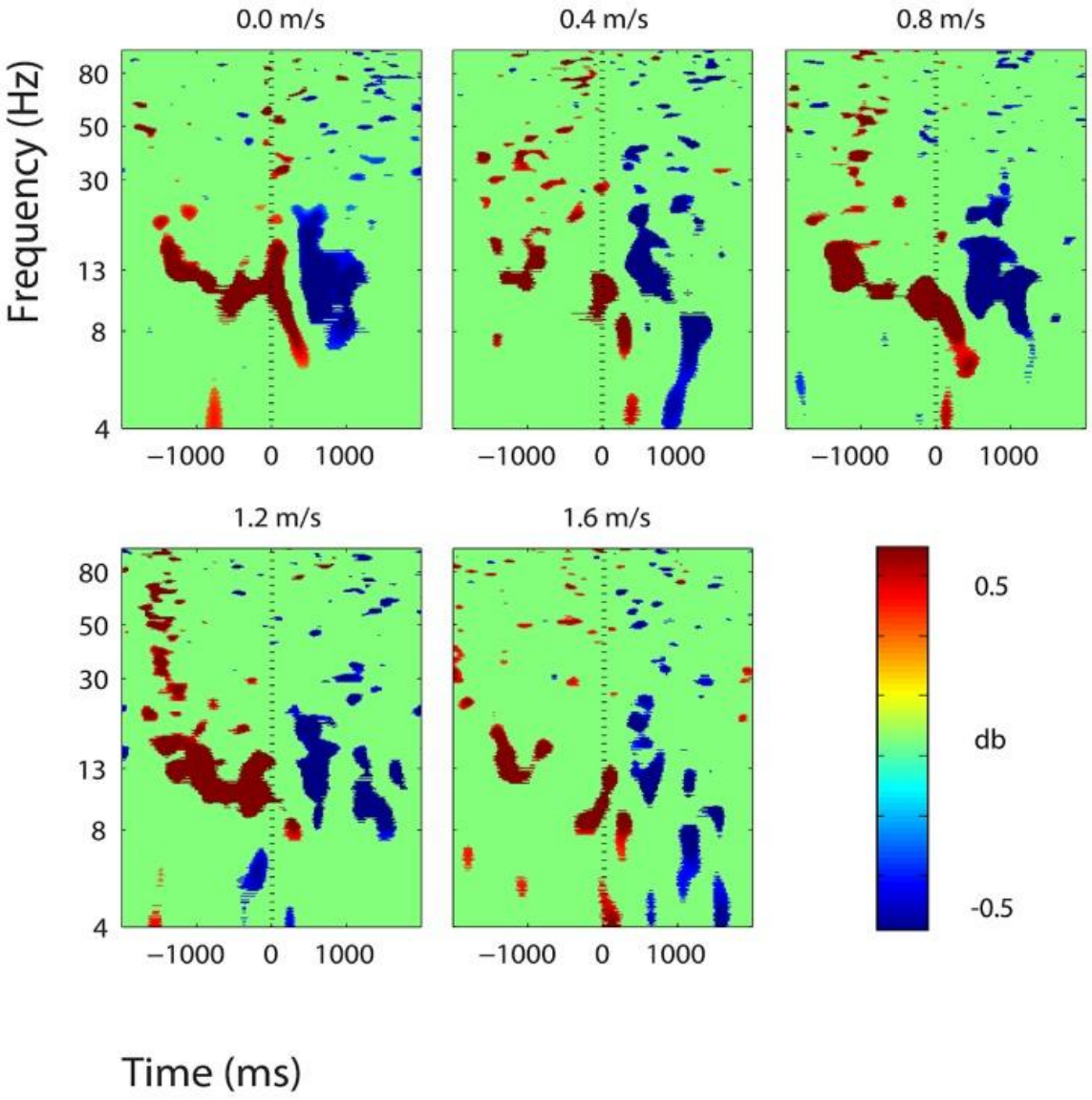

Figure 2-7. ERSPs right BA 7. Event Related Spectral Perturbation (ERSP) plots showing power change around the presentation of a stimulus (a digit and its position in an imagined grid) in the right somatosensory association cortex (BA 7). Red represents a power increase from baseline and blue represents a power decrease from baseline. We set non-significant differences to 0 dB (green). The stand condition ERSP is the average of all three standing Brooks spatial working memory task trials

There were some minor significant spectral shifts in three other clusters, located in the premotor and supplementary motor area, the superior parietal lobule, and the posterior cingulate cortex. In the premotor and supplementary motor area, power in the lower alpha band increased

significantly following stimulus presentation during standing, but not during walking (Figure 8). In the superior parietal lobule and the posterior cingulate cortex, theta (4-7 Hz) power decreased significantly following stimulus presentation during standing and walking at all speeds (Figures 9-10).

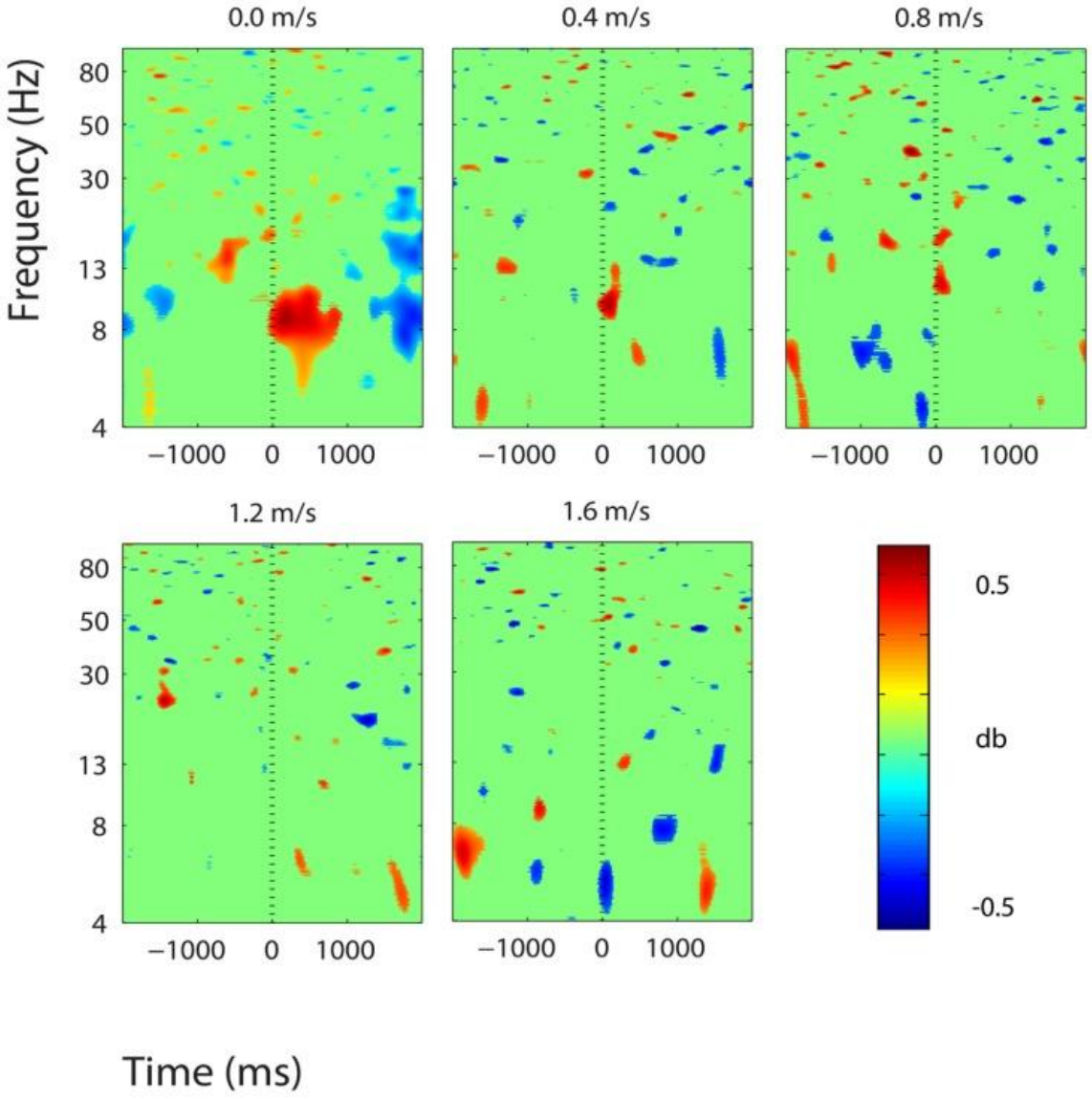

Figure 2-8. ERSPs BA 6. Event Related Spectral Perturbation (ERSP) plots showing power change around the presentation of a stimulus (a digit and its position in an imagined grid) in the premotor and supplementary motor cortex (BA 6). Red represents a power increase from baseline and blue represents a power decrease from baseline. We set non-significant differences

to 0 dB (green). The stand condition ERSP is the average of all three standing Brooks spatial working memory task trials.

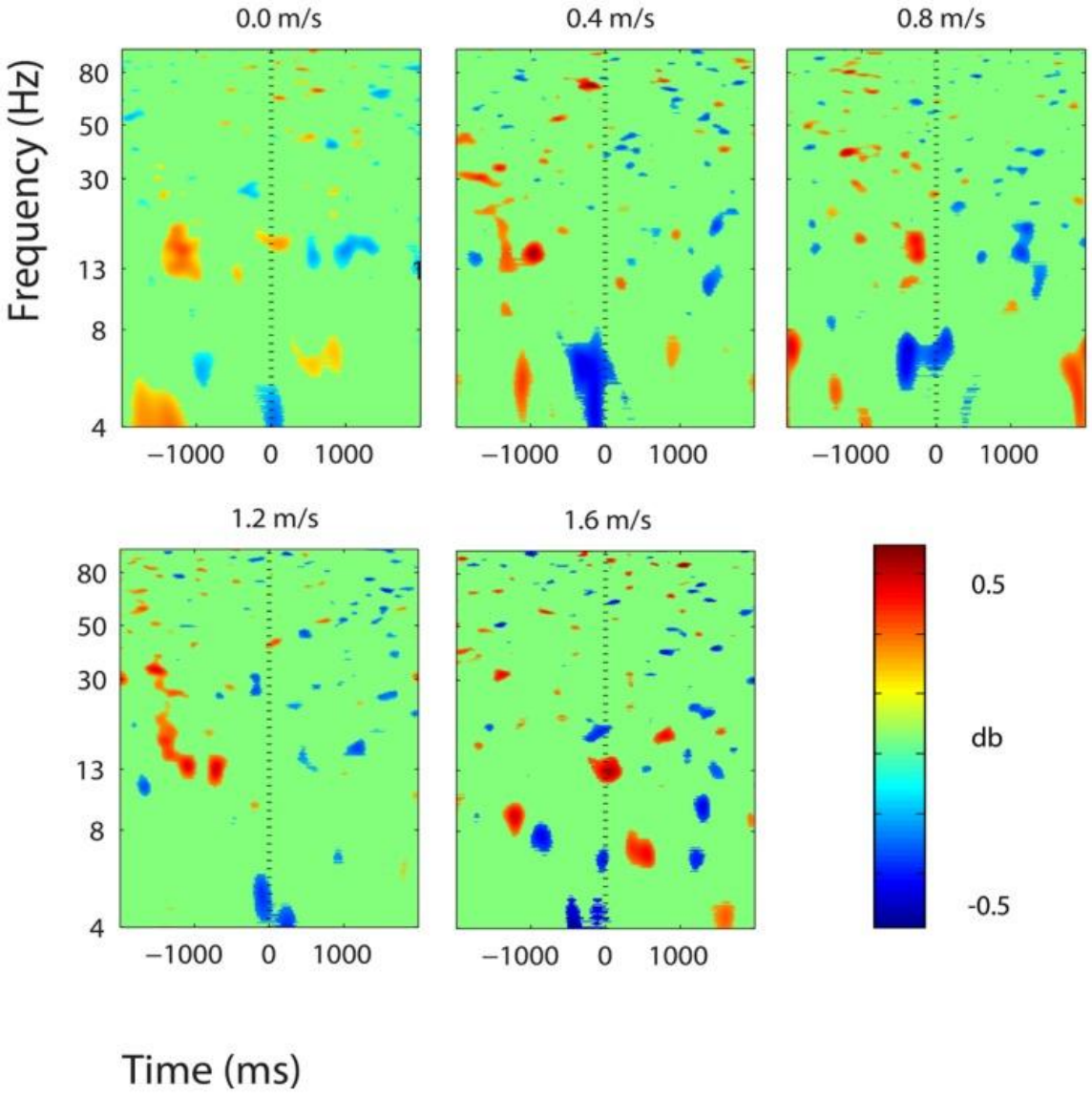

Figure 2-9. ERSPs BA 5. Event Related Spectral Perturbation (ERSP) plots showing power change around the presentation of a stimulus (a digit and its position in an imagined grid) in the right superior parietal lobule (BA 5). Red represents a power increase from baseline and blue represents a power decrease from baseline. We set non-significant differences to 0 dB (green). The stand condition ERSP is the average of all three standing Brooks spatial working memory task trials.

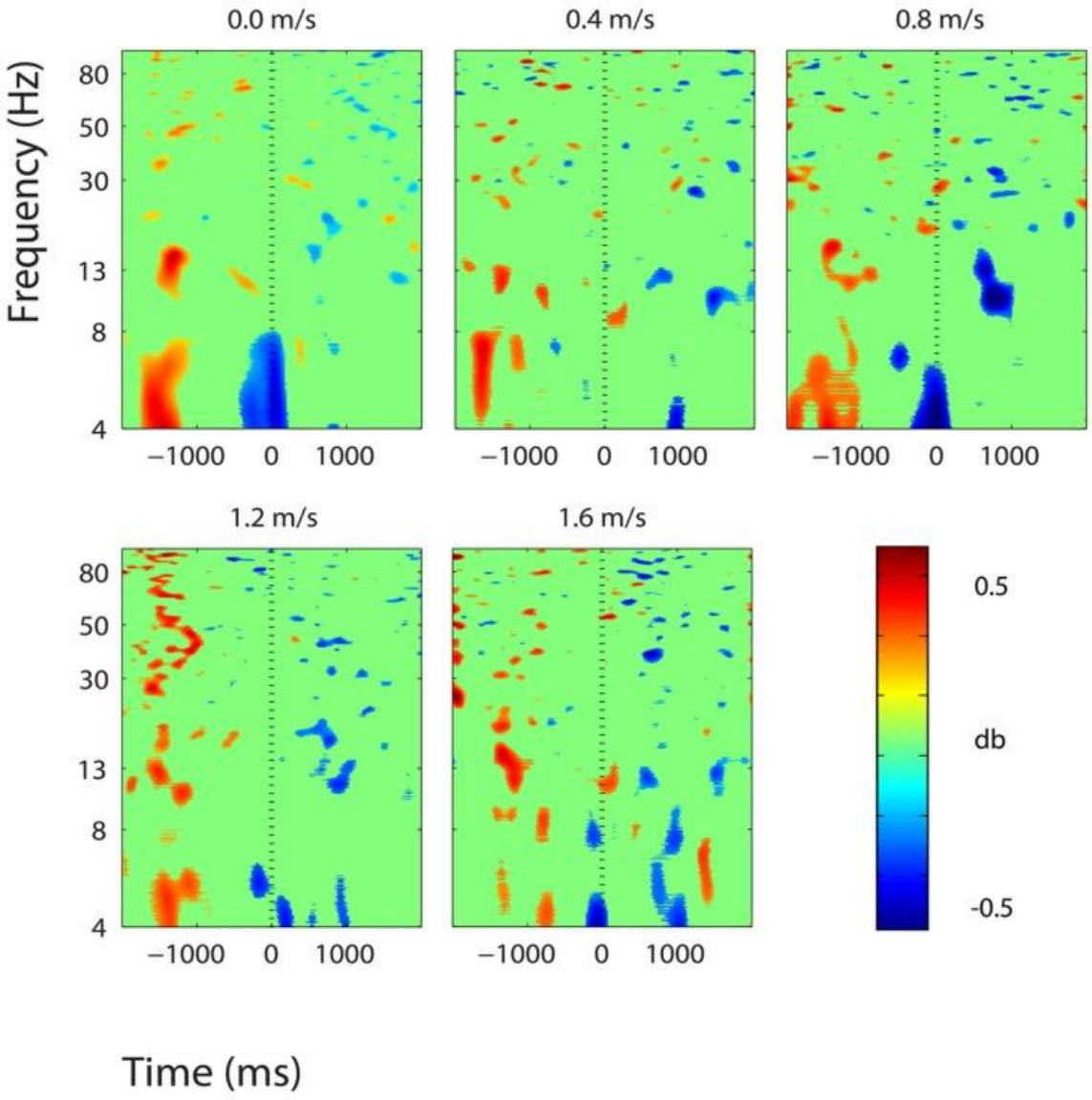

Figure 2-10. ERSPs BA 31. Event Related Spectral Perturbation (ERSP) plots showing power change around the presentation of a stimulus (a digit and its position in an imagined grid) in the posterior cingulate cortex (BA 31). Red represents a power increase from baseline and blue represents a power decrease from baseline. We set non-significant differences to 0 dB (green). The stand condition ERSP is the average of all three standing Brooks spatial working memory task trials.

Clusters containing independent components from more than half of the subjects (>10) were also located in left and right premotor and supplementary motor area (BA 6), left and right posterior cingulate cortex (BA 31), and right anterior cingulate cortex (BA 24, 32) (Figure 11). These six

clusters did not have large event-related spectral power changes linked to stimulus presentation that were consistent across walking speeds (Figure 12).

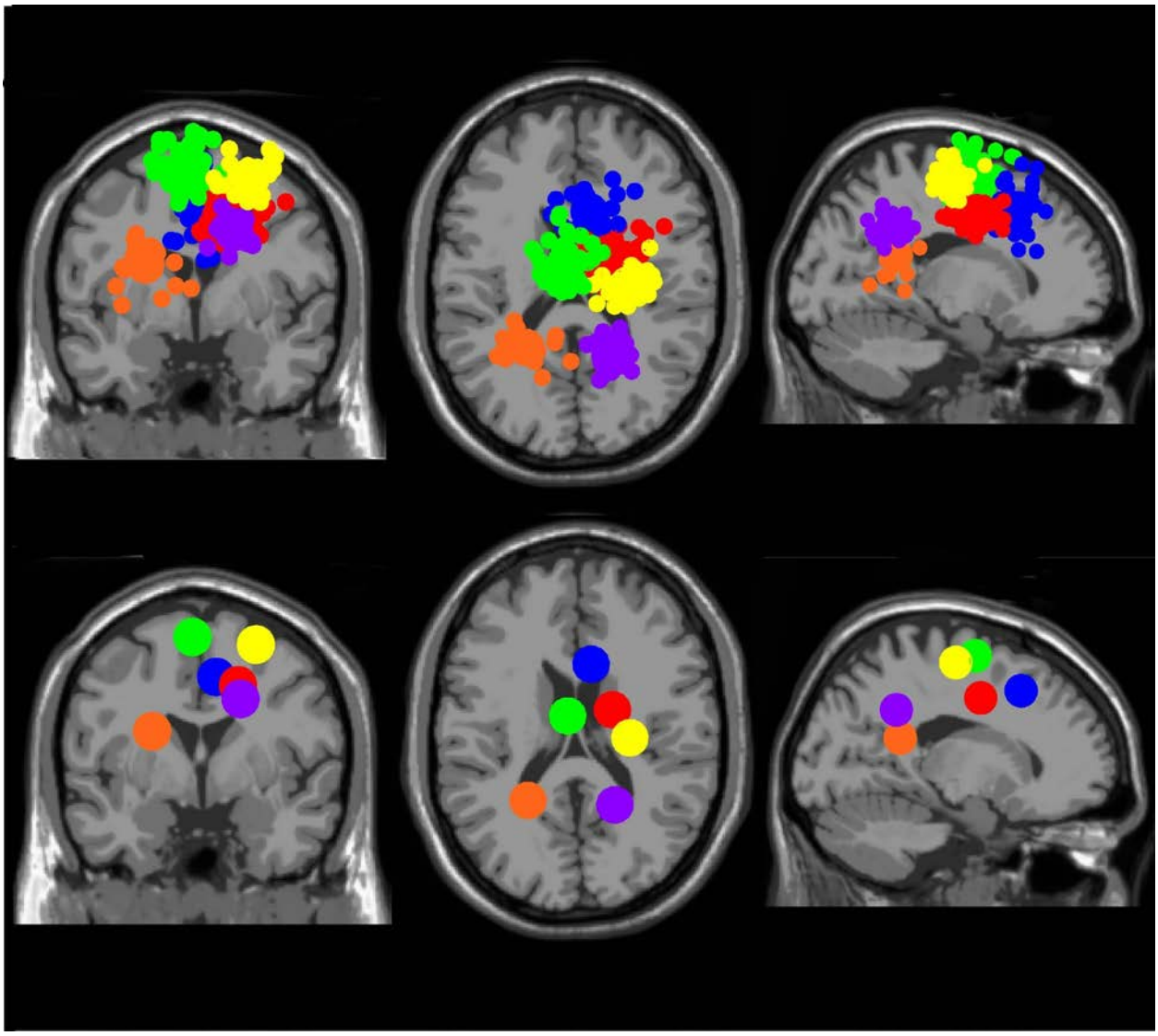

Figure 2-11. Electrocortical Clusters without Event-locked Spectral Shifts. Clusters containing electrocortical sources from >10 subjects but without significant spectral shifts time-locked to stimulus presentation during the Brooks spatial working memory task. Green is left premotor and supplementary motor cortex (BA 6), yellow is right premotor and supplementary motor cortex (BA 6), blue is right anterior cingulate (BA 32), red is right anterior cingulate (BA 24), orange is left posterior cingulate (BA 31), and purple is right posterior cingulate (BA 31). From left to right, the top three images show the centroid locations for each cluster from a horizontal, coronal, and sagittal view. The bottom three images show the independent component dipoles for each cluster from the same three perspectives.

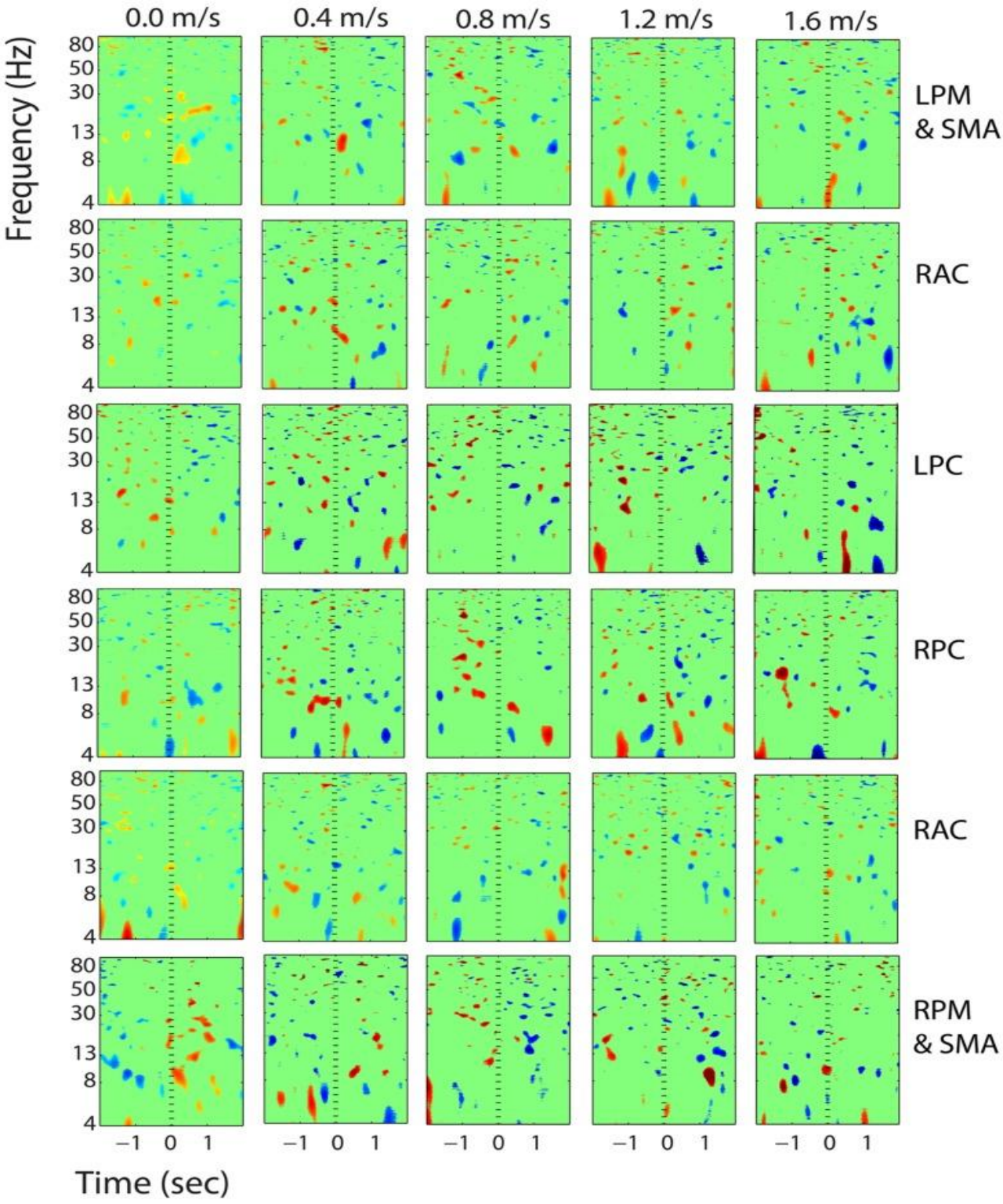

Figure 2-12. ERSPs without Event-locked Spectral Shifts. Event Related Spectral Perturbation (ERSP) plots showing power change around the presentation of a stimulus (a digit

and its position in an imagined grid) in the additional six clusters with independent components from >10 subjects. Each row is one cortical area. From top to bottom, the cortical areas are left premotor and supplementary motor area (LPM&SMA), right anterior cingulate (RAC), left posterior cingulate (LPC), right posterior cingulate (RPC), right anterior cingulate (RAC), and right premotor and supplementary motor area (RPM&SMA). The color scale is from -0.5 db to 0.5 db.

For all six clusters showing significant spectral power shifts temporally linked to stimulus presentation, there was no significant effect of walking speed on spectral power. After analysis with nlmefit and the false discovery rate algorithm, for all six clusters, the p-value calculated by the false discovery rate algorithm was equal to zero. This means that there were no significant p-values, and therefore no significant power changes by speed.

Discussion

Our results indicate that walking speed does not affect spatial working memory task performance or task-related electrocortical activity in young, healthy subjects within the range of speeds measured here. Our subjects showed no change in response accuracy or reaction time for the Brooks spatial working memory task across walking speeds. Their success rate for the task was about 50% regardless of whether they were standing, walking slowly, or walking quickly. We also found no evidence of change in the electrocortical activity devoted to the cognitive task across walking speeds. The event related spectral perturbation graphs in Figures 6-11 reveal similar patterns for standing and all walking speeds (with the exception of the premotor and supplementary motor cortex, Figure 9). The mixed effects model showed no significant trend in spectral power change across speeds. If we had found a speed effect in either task performance or electrocortical activity without the other having a speed effect, our results would have been harder to interpret.

Previous studies have shown that performance of some types of cognitive tasks are affected by walking speed. Tomporowski and colleagues showed that in older adults performing an executive processing task, response times decreased and response errors increased when walking at faster speeds compared with walking at slower speeds (Tomporowski and Audiffren, 2014). When walking freely, young and older adults tend to decrease their walking speed when given cognitive tasks to perform during locomotion (Beauchet et al., 2002;Patel et al., 2014). This decrease in motor performance with dual-task walking and cognition suggest that there are common mental resources devoted to both tasks. Thus, we expected to see a change in cognitive performance and electrocortical activity as walking speed increased. However, the majority of studies reporting dual-task performance costs during locomotion have examined elderly or impaired populations. It may be that young, healthy subjects have an increased ability to walk at high speeds and perform a challenging cognitive task with no performance decrease compared with older subjects. In addition, the type of cognitive task may alter the relative amount of dual-task performance cost, as different cognitive tasks rely on different cortical substrates (Smith et al., 1996). When young, healthy subjects have demonstrated a dual-task performance cost (Melzer and Oddsson, 2004;Grabiner and Troy, 2005;Al-Yahya et al., 2009;Verrel et al., 2009;Szturm et al., 2013;Patel et al., 2014), the cognitive task was not a spatial working memory task.

Across all speeds, the addition of the spatial working memory task caused our subjects to step more widely compared to walking without a cognitive task. Wider steps have been associated with more stable gait (Bauby and Kuo, 2000;McAndrew Young and Dingwell, 2012). Past studies on young, healthy subjects performing cognitive tasks during walking have been inconsistent in finding step width changes (Grabiner and Troy, 2005;Siu et al., 2008;Al-Yahya et

al., 2009). Our spatial working memory task's significant effect on step width in young, healthy subjects could be related to its high difficulty level. Subjects correctly placed only about half of the digits at each speed, indicating that the task was very challenging. Patel et al. found that the complexity of the cognitive task influences the relative dual-task cost during gait (Patel et al., 2014). The lack of dual-task effects on gait kinematics for young, healthy subjects in past studies may be related to this difficulty/complexity effect or to the type of cognitive task, as we discussed above.

When we broke down the kinematic results into periods of encoding vs. retrieval for the cognitive task, we found that the retrieval period showed changes in gait indicative of decreased stability. Step width and step width variability were both greater in the phase of the cognitive task that required the subjects to push buttons on the handheld device (retrieval) compared with the memorization period (encoding). The subjects also took shorter steps during the retrieval period compared to the encoding period. All of these changes in gait kinematics are traditionally seen by individuals that are older and have reduced gait stability (Dubost et al., 2006;Siu et al., 2008;Yogev-Seligmann et al., 2008;Granacher et al., 2011). The encoding task is not unlike many everyday walking tasks such as walking and texting, or walking and dialing a phone number. This suggests that in the real world, performing dual manual and locomotor tasks likely results in humans responding to stability challenges as well.

We found consistent electrocortical activity around stimulus encoding at all walking speeds in the somatosensory association cortex. Event-related spectral perturbations showed substantial alpha (8-13 Hz) synchronization preceding stimulus presentation and alpha desynchronization following stimulus presentation during the Brooks task. This area of the parietal lobe is involved

in locating objects in space and is engaged during spatial working memory tasks (Carlesimo et al., 2001). We presented a stimulus every four seconds during the Brooks task. Alpha power in the left, right, and central portions of the somatosensory association cortex increased approximately 1 second before the presentation of the stimulus (a digit and its corresponding position in the grid) and remained elevated until shortly after stimulus presentation. Alpha power in the somatosensory association cortex decreased approximately 0.5 seconds after stimulus presentation. This could represent neural encoding of the digit and its position in working memory. The alpha power fluctuation was stronger in the right than in the left somatosensory association cortex, which may indicate that this brain area shows a right hemisphere dominance for locating objects in space. Eighteen of the twenty subjects were right-hand dominant.

We found small, significant theta power decreases around stimulus encoding in two brain areas: the right superior parietal lobule and the central posterior cingulate. Theta power modulations during memory tasks have been associated with memory encoding and maintenance by previous electrophysiology studies (Bastiaansen et al., 2002;Friese et al., 2012;Itthipuripat et al., 2013;Lenartowicz et al., 2014). Bastiaansen and colleagues found sustained theta power decreases in frontal electrodes during the retention phase of a spatial working memory task (Bastiaansen et al., 2002). Burke and colleagues also found decreases in theta phase synchrony during memory encoding (Burke et al., 2013). Many studies have shown theta increases in frontal brain regions during memory encoding and maintenance (Itthipuripat et al., 2013;Lenartowicz et al., 2014). However, we did not find any theta power increases in the frontal brain areas during performance of our task. It could be that during walking, these areas are engaged in gait-related processing, so cognitive task-related electrocortical shifts are undetectable within the gait related electrocortical activity. A host of functional near-infrared

spectroscopy studies have found that the frontal cortical areas are highly engaged during human walking, even without a secondary task (Miyai et al., 2001;Suzuki et al., 2004;Harada et al., 2009). In addition, in a previous study from our lab, we also found electrocortical evidence of frontal cortical involvement in human walking without a cognitive task (Gwin et al., 2011). Our analysis of spectral perturbations in electrocortical activity was specifically limited to changes synchronized to stimulus presentation.

On a similar note, activity in the premotor and supplementary motor cortex may demonstrate some overlap between cognitive and motor processing (Figure 9). During standing, power in the lower alpha band increased around stimulus presentation, and alpha and beta power decreased shortly thereafter. During walking, this effect was not visible. Studies have shown that the premotor and supplementary motor cortex is engaged during walking (Gwin et al., 2011). During walking this area was likely engaged in motor processing, and cognitive-related activity was either not present or undetectable.

Some researchers have questioned how much mechanical artifact is present in walking EEG data synchronized to the gait cycle (Castermans et al., 2014). Previous studies have shown that EEG during walking is viable for non-gait synchronized data, as the approach of synchronizing EEG data to cognitive events not coupled to gait allows mechanical artifacts to wash out (Gramann et al., 2010). We observed the same pattern of neural activity at all speeds from standing (0.0 m/s) to very fast walking (1.6 m/s). This result indicates that EEG and ICA can reveal neural activity from a continuous cognitive task even when a subject is moving quickly. To our knowledge, our results are the first to show that high-density EEG and ICA can allow for the study of continuous cognitive dynamics at high walking speeds. This has important implications for the field of

mobile brain imaging, as it suggests EEG could be used even in real-world environments that include walking at normal speeds.

Our study had some limitations that prevent us from drawing broad conclusions about the effects of speed on spatial working memory. First, we only examined young, healthy subjects. It is possible that we would have seen a larger effect in gait parameters and task performance if we had tested elderly subjects. Future studies should examine the neural and performance responses of elderly and neurologically impaired individuals. Second, we only examined a single cognitive task and a single cognitive task difficulty level. While unlikely, it is possible that an easier task or a harder task may have resulted in a different outcome. Third, the majority of the subjects in this study were males. There is some evidence that males may walk with increased variability under dual-task conditions. Hollman and colleagues had older adults walk and performed a backward spelling task (Hollman et al., 2011). Both genders increased their variability when walking with the cognitive task, however the variability increase during dual-task walking was greater in men than women. Finally, we did not assess our subjects' preferred speed. A study by Schaefer et al. showed that children and young adults improved their cognitive performance on a working memory task while walking at their preferred speed on a treadmill (Schaefer et al., 2010). The ideal dual-task cost study would include a range of cognitive tasks and difficulty levels, to separate out overlap in neural substrates between walking and various cognitive tasks. Our findings raise some interesting questions about dual-tasking. A popular view suggests that because walking requires mental effort, performing both walking and thinking can decrease thinking ability compared with thinking while standing still (Kahneman, 2013). Our results do not support that conclusion. For our spatial working memory task, mental performance did not change for walking vs. standing. Similarly, a recent study on the use of a treadmill desk found

that human subjects performed equally well on a range of cognitive tasks for slow walking compared to standing (Alderman et al., 2014). John and colleagues (John et al., 2009) also reported that subjects performing slow walking at a treadmill desk had no significant differences in selective attention, processing speed, or reading comprehension compared to sitting at a desk. Our study only examined a single cognitive task, but we found no detrimental effects over a wide range of walking speeds on cognitive ability.

Other researchers have suggested that moving your body may actually improve creativity. Slepian and Ambady (Slepian and Ambady, 2012) found that subjects performed better on cognitive tasks related to creativity when moving their arms in fluid movements compared with not moving their arms. Longer term studies have found that chronic exercise also seems to increase creativity, but that is on the time scale of weeks or months (Flaherty, 2011). Putting together all of these observations with our own results, we suggest that people should not be concerned that walking while thinking will impair their cognitive performance. All in all, our study demonstrates that in young, healthy subjects perform equally well on a challenging spatial working memory task during walking at a range of speeds as during standing. Given the many benefits of walking (Rippe et al., 1988;Hardman and Morris, 1998), people should be encouraged to walk and think whenever possible.

Chapter 3: Isolating gait-related movement artifacts in electroencephalography during human walking

This chapter has been previously published:

Kline JE, Huang HJ, Snyder KL, Ferris DP. Isolating gait-related movement artifacts in electroencephalography during human walking. *J Neural Eng* 12(4):046022, 2015.

Abstract

Objective: High-density electroencephalography (EEG) can provide insight into human brain function during real-world activities with walking. Some recent studies have used EEG to characterize brain activity during walking, but the relative contributions of movement artifact and electrocortical activity have been difficult to quantify. We aimed to characterize movement artifact recorded by EEG electrodes at a range of walking speeds and to test the efficacy of artifact removal methods. We also quantified the similarity between movement artifact recorded by EEG electrodes and a head-mounted accelerometer. Approach: We used a novel experimental method to isolate and record movement artifact with EEG electrodes during walking. We blocked electrophysiological signals using a nonconductive layer (silicone swim cap) and simulated an electrically conductive scalp on top of the swim cap using a wig coated with conductive gel. We recorded motion artifact EEG data from nine young human subjects walking

on a treadmill at speeds from 0.4-1.6 m/s. We then tested artifact removal methods including moving average and wavelet-based techniques. Main Results: Movement artifact recorded with EEG electrodes varied considerably, across speed, subject, and electrode location. The movement artifact measured with EEG electrodes did not correlate well with head acceleration. All of the tested artifact removal methods attenuated low-frequency noise but did not completely remove movement artifact. The spectral power fluctuations in the movement artifact data resembled data from some previously published studies of EEG during walking. Significance: Our results suggest that EEG data recorded during walking likely contains substantial movement artifact that: cannot be explained by head accelerations; varies across speed, subject, and channel; and cannot be removed using traditional signal processing methods. Future studies should focus on more sophisticated methods for removing of EEG movement artifact to advance the field.

Introduction

Measuring brain activity during human walking has the potential to advance both basic neuroscience and functional technologies. Imaging the brain during movement can help determine what brain areas are involved in neuromotor control and how they interact during motor activities. Further, real-time information about brain processes during everyday activities as people walk could allow for the design of more broad-ranging brain machine interfaces. In addition, mobile brain imaging devices would provide valuable information about the brain activity patterns of individuals with neural disorders. For these goals to be achieved during locomotion, it is imperative to: 1) be able to identify specific brain sources, which requires good

spatial resolution, 2) be able to observe split-second neural changes within a stride, which requires good temporal resolution, and 3) be able to extract strictly neural signals.

Advanced electroencephalography (EEG) technologies allow for novel insight into human brain function during whole-body movements. EEG has inherently good (millisecond) temporal resolution, and inverse source modeling techniques can provide spatial localization in the range of 1 cm (Makeig and Jung, 1996;Makeig et al., 2004a;Makeig et al., 2004b;Mullen et al., 2011). Functional near-infrared spectroscopy (fNIRS) has been used to study walking previously (Miyai et al., 2001;Suzuki et al., 2004;Harada et al., 2009), but it relies on a hemodynamic response, which has poorer temporal resolution. EEG offers better temporal resolution than fNIRS (Villringer and Chance, 1997;Irani et al., 2007), because EEG measures fast electrical potential changes rather than a slow metabolic signal. Combined with advanced statistical techniques, EEG can have comparable spatial resolution to fNIRS (Makeig et al., 2004a;Makeig et al., 2004b). Our laboratory has recorded electrocortical spectral fluctuations during treadmill walking in healthy, young adults (Gwin et al., 2011;Sipp et al., 2013). Other groups have also proved the feasibility of measuring scalp electrocortical signals during human walking, at speeds ranging from 0.42 m/s to 1.9 m/s, to provide insight into brain function (Gramann et al., 2010;Cheron et al., 2012;Lau et al., 2012;Severens et al., 2012;Wagner et al., 2012;Seeber et al., 2014; 2015) .

EEG recordings are a mixture of electrocortical and other signals, which ideally need to be separated to examine the brain activity. Other signals recorded by EEG systems include muscle and heart activity, eye movement, line noise, electromagnetic fields, and movement artifact (Figure 1(a); (Gwin et al., 2010)). To identify and remove these additional signals, first and

foremost, researchers can use visual inspection of EEG data to reject channels and time periods with large movement artifacts. There are also relatively simple frequency-based methods for removing artifact. Line noise can be separated by identifying and removing power at a frequency of 50 or 60 Hz. Either all power at this frequency can be removed via a notch filter, or only that which is independent of data at other frequencies. If the primary focus of a study is on non-gait related cognitive tasks, a moving average artifact template can be used to reject movement artifacts (Gwin et al., 2011). The drawback of this technique is that it also removes electrical brain activity that is time-locked to the gait cycle. Wavelet-based cleaning methods have been used in previous EEG studies to identify or remove low-frequency spectral fluctuations (Daubechies, 1988;Adeli et al., 2003).

There are additionally more complex, comprehensive mathematical methods for removing artifact from neural data. Blind source separation techniques, such as Independent Component Analysis (ICA) and Canonical Correlation Analysis (CCA) (Sweeney et al., 2013), have been successful at separating eye and muscular artifacts from EEG data (Jung et al., 2000a;Jung et al., 2000b), but they may be less successful with movement artifact due to the lack of independence between different noise signals. Additionally, Artifact Subspace Reconstruction (ASR) (Mullen et al., 2013) has also been used to remove artifacts from EEG recordings. ASR is a more complex, sophisticated method for movement-related artifact removal, but is beyond the scope of this paper. However, it will be included in a future analysis of how ASR and other more sophisticated techniques work in isolation and in combination to remove gait-related artifact.

Another approach to determining how to separate movement artifacts from scalp EEG during human walking is to focus on characterizing the electrical artifacts induced by gait. Castermans

and colleagues recently compared spectral fluctuations over the gait cycle in EEG data and accelerometer data. They found common harmonics in the spectra of the EEG and the accelerometer that roughly corresponded to the subjects' fundamental stepping frequency and increased with speed (Castermans et al., 2014). However, because accelerometers and EEG electrodes measure fundamentally different quantities, gait-related movement artifacts may differ between the two. Small movements of electrodes relative to a subject cause the electrodes to register a change in voltage, whereas the accelerometer only measures changes in the head's acceleration relative to the environment. Using EEG electrodes to quantify artifact induced by head movement during locomotion is also problematic because the EEG will contain a mixture of true electrocortical signals and artifact signals, with no clear way to distinguish the relative contributions of the two. If we could explicitly determine the spectral and temporal properties of the movement artifact, it might be possible to remove the artifact while keeping the real electrocortical content that is synchronized to the gait cycle. However, to truly characterize movement artifact in EEG recordings, we must first isolate it.

The purpose of this study was to isolate, record, and characterize movement artifact in EEG during human walking. We used a nonconductive layer, a silicone swim cap, to block all neural, muscular, ocular, and other physiological signals from the EEG electrodes (Figure 1(a)). While the signal we recorded likely contained nonphysiological electrical signals and movement artifact, the nonphysiological electrical signals, such as line noise and electromagnetic field noise, occur in a narrow frequency band and are small in magnitude, respectively, leaving our data dominated by movement artifact. We therefore refer to the data recorded by the EEG electrodes as movement artifact data. We placed a wig coated with conductive gel over the swim cap to simulate an electrically conductive human scalp with hair. Nine healthy subjects walked

on a treadmill over a range of speeds, while we recorded movement artifact data, head accelerations, and kinematic data. We hypothesized that EEG electrodes isolated from any electrophysiological signals would show gait-linked spectral fluctuations that varied across speed. We also tested the ability of a few simple cleaning methods to remove this movement artifact. Characterizing and attenuating walking-related movement artifact in EEG electrodes should improve our ability to study brain dynamics during walking.

Material and Methods

Data Collection

Nine healthy young adults (27.0 +/- 4.8; male=4, female=5) with no known musculoskeletal or neurological deficits participated in the study. The University of Michigan Institutional Review Board approved the study protocol, and all subjects gave written informed consent.

We devised a multi-layer approach to isolate and measure movement artifact with EEG electrodes (Figure 1(b); Active II, BioSemi, Amsterdam, The Netherlands). First, we placed a nonconductive layer, a silicone swim cap, over the subject's scalp. The nonconductive layer prevents electrophysiological signals from propagating to the electrodes. To measure voltage differences generated by movement, the recording electrodes needed to be in contact with a conductive medium. To achieve this, we used a wig that was coated with conductive gel to simulate a scalp with hair. This was placed directly over the swim cap. We then placed the EEG cap over the simulated scalp and gelled the electrodes as customary for EEG studies (Gwin et al., 2011). To view whether the silicone swim cap was blocking electrophysiological signals from the EEG electrodes, we asked subjects to blink their eyes and clench their jaw as we visually

inspected the channel data. We ensured that no muscle or eye artifact was visible in the EEG traces. To verify that we were measuring movement artifact, we asked subjects to nod their head up-and-down and shake their head from side-to-side, and we also physically shook the wires as we visually inspected the channel data for movement artifacts. Large movement artifacts were visible in the EEG traces during head movement and shaking for all subjects.

We also estimated how well the resistances of our simulated scalp compared with the resistance of a natural human scalp (~0.001-0.1 Mohm for dry skin, (Fish et al., 2003)). We used a multimeter to measure the resistances between the ground and the electrodes on the simulated scalp (0.9 ± 0.4 Mohm). We also checked that the BioSemi electrode offsets were <20 mV, as recommended by BioSemi's website (www.biosemi.com). The BioSemi system uses active electrodes, which are designed to reduce current flow through the skin-gel-electrode interface and thus reduce extraneous voltages from changes in impedance related to changes in the skin-gel-sensor interface. The measured multimeter resistances of our simulated scalp and the voltage offsets provided by BioSemi suggest that the electrode characteristics were similar for the simulated scalp and actual human scalp.

(a)

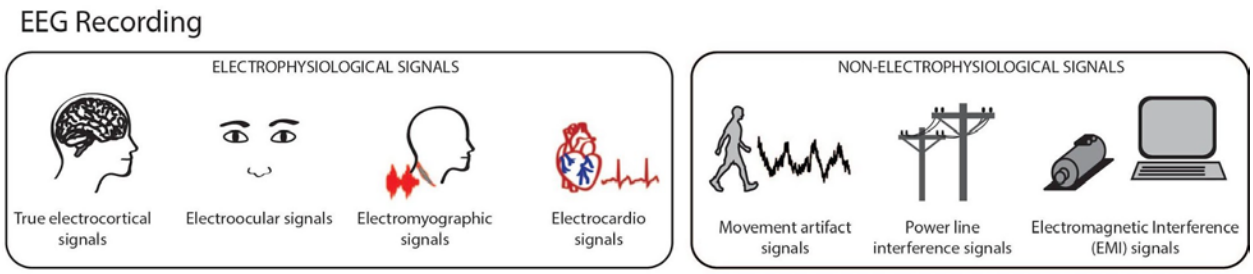
EEG Recording
ELECTROPHYSIOLOGICAL SIGNALS
True electrocortical signals
Electroocular signals
Electromyographic signals
Electrocardio signals
NON-ELECTROPHYSIOLOGICAL SIGNALS
Movement artifact signals
Power line interference signals
Electromagnetic Interference (EMI) signals

(b)

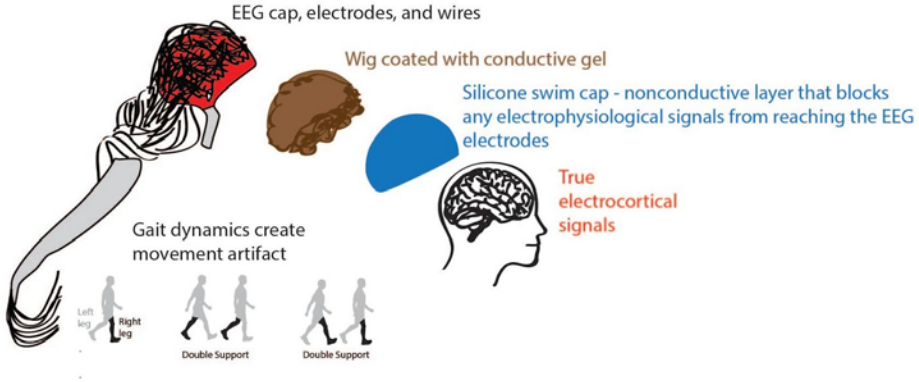
EEG cap, electrodes, and wires
Wig coated with conductive gel
Silicone swim cap - nonconductive layer that blocks any electrophysiological signals from reaching the EEG electrodes
True electrocortical signals
Gait dynamics create movement artifact
Left leg
Right leg
Double Support
Double Support

(c)

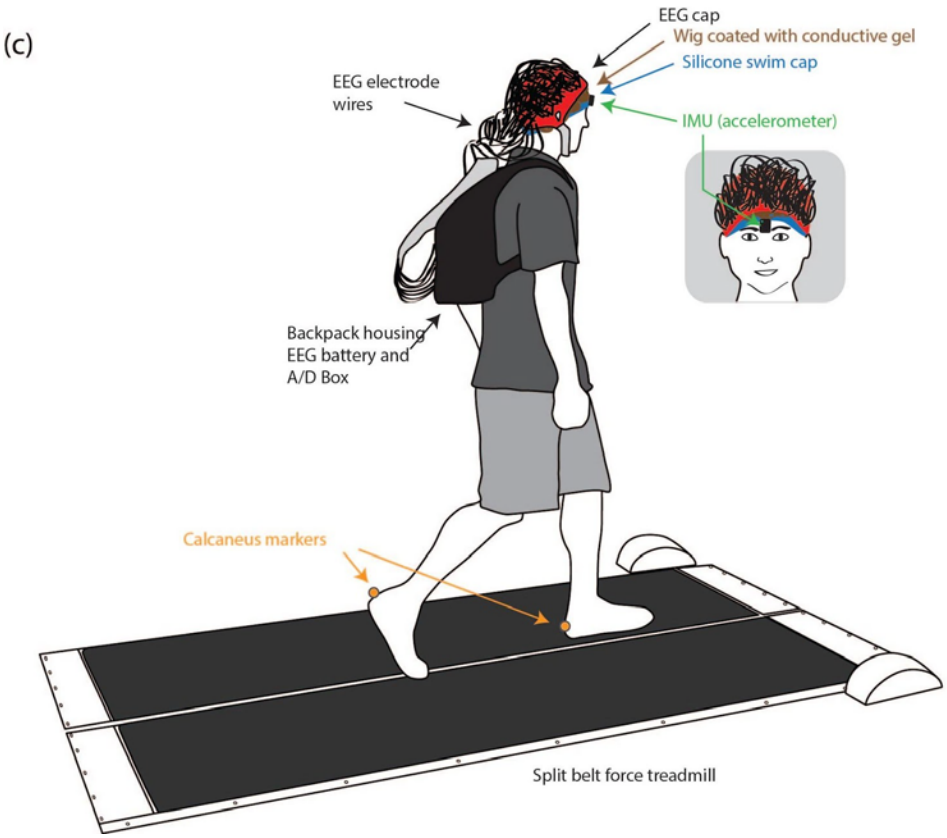
EEG cap
Wig coated with conductive gel
Silicone swim cap
EEG electrode wires
IMU (accelerometer)
Backpack housing EEG battery and A/D Box
Calcaneus markers
Split belt force treadmill

Figure 3-1. Experimental Setup. Conceptual schematic and experimental set up. a) All of the signals that contribute to scalp EEG recordings, categorized as electrophysiological or non-electrophysiological. b) Schematic of the methodological concept for isolating and measuring gait-induced movement artifact in EEG recordings. A silicone swim cap blocks true electrocortical signals while a simulated conductive scalp and a conductive wig allows the electrodes to measure voltage differences resulting from gait dynamics. c) Schematic of the experimental setup. Subjects walked at 4 speeds (0.4, 0.8, 1.2, and 1.6 m/s) on a custom split-belt force measuring treadmill. Trajectories of the calcaneus markers were recorded. An inertial measuring unit (IMU) with a tri-axial accelerometer placed on the forehead above the nose measured accelerations of the head during walking.

Subjects walked on a custom force treadmill at a range of speeds (0.4, 0.8, 1.2, 1.6 m/s) as we recorded movement artifact data, lower limb kinematics, and accelerations of the head (Figure 1C). Subjects walked at each speed for 10 minutes, and we randomized the order of the speeds. We also collected 10 minutes of sitting data at the beginning and end of the walking portion of the experiment. We used a ten-camera motion capture system (Vicon Nexus, Oxford, UK) to record kinematic trajectories of calcaneus markers, one on each foot. We recorded ground reaction forces for each lower limb as subjects walked. For the final six of the nine subjects, we used double-sided tape to place an inertial measuring unit (IMU) with a tri-axial accelerometer (The Opal, APDM, Inc., Portland, OR) on the subject's forehead along the midline of the nose and covered the accelerometer with an additional piece of tape (Figure 1C). We placed the accelerometer on the forehead in order to get the best estimate of the acceleration of the head without interfering with the movement artifact recorded in any of the EEG channels. We recorded 5 minutes of accelerometer data for each speed. The sampling frequencies were 512 Hz, 100 Hz, 1000 Hz, and 128 Hz for the EEG, motion capture, ground reaction force, and accelerometer data, respectively.

Data Analyses

We compared the time courses of the accelerometer data, ground reaction forces, and movement artifact signal. We first aligned all of the data to a common trigger, a square wave of a constant frequency sent simultaneously to the different recording systems. We smoothed the ground reaction forces using a moving average of a 50-ms time window.

To analyze the data with respect to the gait cycle, we used the calcaneus markers to identify gait events. We applied a 6 Hz low-pass Butterworth filter to smooth the kinematic data. The gait cycle consisted of the following gait events: initial left toe-off (LTO), left heel-strike (LHS), right toe-off (RTO), right heel-strike (RHS), and the subsequent left toe-off. Heel-strikes corresponded to the times of the troughs of the calcaneus marker vertical position and toe-offs corresponded to the times of the peaks of the calcaneus marker velocity in the vertical direction (Kline et al., 2014).

We processed the EEG movement artifact signals offline using customized MATLAB scripts and EEGLAB (Delorme and Makeig, 2004). We performed initial analyses using all of the electrodes, but eventually focused our analyses on 5 electrodes spatially distributed around the head at the front (E12), back (A19), left (G11), right (C18), and top center (A1). These positions are relative to a BioSemi 256 channel headcap (http://www.biosemi.com/headcap.htm). We high-pass filtered the movement artifact signals using a two-way least squares FIR filter with a cutoff frequency of 1 Hz to remove drift. We divided the data into epochs corresponding to gait cycles, time-locked to left toe-off. To be as consistent as possible with previous published studies, we re-referenced the data to the average of all 256 channels (Gwin et al., 2011;Sipp et al., 2013). We rejected epochs that were greater than 3 standard deviations from the means of the

gait event times. We then used the remaining epochs as the raw data that we included in further analyses.

We applied three movement artifact cleaning methods (discussed below) to the movement artifact data. For the uncleaned and the three cleaned data sets, we calculated changes in spectral power relative to baseline (event related spectral perturbations: ERSPs) according to Gwin et al. (Gwin et al., 2011). Briefly, this involved computing a spectrogram for each channel and epoch of data. We time-warped the spectrograms so that the gait events occurred at the same relative time within the gait cycle, to account for differences in absolute timing from stride to stride. We averaged the spectrograms for all epochs for the same channel and condition. To visualize power fluctuations about the baseline frequency spectrum, we subtracted the average frequency spectrum for the whole gait cycle from the frequency spectrum at each time point. We then averaged these ERSPs across all subjects (Makeig, 1993;Makeig et al., 2004a). We used bootstrapping methods available in EEGLAB (Delorme and Makeig, 2004) to determine regions of significant difference from baseline ($p < 0.05$).

Furthermore, we wanted to quantify how similar the ERSP plots were across subject, speed, and electrode location. An ERSP is a three dimensional matrix of time by frequency by power, with the power values representing a power change from baseline. We used the Matlab ‘corr’ function to compute a pairwise linear correlation coefficient for the power values for our ERSP comparisons (Tables 1-2). We focused our analyses on channel A1 and 1.2 m/s. Channel A1 in the BioSemi EEG system is comparable to Cz in a traditional 10-20 system, and is closest to the motor cortex, where we would expect there to be significant activity during walking in a true

EEG study. Preferred walking speed is consistently found to be 1.2-1.3 m/s, leading us to focus on 1.2 m/s, the closest walking speed to preferred that we collected.

Movement Artifact Cleaning Methods

We applied three potential artifact cleaning methods: 1) moving average, 2) wavelets, and 3) moving average + wavelets. The first artifact cleaning method we used was a moving average, outlined in (Gwin et al., 2010). For the moving average, we specified the number of time-warped strides to average before and after the current stride and the low-pass filter cutoff frequency to apply to the average stride data. We subtracted this low-pass filtered time-warped average stride data from the raw data for the current stride. We used 10 strides and a 10 Hz low-pass filter cutoff, based on (Gwin et al., 2010). We then detrended the data, as the moving average processing sometimes introduced a linear trend into the data. The second artifact cleaning method was wavelets. Using Daubechies 4 wavelets, we removed signal content at frequencies below 8 Hz and applied the wavelets to the whole stride. The third artifact cleaning method combined the moving average and wavelets. We first applied the moving average (10 strides, 10 Hz cutoff) and then the wavelet method (8 Hz over the whole stride). The moving average method occasionally introduced artifacts (<1% of the epochs). We identified epochs with values above a threshold of 100 μV and rejected them from all files to ensure that all artifact cleaning methods analyzed the same strides.

Accelerometer Analyses

We compared the movement artifact signals measured using the EEG system with the head accelerations in all three directions (vertical, mediolateral, and anterior-posterior) measured using an accelerometer placed on the forehead. We used a fast Fourier transform (FFT) to compute the frequency spectra of each measure for the entire length of the data (EEG frequency resolution: 0.0017 Hz, accelerometer frequency resolution: 0.0033 Hz). We downsampled the movement artifact data recorded with the EEG system to 128 Hz, to match the sampling frequency for the accelerometer. Because there is most likely a time lag between the movement artifact signals recorded in the EEG electrodes and the head acceleration, we calculated the cross-correlation between the time series of each head acceleration direction and each electrode channel. We used MATLAB's xcorr function to find the lag that corresponded with the maximum correlation for each combination of head acceleration direction and electrode channel (3 head acceleration directions x 256 EEG channels). Because the maximum correlations mostly occurred between the vertical head acceleration and movement artifact signals, we shifted the time series data by the lag that corresponded to the maximum correlation between the vertical head acceleration direction and each channel. The lag time used to align the movement artifact signal with the head acceleration was specific to each channel. We then performed a linear regression using the whole time series (~5 minutes) where an individual channel movement artifact signal was the response and all three head acceleration directions were predictors using MATLAB's fitlm function. We repeated this linear regression analysis for each electrode channel to determine how much of the variation in the movement artifact signal recorded by that specific EEG electrode was due to the accelerations. To examine time-frequency characteristics,

we also compared ERSPs for the accelerometer data with the ERSPs for the movement artifact data. To allow for fair comparison, we computed ERSPs for the accelerometer data using the same process described above for the movement artifact data.

Mastoid Experiment: Comparison of Data from Simulated Scalp Interface and Human Skin Interface

To verify that the electrode/simulated scalp interface was fundamentally similar to an electrode/human skin interface, we had one of our nine subjects return for an additional experiment (Figure 8(a)). To obtain movement artifact data for the electrode/simulated scalp interface, we set up the experiment as previously described using the silicone swim cap and wig coated with conductive gel. The subject walked on the treadmill for five minutes at 1.2 m/s while we collected movement artifact data on the simulated scalp interface. To obtain movement artifact data for an electrode/human skin interface, we placed one EEG electrode on the subject's left mastoid, a bony prominence known to have minimal electrophysiological signal. The BioSemi system uses two separate electrodes (common mode sense, CMS, electrode; driven right leg, DRL, electrode) to increase the common mode rejection ratio, instead of using a single ground electrode. There was not enough space on the subject's mastoid to place the EEG electrode and the two BioSemi reference electrodes. We therefore placed the BioSemi CMS reference electrode on the left mastoid, next to the EEG electrode we were recording from, and the DRL reference electrode on the right mastoid. The subject again walked for five minutes at 1.2 m/s while movement artifact data were recorded.

To determine if the two interfaces recorded movement artifact of a similar pattern and magnitude, we applied the ERSP analysis described above to both control datasets. For the electrode/simulated scalp data, we computed ERSP plots for the channels closest to the left mastoid, G21 and G22 (http://www.biosemi.com/headcap.htm). For the electrode/human skin data, we computed an ERSP plot for the electrode placed on the subject's mastoid. We used the correlation method described above to compute a measure of similarity between the simulated scalp and mastoid ERSPs.

Results

The EEG electrodes measured movement artifact waveforms that varied across speed and electrode location. Waveforms increased in amplitude as walking speed increased (Figure 2). At the slowest speed, little movement artifact was detected. At the fastest speed, the movement artifact waveforms were more evident. The movement artifact also varied between electrode locations (Figure 2).

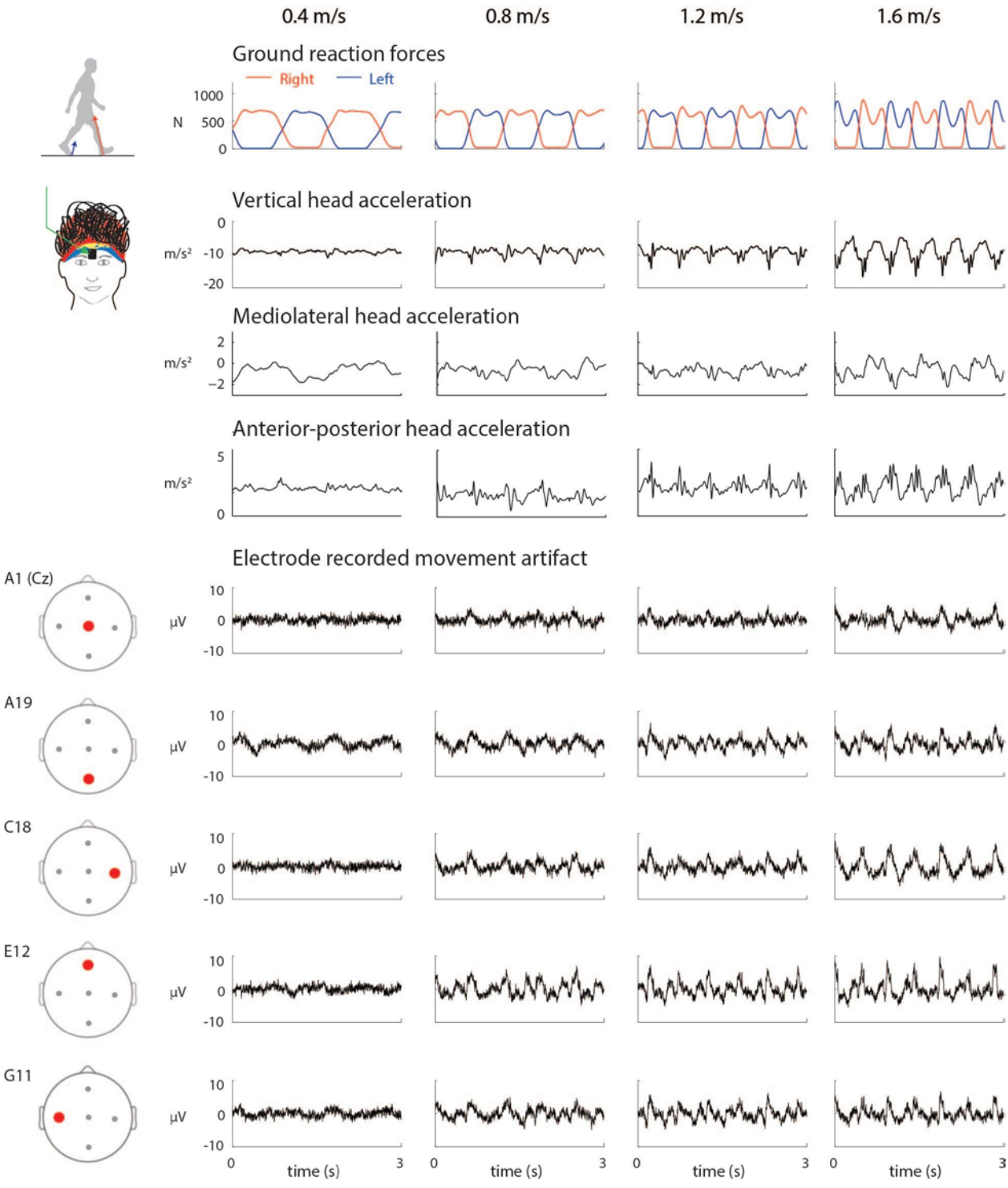

Figure 3-2. Time courses. Time courses of movement artifact and accelerometer data**.** Time courses of the ground reaction forces for the right and left legs, head accelerations (vertical, mediolateral, and anterior-posterior), and movement artifacts recorded in 5 electrodes (A1, A19, C18, E12, and G11) for the 4 walking speeds (0.4, 0.8, 1.2, and 1.6 m/s) for a single subject.

The time course waveforms of the head acceleration and movement artifact signals were different (Figure 2). During single support (when only one leg is in contact with the ground), there was typically a single peak in the accelerometer time series but multiple peaks and valleys in some of the electrode time series. The vertical accelerations of the head did not correlate well with the movement artifact signals measured by the electrodes (Figure 3). A phase space plot of the E12 electrode voltage versus the vertical head acceleration appeared to have no clear relationship across speeds (Figure 3(a)). The correlation coefficients were greatest for the vertical head acceleration and the movement artifact signals recorded in the EEG electrodes compared to the mediolateral and anterior-posterior accelerations (Figure 3(b)). At the normal walking speed (1.2 m/s), the average correlation coefficient was 0.35 ± 0.07 for the vertical, 0.14 ± 0.03 for the mediolateral, and 0.17 ± 0.04 for the anterior-posterior head accelerations. Additionally, the group average correlation coefficients increased with walking speed (Figure 3(b)). For the vertical direction, the average correlation coefficient was 0.18 ± 0.06, 0.37 ± 0.09, 0.35 ± 0.07, and 0.31 ± 0.08, from the slowest (0.4 m/s) to fastest (1.6 m/s) walking speed respectively. The linear regressions using the head accelerations in all three directions had an overall average R-squared of 14.3 ± 0.05, for the 5 primary channels we focused on, and across all speeds (Table 3). This indicates that the head accelerations only account for ~14% of the variance of the movement artifact signal recorded by the EEG electrodes.

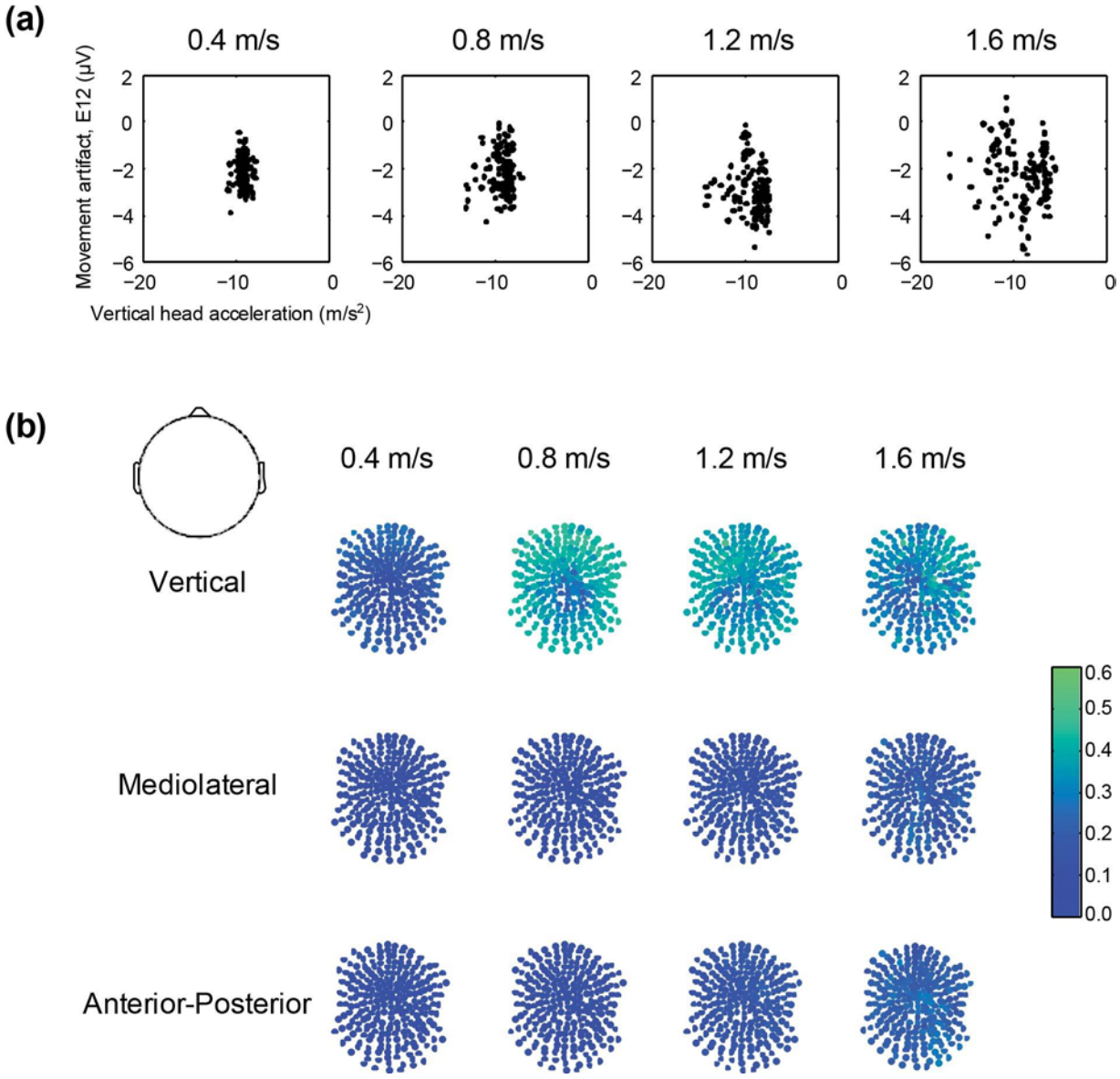

Figure 3-3. Correlations between Accelerometer and EEG. Correlations between accelerometer and the frontal electrode movement artifact. a) Vertical head acceleration was plotted against movement artifact recorded in the frontal electrode (E12) for a stride of data for a single subject (same data as in Figure 2). b) Correlation coefficients between all three head accelerations and each electrode recorded movement artifact signals were generally < 0.4. Dark blue represents uncorrelated signals, correlation coefficient = 0.0 and green equals a correlation coefficient of 0.6.

Table 3-3. Intersubject mean and standard deviation R-squared values for linear regressions. These values were calculated using all three acceleration directions as variables for each electrode channel and speed.

Speed	Top (A1, Cz)	Back (A19)	Right (C18)	Front (E12)	Left (G11)
0.4	4.8 ± 9.1	6.2 ± 7.7	9.6 ± 11.1	9.5 ± 13.3	3.9 ± 4.6
0.8	15.1 ± 13.6	14.0 ± 12.8	23.2 ± 13.4	21.9 ± 12.7	21.7 ± 10.5
1.2	16.4 ± 10.9	16.5 ± 9.8	17.8 ± 7.0	13.8 ± 4.6	19.6 ± 10.9
1.6	13.0 ± 8.3	12.9 ± 9.4	18.0 ± 13.5	11.9 ± 11.6	15.4 ± 10.0

Although there was some overlap, particularly for the lower frequencies, the frequency spectra for the accelerometer and the movement artifact data revealed spectral power harmonics at different frequencies and over different frequency ranges. (Figure 4). The accelerometer frequency spectra in the vertical direction had large peak amplitudes up to 20 Hz at the fastest walking speed. The movement artifact frequency spectra and accelerometer frequency spectra in the mediolateral and anterior-posterior directions had large peak amplitudes up to 10 Hz at the fastest walking speed. Movement artifact signal spectra amplitudes increased with faster walking speeds for the head accelerations in all three directions and all the electrodes.

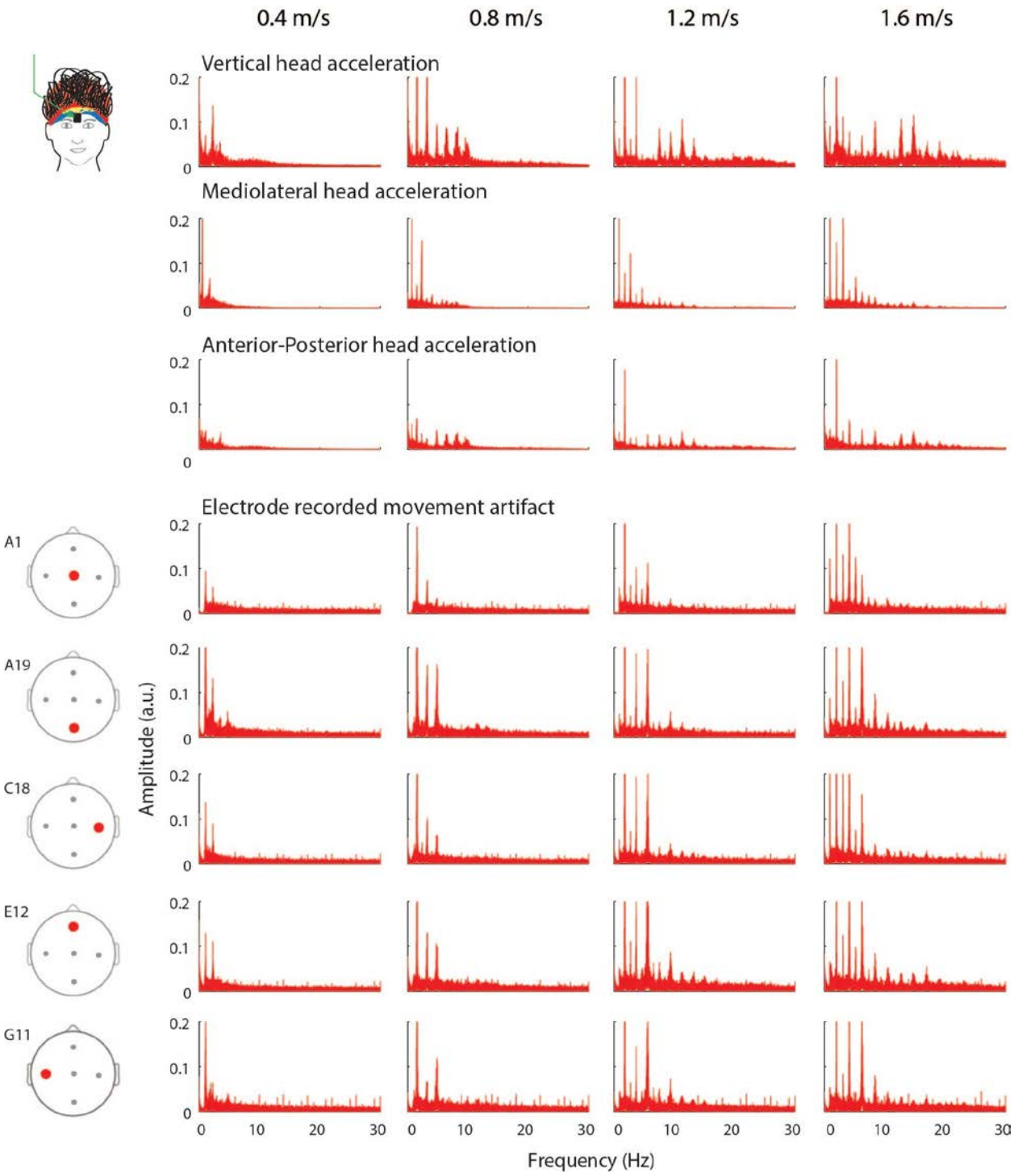

Figure 3-4. Accelerometer and EEG Spectra. Frequency spectra for the accelerometer and electrode movement artifacts. Frequency spectra of the head accelerations (vertical, mediolateral, and anterior-posterior) differed from the spectra of the electrode recorded movement artifacts (A1, A19, C18, E12, & G11). Each column is a walking speed, increasing from left to right.

There were different distinctive patterns of movement artifact in the individual subject ERSPs that varied across walking speeds (Figure 5, Table 1). The individual subject ERSPs highlighted that the movement artifact varied from subject to subject. As an example, we quantified the ERSP correlation coefficients across subjects for channel A1 at 1.2 m/s. Average correlation values were low (mean 0.09) and had a high standard deviation (0.11). These values indicated a high inter-subject variability. (For the raw data values, see Table 1 in the supplement). For many of the subjects, the pattern of spectral power change was variable across speeds. We quantified this variability by calculating correlation coefficients (Table 1), which revealed low correlation values when averaged across subjects. Individual subject ERSPs consistently indicated that the magnitude of the movement artifact and the maximum frequency at which it occurred increased with increasing walking speed. The individual subject ERSPs for the vertical head acceleration showed broadband spectral fluctuations, which were not consistently observed in the movement artifact ERSPs for all subjects and speeds (Figure 5).

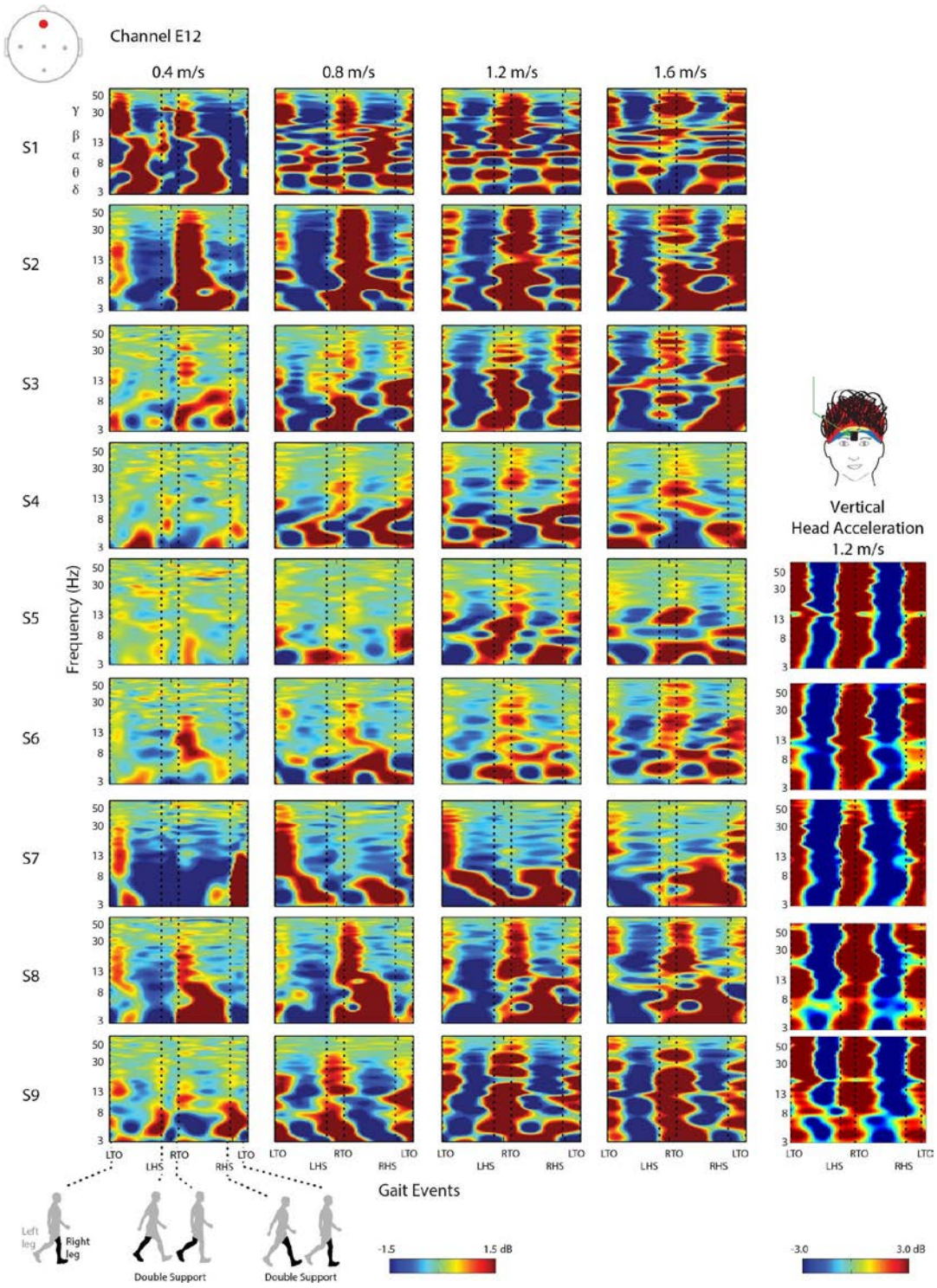

Figure 3-5. Individual ERSPs. ERSP plots for individual subjects for both the head mounted accelerometer and channel A1. ERSP plots for individual subjects at channel A1 reveal inter-subject variability in the movement artifact data. ERSP plots of individual subject accelerometer

data show that an accelerometer captures less inter-subject variation. Each row is a subject and each column is a walking speed, increasing from left to right. Red represents a power increase from baseline, and blue represents a power decrease from baseline. The x-axis is one gait cycle: left toe-off (LTO), left heel-strike (LHS), right toe-off (RTO), right heel-strike (RHS), and left toe-off again. Double support occurs between the dotted lines of LHS and RTO and between RHS and LTO. Note the different y axes and color bar power scales.

Table 3-1. Mean ERSP correlation ± standard deviation across speeds for all nine subjects at channel A1.

	0.4 m/s	0.8 m/s	1.2 m/s	1.6 m/s
0.4 m/s	1	0.25 ± 0.13	0.02 ± 0.15	0.19 ± 0.16
0.8 m/s		1	0.08 ± 0.09	-0.04 ± 0.19
1.2 m/s			1	0.04 ± 0.12
1.6 m/s				1

Additionally, the ERSPs for the different electrode locations showed different patterns of movement artifact, which also varied across walking speed (Figure 6, Tables 1 and 2). Depending on the electrode location, the movement artifact differed, particularly with respect to the magnitude. The midline electrodes (A1, A19, & E12) generally recorded larger movement artifacts than the lateral electrodes (C18 & G11) (Figure 6). Based on the magnitude of the fluctuations in the ERSPs, the electrode on the front of the head (E12) was the most susceptible to movement artifacts compared with the other electrodes.

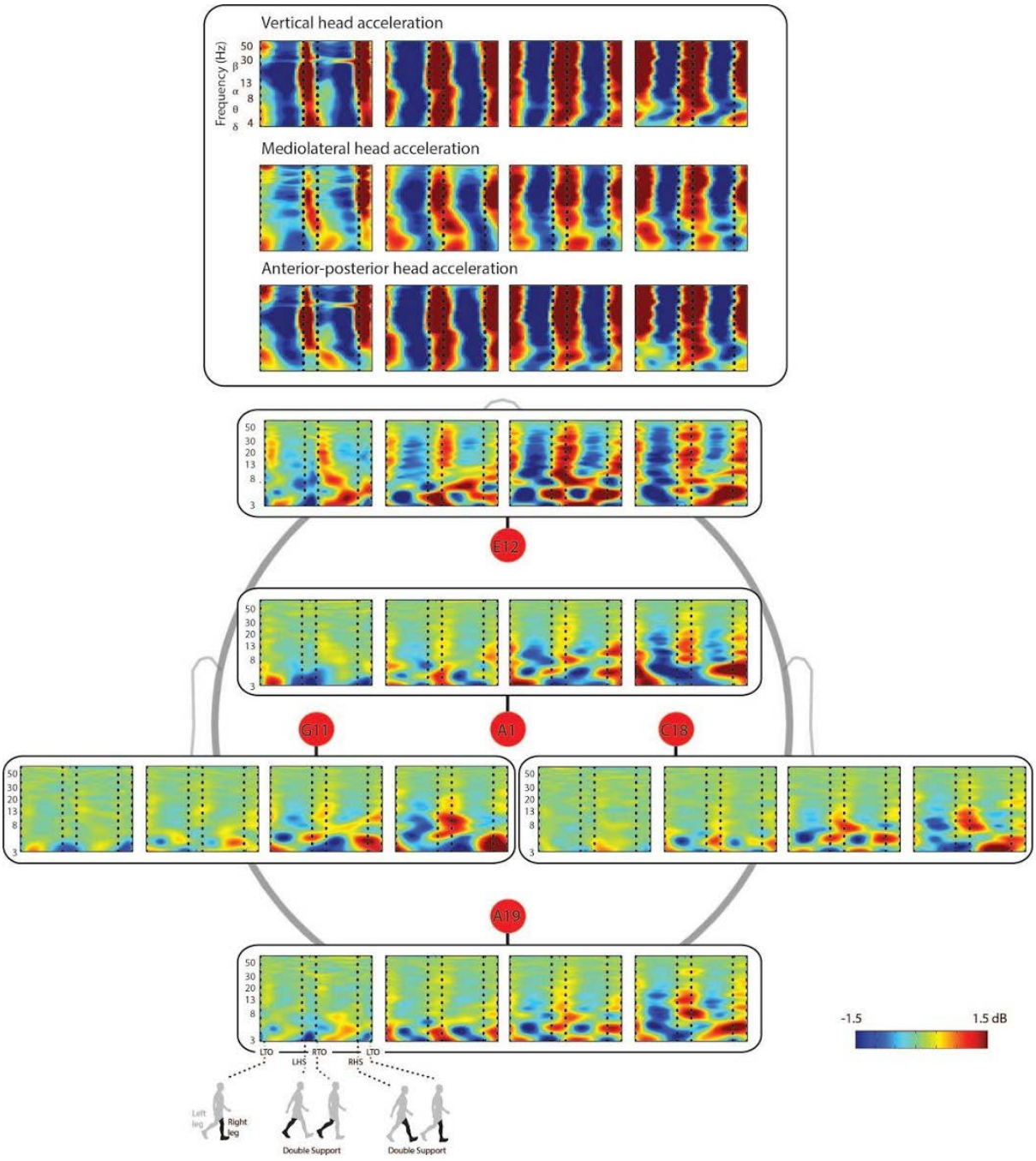

Figure 3-6. Group Averaged ERSPs. Group averaged ERSP plots oriented with respect to the head. ERSPs for the head accelerations in all three directions (vertical, mediolateral, and anterior-posterior) showed similar broadband synchronization and desynchronization patterns. ERSPs of the electrode-recorded movement artifact plotted spatially illustrate that midline electrodes (A1, A19, & E12), particularly in the front of the head (E12), were more susceptible to movement artifacts than lateral electrodes (C18 & G11). Red represents a power increase from baseline, and blue represents a power decrease from baseline. Each plot for each electrode is a

walking speed, increasing from left to right. The x-axis is one gait cycle: left toe-off (LTO), left heel-strike (LHS), right toe-off (RTO), right heel-strike (RHS), and left toe-off again. Double support occurs between the dotted lines of LHS and RTO and between RHS and LTO.

Table 3-2. Mean ERSP correlation ± standard deviation across channels for all nine subjects at 1.2 m/s.

	A1	A19	C18	E12	G11
A1	1	0.47 ± 0.35	0.28 ± 0.34	0.38 ± 0.35	0.47 ±0.33
A19		1	0.53 ± 0.25	0.46 ± 0.38	0.43 ± 0.34
C18			1	0.41 ± 0.32	0.16 ± 0.28
E12				1	0.42 ± 0.29
G11					1

There were some consistent patterns across speeds in the ERSPs for individual subjects (Figure 5) and for different electrodes (Figure 6). During the double support period (when both legs are in contact with the ground), there tended to be synchronization in the 8-30 Hz range at the fastest speed (1.6 m/s). At the slowest speed (0.4 m/s), double support tended to show a desynchronization in the 4-7 Hz range. In contrast, during the single support period, there was typically a strong desynchronization at the fastest speeds and a slight desynchronization at the slower speeds. However, correlation coefficient values reveal that these patterns are not completely consistent across all subjects and electrode locations (Tables 1 and 2). The mean

ERSP were most highly correlated for the two lowest speeds, 0.4 and 0.8 m/s. However, significant changes in pattern occurred from the slowest to the fastest speed, as evidenced by both the ERSPs and correlation values. Additionally, ERSPs for the accelerometer data in all three directions showed broadband synchronization and desynchronization, in contrast to the ERSPs for the movement artifact (Figure 6).

The moving average, wavelet, and moving average + wavelet cleaning methods attenuated but did not remove all movement artifacts (Figure 7). We found that the cleaning methods had some success attenuating low-frequency, gait-related movement artifact at the slowest speed. Though the moving average and wavelet methods seemed to perform similarly, the combination of both seemingly had modest improvements over either method alone at these slower speeds. However, there was little quantitative difference between the two methods. At the fastest speeds, none of the cleaning methods we examined had much success attenuating the stride-locked movement artifact.

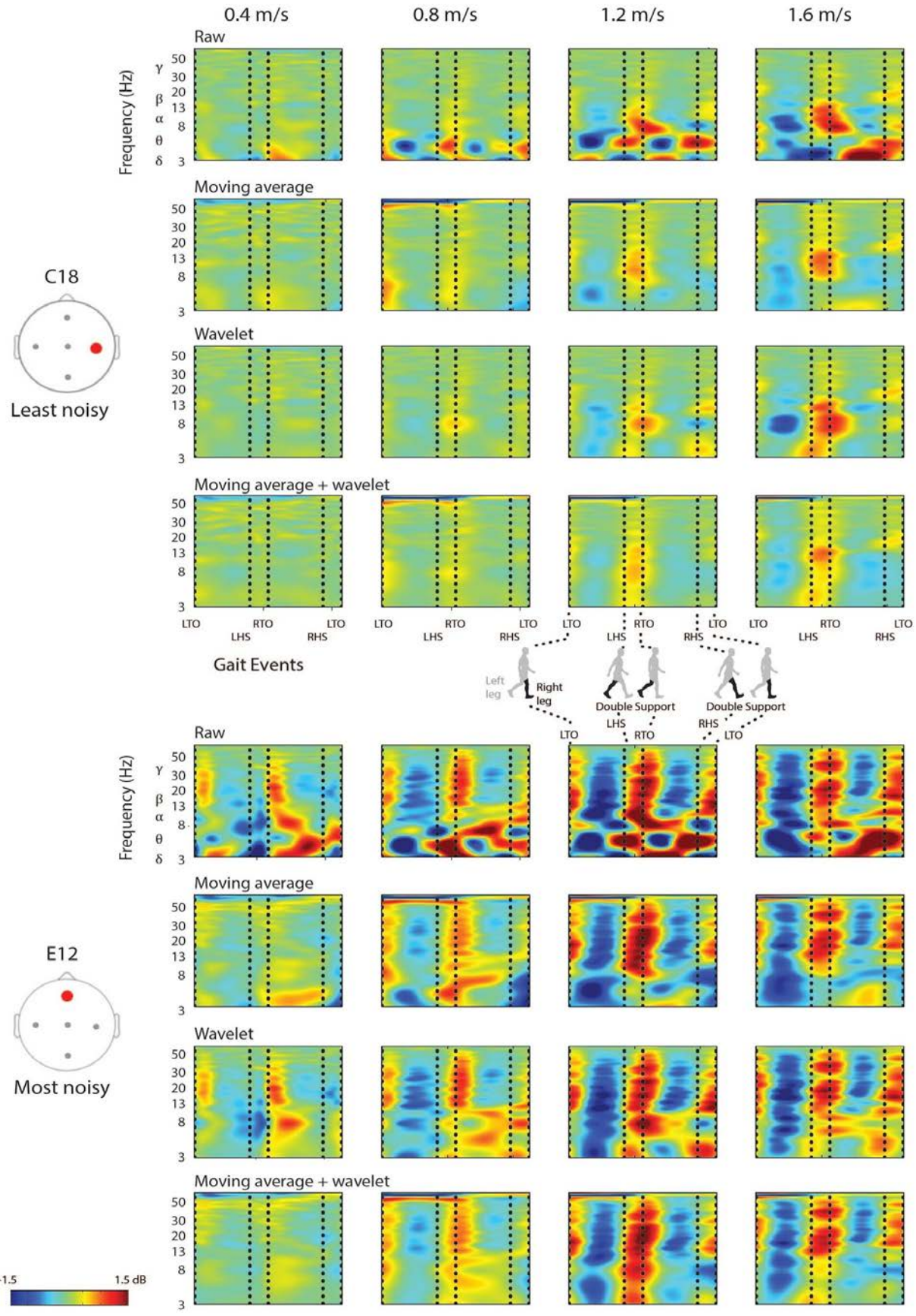
0.4 m/s
0.8 m/s
1.2 m/s
1.6 m/s
Raw
Moving average
Wavelet
Moving average + wavelet
Frequency (Hz)
γ
β
α
θ
δ
50
30
20
13
8
3
C18
Least noisy
LTO
RTO
LHS
RHS
Gait Events
Left leg
Right leg
Double Support
E12
Most noisy
-1.5
1.5 dB

Figure 3-7. Group averaged cleaned ERSPs. Group averaged ERSP plots of the moving average, wavelet, and moving average + wavelet cleaning methods reveal that movement artifact remained despite cleaning. The cleaning results for the least noisy (C18) and most noisy (E12) channels are shown. Each row is a cleaning method and each column is a walking speed, increasing from left to right. Red represents a power increase from baseline, and blue represents a power decrease from baseline. The x-axis is one gait cycle: left toe-off (LTO), left heel-strike (LHS), right toe-off (RTO), right heel-strike (RHS), and left toe-off again. Double support occurs between the dotted lines of LHS and RTO and between RHS and LTO.

Mastoid data comparison

The ERSPs from the mastoid experiment indicated that EEG electrodes placed on the simulated scalp interface recorded movement artifact of a similar pattern and magnitude as EEG electrodes placed on human skin (Figure 8B). The mastoid ERSP and the ERSPs for channels G21 and G22 on the simulated scalp showed similar movement artifact magnitude and timing in all but the highest frequencies. The correlation coefficients for the mastoid ERSP and the ERSPs for channels G21 and G22 were 0.54 and 0.57, respectively.

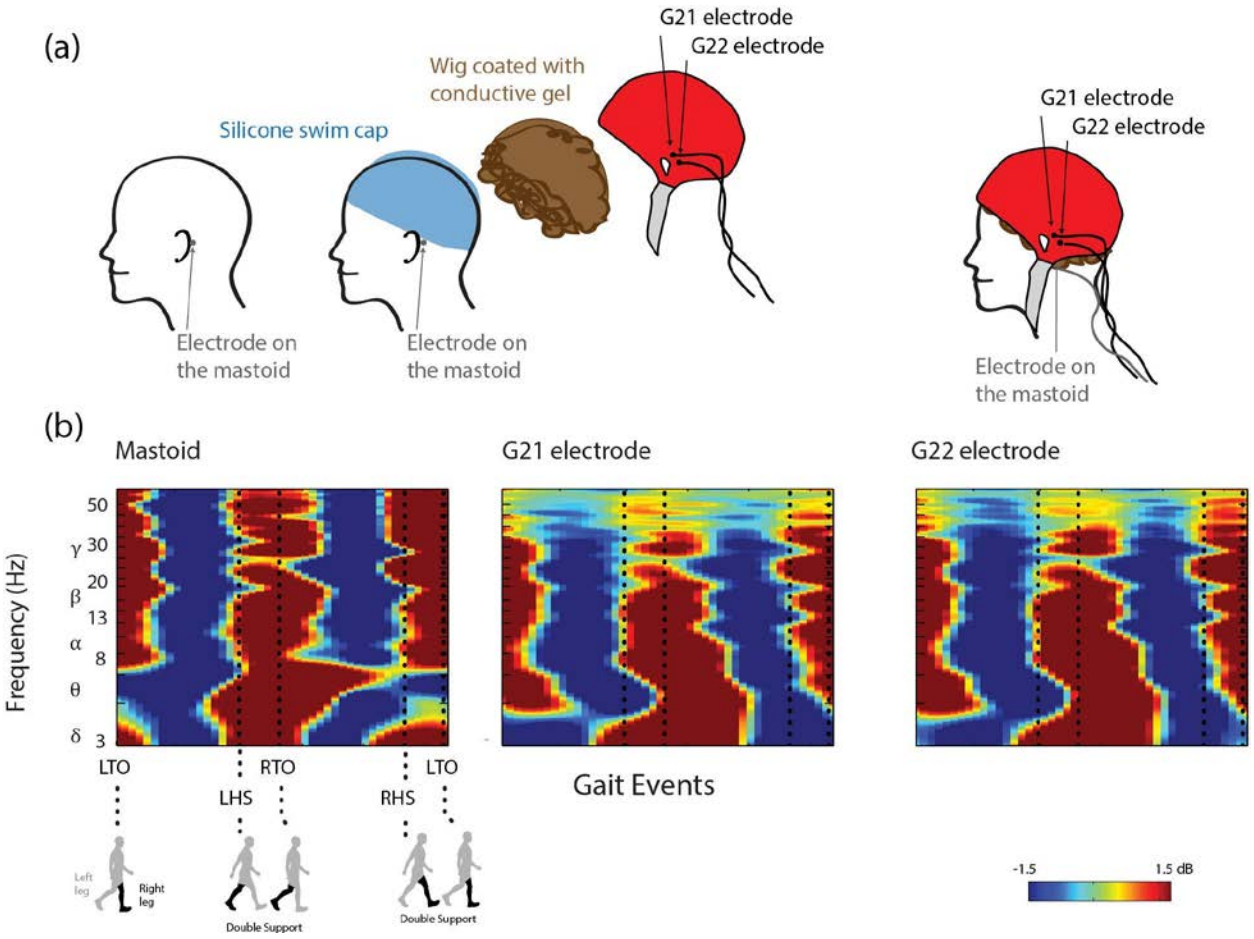

Figure 3-8. Mastoid ERSP. Schematic of the setup and ERSP plots for the mastoid experiment. **a)** To examine the electrode/human skin interface, an electrode was placed on the left mastoid underneath the swim cap. To examine the electrode/simulated scalp interface, the two electrodes closest to the left mastoid, G21 and G22, were used to measure movement artifact from the simulated scalp comprised of the wig coated with conductive gel placed over the swim cap. **b)** ERSP plots for the mastoid, G21, and G22 electrodes show similar broadband spectral fluctuations between 3-64 Hz.

Discussion

The main finding of the study was that movement artifact patterns recorded in EEG electrodes during walking had large spectral fluctuations over the gait cycle that increased in amplitude as walking speed increased. As speed increased, not only did the amplitude of the spectral fluctuations increase, but the spectral fluctuations appeared in higher frequency bands. Another

important finding was that the movement artifact patterns recorded by the EEG electrodes varied substantially across subjects and among electrodes located at different areas of the head. We applied some simple cleaning methods, moving average and wavelets, to the artifact data, but these cleaning methods were insufficient to remove all movement artifact. A third key finding of the study was that data from an accelerometer placed on the forehead had poor correlation with the movement artifact recorded by the EEG electrodes. There were substantially different spectral fluctuations between the EEG electrode data and the accelerometer data, however there were some similarities. Above 0.4 m/s the artifact spectral fluctuations were similar to the accelerometer spectral changes at 8-30 Hz for some subjects, but the timing was slightly shifted. Altogether, our findings highlight and quantify limitations in current EEG techniques and data cleaning methods. New approaches need to be developed to account for movement artifact patterns, especially at faster walking speeds, that affect EEG electrode data in order to improve interpretation of electrocortical activity during human locomotion.

Several past studies have found spectral power increases during double support and spectral power decreases during single support at alpha and beta frequencies of scalp EEG at normal walking speeds, 0.78-1.25 m/s (Gwin et al., 2011;Cheron et al., 2012;Severens et al., 2012). These fluctuations have been reported to be caused by neural activity. Our pure movement artifact data, which contains no neural activity, also found that some subjects showed increased spectral power during double support and decreased spectral power during single support at faster walking speeds. This suggests that the spectral fluctuations reported in the previous studies reflect a combination of neural activity and movement artifact. Some studies conducted at faster walking speeds may have reported relatively little neural activity compared to artifact. Other studies at slower walking speeds, 0.22-0.60 m/s, have shown some increases in spectral power

during double support in alpha and beta frequencies as well (Wagner et al., 2012;Sipp et al., 2013). However, the magnitude and duration of the increased spectral power at double support in our artifact data appears to be reduced substantially for the slower walking speeds. EEG data recorded at slower speeds are less likely to be contaminated with movement artifacts, especially in the higher frequency bands. Though using slower walking speeds may minimize movement artifact, it may also fundamentally change the motor task from rhythmic walking to a discrete stepping task, and so may limit the conclusions that may be drawn from such a study. Future studies may have to balance minimizing movement artifact with using speeds that are fast enough to be representative of typical human walking.

Simple cleaning methods do not appear to sufficiently attenuate movement artifacts in EEG collected at fast walking speeds. We tested a moving average artifact template that had successfully reduced EEG movement artifact in a study of non-gait related cognitive events during walking and running (Gwin et al., 2010). We also tested Daubechies wavelets as a means to identify and remove low frequency artifact. We chose Daubechies wavelets based on their previous usage in EEG studies to identify low frequency spectral fluctuations (Daubechies, 1988;Adeli et al., 2003). Both the moving average and wavelet artifact cleaning methods performed similarly in our study, but substantial movement artifacts remained at faster speeds (Figure 7). Consistent with previous results, the moving average worked well for removing artifacts that had a consistent pattern across occurrences (Chowdhury et al., 2014). Because stride to stride changes in movement patterns lead to differences in movement artifact, this cleaning method could only remove the noise that was consistent from stride to stride. In addition to the results presented, we also tested other values of stride numbers (±3 strides) and filter cutoff frequencies (30 Hz) for the moving average template. There were no noticeable

differences between the other values tested and the ones used for the current figures. The moving average template did tend to exacerbate electrical line noise (60 Hz) (Figure 7). The wavelet filter was less computationally expensive but eliminated almost all information below a given frequency (Figure 7). As a result, wavelets are not useful for targeting gait-related movement artifact and retaining low frequency electrocortical activity.

EEG studies that use cognitive tasks that are not synchronized to the gait cycle are much less likely to have data interpretation affected by movement artifacts. For example, using a visual oddball task or another cognitive task that is not synchronized to the gait cycle allows for any movement related artifacts (and true electrocortical activity synchronized to the gait cycle) to wash out over a large number of cognitive events (Gramann et al., 2010;Gwin et al., 2010;Kline et al., 2014). For future research examining electrocortical activity during human locomotion, it would be beneficial to include a repetitive cognitive event non-synchronized to the gait cycle for analysis of EEG data.

Our results indicate that an accelerometer does not record the same movement artifact signal that EEG electrodes record. Past studies have used accelerometers to measure movement artifacts in non-ambulatory tasks such as nodding and shaking of the head (Sweeney et al., 2010;O'Regan et al., 2013;O'Regan and Marnane, 2013). More recently, Castermans et al. used head-mounted accelerometers during walking and found patterns of synchronization and desynchronization in the data, especially at faster walking speeds (Castermans et al., 2014). Our results showed that movement patterns varied substantially across speed, subject, and electrode placement. There was greater complexity and variation than could be described by the simple patterns of desynchronization and synchronization found in accelerometer data. We also found that the

accelerometer data did not correlate well with the movement artifact data recorded by our simulated scalp electrodes. Small movement differences between the accelerometer, the electrodes, and their respective wires may contribute to the differences between the movement artifact in the accelerometer data and electrode data. Even with a wireless EEG system, it is possible that the relative motion of the electrodes to the scalp could still generate movement artifacts. The electrodes likely move side-to-side and up-and-down relative to the scalp or simulated scalp, which may lead to voltage drops. Passive electrodes are more susceptible to sudden changes in impedance and capacitance that can lead to sudden changes in voltage. Active electrodes like the ones used in this study may be less susceptible to sudden changes in voltage because active electrodes likely have more stable impedances, which can be observed in real-time in the Biosemi software program as stable voltage offset values.

Although our simulated scalp does not have exactly the same mechanical properties of real human scalp, the comparison of mastoid data and simulated scalp data suggests that it is close enough to capture similar movement artifact waveforms (Figure 8). The two sets of ERSPs are strongly correlated. However, there are substantive differences between the mastoid ERSPs and simulated scalp ERSPs at higher frequencies. The hair fibers of the wig likely provided some damping effect on the movement of the electrode. This could have attenuated the movement artifact recorded by the simulated scalp electrodes at the highest frequencies.

The most accurate approach for recording movement artifact signals in EEG may be to block the electrophysiological signals in some electrodes during data collection so that those electrodes record only the movement artifact. An EEG system that simultaneously measured movement artifact and movement artifact plus neural signal would allow for an interpolative subtraction

process that could remove the movement artifact in real-time. This method would not need to rely on data averaged over time and might even be able to be employed in an ongoing basis during data collection. Movement artifact subtraction performed in real-time would advance mobile brain imaging and brain-computer interfaces substantially compared to the current status quo. An interpolative subtraction process would be useful when recording EEG during any full body movement where substantial artifacts occur, including with patient populations with spasticity or other movement disorders.

Chowdury et al. recently explored the possibility of using an interpolative subtraction process to attenuate magnetic resonance imaging (MRI) noise from EEG recordings. They used a reference layer with similar conductivity to the human head to allow subtraction of movement-related and MRI-related artifacts during simultaneous EEG-fMRI recordings (Chowdhury et al., 2014). They explored only small (≤7 mm) head movements rather than larger head movements that are more characteristic of human gait. Their reference layer consisted of an agar, water, and sodium mixture that was not very durable. This idea has potential for separating movement artifact from EEG signals in walking, but further work needs to be done to modify the approach for walking applications.

Our study had a few limitations that prevent us from drawing broader conclusions about the relationship between movement artifact and EEG data recordings. First, there was substantial inter-subject variability in the movement artifact signal. This inter-subject variability may have been due to individual gait patterns, electrode cap fit, and/or differences in the preparation of the wig set up for each subject. There was also variability across subjects in head shape, head size, and hair characteristics. All of these head and hair properties could have led to differences in

pressure between the electrodes and the scalp. In our preparation, the swim cap did not lay perfectly smooth over the subject's head. This swim cap effect may also have contributed to the variability we observed across subjects and electrodes. Additionally, our conductive wig preparation had resistances greater than the resistances reported for dry skin. Designing a conductive scalp with resistive properties that more closely match actual scalp may improve the quality of the isolated movement artifact recorded in the EEG electrodes. Despite these limitations, this simple method for isolating and measuring the movement artifact recorded in the EEG electrodes seems to be promising for capturing gait-induced movement artifacts in EEG.

Conclusion

The relative amounts of true electrocortical signal and movement artifact in scalp EEG collected during human locomotion is difficult to determine. We created a novel approach for isolating pure movement artifact with EEG electrodes. The results from our simulated scalp protocol indicate that gait-related movement artifact can have varying magnitudes and patterns across subjects, conditions, electrodes, and strides. These differences are more complex than can be captured merely by accelerometry or eliminated by simple artifact cleaning techniques. The similar patterns of spectral fluctuation in our purely artifactual data and in previous studies of neural activity during walking suggest that the results of those studies need to be interpreted with caution. One possibility for future studies is to simultaneously measure movement artifact so that it can be characterized and removed from the neural data recorded by EEG. Ultimately, designing more sophisticated techniques that target gait-related artifact for individual strides would allow for more complete gait-related movement artifact attenuation in EEG recordings

during walking, which could greatly improve brain-machine interfaces and neurorehabilitation technologies.

Supplementary Materials

Supplementary Table 3-1. ERSP correlations across subjects for channel A1 at 1.2 m/s.

	1	2	3	4	5	6	7	8	9
1	1	0.59	0.12	0.28	-0.03	-0.06	0.07	0.02	0.23
2		1	0.27	0.39	-0.10	-0.03	0.10	0.27	0.47
3			1	0.33	-0.09	-0.07	-0.30	0.30	0.24
4				1	0.19	0.10	0.36	0.48	0.16
5					1	-0.15	0.39	0.04	0.04
6						1	0.21	-0.19	0.01
7							1	0.07	0.21
8								1	0.06
9									1

Chapter 4: Cortical Spectral Activity and Connectivity during Active and Viewed Arm and Leg Movement

Introduction

An interesting feature of cortical control of human movements is that active movement and viewed movement recruit many of the same neural structures in the human brain (Prinz, 1997). "Mirror neurons," which fire in response to both active and viewed movements were first discovered in monkeys (di Pellegrino et al., 1992). Since then, a slew of neuroimaging studies have confirmed that a similar neural mechanism exists in humans. Electroencephalography (EEG) studies have demonstrated desynchronization in the human motor cortex during both active and viewed movement (Cochin et al., 1998;Cochin et al., 1999;Calmels et al., 2006;Avanzini et al., 2012;Cevallos et al., 2015). Studies with functional magnetic resonance imaging (fMRI) have found overlapping cortical activation during active and viewed movement (Iacoboni et al., 1999;Buccino et al., 2001;Grezes et al., 2003;Manthey et al., 2003).

Because of the overlap in cortical recruitment for both active and viewed movement, some scientists have suggested that action observation could improve motor rehabilitation in patients with chronic stroke, Parkinson's disease, or cerebral palsy (Buccino, 2014). In adults with upper-limb impairment following a stroke, significant improvements in functionality were seen after eighteen consecutive days of action observation therapy (Ertelt et al., 2007). In children with cerebral palsy, a similar duration of action observation therapy increased spontaneous use of the

affected hand (Buccino et al., 2012). Given the potential therapeutic benefits of viewed movement, knowledge of the differences in cortical connectivity during active and viewed movement could provide insight for rehabilitation after a brain injury. It might also suggest potential rehabilitation targets accessible through transcranial magnetic stimulation.

Human locomotion likely involves a distribution of cortical and spinal control, which may affect the potential benefits of viewing locomotion. Humans regularly coordinate arm and leg movements during locomotion or locomotion-like movements. In quadrupedal animals, the coordination of rhythmic limb behaviors relies heavily on collections of oscillatory neurons in the spinal cord, known as central pattern generators (Brown, 1914;Grillner, 1975;Grillner et al., 1995;Marder and Calabrese, 1996;Duysens and Van de Crommert, 1998;Juvin et al., 2005;Rossignol et al., 2006). In humans, rhythmic limb movement likely depends on a combination of cortical and spinal control. Functional near infrared spectroscopy studies (Miyai et al., 2001;Harada et al., 2009) and electroencephalography (EEG) studies (Gwin et al., 2011;Severens et al., 2012;Sipp et al., 2013) have shown cortical activation during human steady-state walking. There is also indirect evidence for central pattern generators in humans. This evidence includes primitive stepping-like motions in infants (Yang et al., 2005), rhythmic lower limb contractions in a patient with a complete spinal cord injury when the limbs are moved through the motion of gait (Wernig and Phys, 1992;Dobkin et al., 1995), and vibration-induced air stepping in healthy subjects (Isaev et al., 2004). Because humans likely share features of quadrupedal neural control but have adapted to become predominantly bipedal, there may be differences in the relative contributions of cortical and spinal control during rhythmic movement involving the arms and legs.

One way to examine cortical control is to use effective connectivity to find the causal relationship between brain regions. Positron emission tomography (Cabeza et al., 1997;Rosenbaum et al., 2010) and fMRI (Biswal et al., 1995;Greicius et al., 2003;Kiran et al., 2015) are frequently used to study effective connectivity. However, these modalities require participants to remain stationary and therefore cannot examine brain connectivity during unconstrained full-body motion. Another approach for studying real-world activities is to use high-density EEG, independent component analysis (ICA), and source localization techniques (Gwin et al., 2010;Gramann et al., 2011;Gwin et al., 2011;Sipp et al., 2013;Kline et al., 2014). Although this EEG approach does not have the spatial resolution of fMRI connectivity studies, it does provide excellent temporal resolution with spatial resolution of around 1 cm (Mullen et al., 2011). Lau and colleagues combined high-density EEG, ICA, and source localization with Granger causality to show that sensorimotor cortical connectivity was greater for standing compared to walking (Lau et al., 2012). Using a similar approach may provide additional insight into brain function as it relates to active and viewed movement.

The overall purpose of this study was to quantify the differences in cortical spectral fluctuations and effective connectivity during active and viewed rhythmic limb movements. Our overall hypothesis was that we would be able to detect similar but weaker electrocortical spectral fluctuations and effective connectivity during viewed limb movement compared to active limb movement due to the similarities in neural recruitment. We tested different combinations of arm and leg movements (arms and legs, legs only, and arms only), because we hypothesized that active rhythmic legs only movements would show little spectral fluctuations based on evidence that suggests that rhythmic leg movements likely use spinal control (Sakamoto et al.,

2007;Sakamoto et al., 2014). Additionally, some have suggested that the mirror neuron system is highly involved in human social interaction (Gallese et al., 2004;Oberman et al., 2007). Therefore, humans may have differences in cortical activity when viewing themselves compared to viewing someone else perform a movement. If there are indeed differences in electrocortical spectral fluctuations for different combinations of active arms and legs movements or viewing perspective, we hypothesized that there would also be similar relative differences in effective connectivity for viewing those arm and leg movements. To test these hypotheses, we had subjects perform different combinations of arm and leg rhythmic movements on a recumbent stepper while we videotaped them. The subjects later viewed video playback of themselves and another individual performing the movements. We recorded EEG data for all conditions.

Materials and Methods

Subjects and experimental setup

Ten healthy adults (mean age 25.6 ± 4.4, 5 females) with no history of neurological disease or musculoskeletal injuries participated in this study. All participants signed a consent form approved by the University of Michigan Institutional Review Board.

We used a customized recumbent stepping machine (TRS 4000, NuStep, Ann Arbor, MI) with an adjustable level of resistance and an isokinetic motor (Huang et al. 2009). The stepping machine combined features of a stair stepper and a recumbent bicycle. The handles and pedals were coupled so that the left handle and right pedal moved together.

Before data collection, we fitted the subjects with a 256-channel EEG cap (Biosemi ActiveTwo, Amsterdam, The Netherlands). We digitized the position of each electrode relative to the subject's head using a digitizer (Zebris, Germany). All electrode offsets were <20 mV. We recorded EEG data at 512 Hz for all conditions.

Subjects initially practiced stepping on the device at a range of resistances. We set the resistance to a level that the subjects deemed challenging but not uncomfortable. We secured a Velcro strap around the subject's midsection to minimize torso movement and strapped the subject's feet to the pedals (they remained strapped to the pedals for the two active leg conditions). We placed the EEG amplifier on a platform directly behind the subject and draped the electrode leads over a bar (Figure 1). Directly in front of the subject, we placed a large mirror (79 cm X 168 cm). A screen above the mirror displayed visual cues that set the pace of the movement. We mounted a video camera at the subject's eye level, approximately six inches to the left of the head, pointed at the mirror. This allowed us to record videos of the subject exercising from the subject's viewpoint.

Data Collection

The subjects performed rhythmic arm and leg movement on the device (active conditions) and then sat quietly and viewed video playbacks of themselves and another individual performing the same movements (viewed conditions). During the active conditions, we also recorded position data based on the motor position signal of the recumbent stepper. (The maximum motor position signal corresponded to the right pedal being fully extended). We synchronized the data streams using a square wave of constant frequency sent simultaneously to all recording systems.

The subjects moved on the device in three different ways in the following order: 1) with both their arms and their legs, 2) with their legs only, and 3) with their arms only. During the legs only condition, the subjects moved with their hands folded comfortably in their lap. During the arms only condition, the subjects moved with their feet resting on the floor, or on foot rests for shorter subjects.

The visual cues paced the subjects to moved at 70 arm or leg extensions per minute. The cues consisted of a pair of squares at opposite sides of a central fixation point. The squares shaded from white to black at a fixed rate (1.16 Hz) and were 180 degrees out of phase with each other. The subjects kept their eyes on the fixation point and moved so that the corresponding limb was fully-extended when the left or right square turned black. For the combined arms and legs condition, legs were given precedent, and the subjects moved so that the corresponding leg was fully extended when a square turned black. The subjects were allowed to practice exercising in synchrony with the cues as needed. We recorded a five minute video of the subject exercising, as seen in the mirror, during each active condition.

During the viewed conditions, we removed the mirror that had been in front of a video projection screen (84 cm X 165 cm) (Figure 1). On the screen, we then played a total of seven five-minute videos to the subject in a randomized order. The videos were: 1) playback of the subject exercising with both their arms and legs, 2) playback of the subject exercising with their legs only, 3) playback of the subject exercising with their arms only, 4-6) pre-recorded videos of another individual exercising in the three ways described above, 7) a control video of the recumbent stepper moving on its own, with no one seated in it. The video playback was adjusted to be life-size. During the

viewed conditions, we gave the subjects a fixation point on the center of the screen, roughly at the center of the torso of the individual in the video, to prevent large eye movements during viewing.

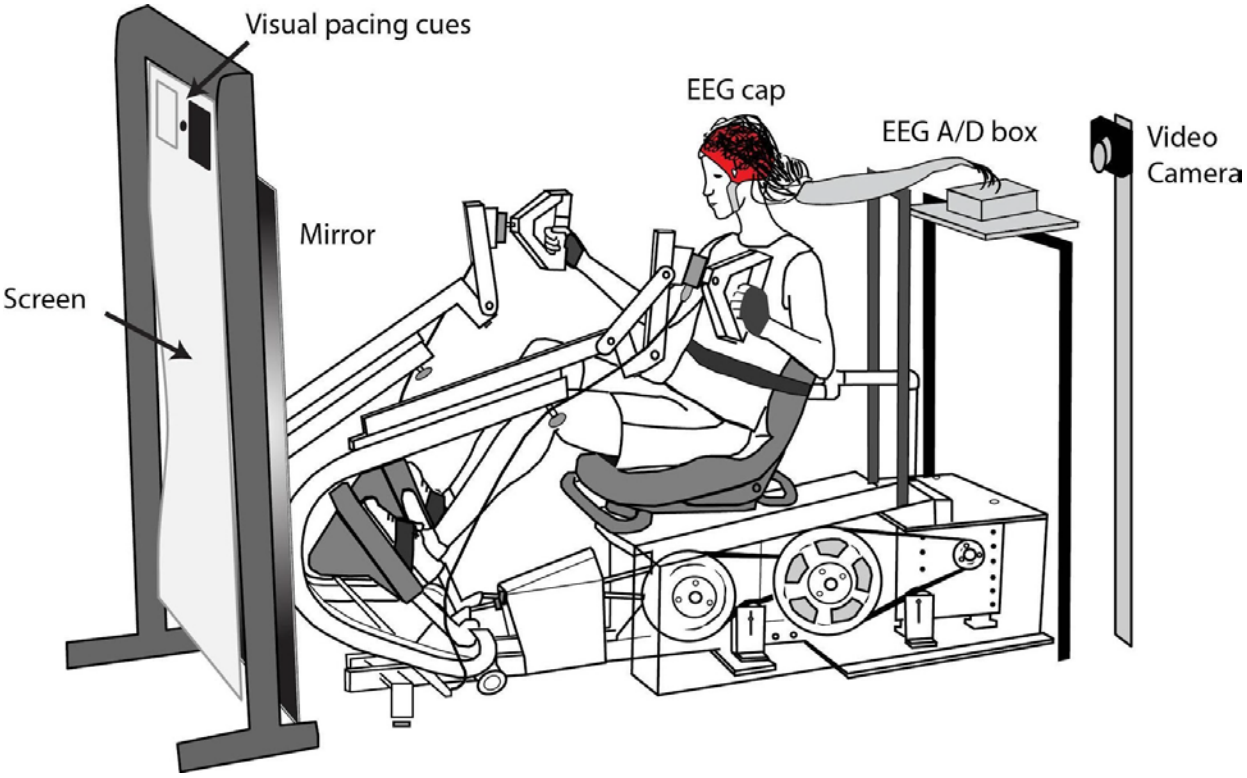

Figure 4-1. Experimental setup. Subjects moved to the pace of visual cues with 1) both their arms and legs, 2) their legs only, and 3) their arms only. A video camera to the left on the subject's head recorded videos of the subject exercising, as viewed in the mirror, for the three active conditions. For the viewed conditions, we removed the mirror, and projected life-size video playbacks of the subject or another individual exercising. The subjects remained seated in the stepping device during the viewed conditions. We recorded EEG during all conditions.

Data Processing

We post-processed the EEG signals using custom scripts in EEGLAB (Delorme and Makeig, 2004). First, we merged the EEG recordings into a single dataset and high-pass filtered above 1 Hz to remove drift. We rejected channels exhibiting substantial artifact based on the methods of Gwin and colleagues (Gwin et al., 2010). These rejection guidelines did not reject enough channels

to ensure good convergence of our ICA algorithm, therefore we altered the cutoffs slightly to reject an average of 140 channels per subject and re-referenced the remaining channels to a common average reference. Next, we rejected EEG time windows with high artifact across all channels based on visual inspection. To these cleaned datasets we applied infomax (Bell and Sejnowski, 1995) independent component analysis (ICA) as implemented on GPU by CUDAICA (Raimondo et al., 2012). This parsed the data into spatially fixed, temporally independent component (IC) signals (Makeig et al., 1996). The EEGLAB DIPFIT function (Oostenveld and Oostendorp, 2002) modelled each IC as an equivalent current dipole within a boundary element head model based on the MNI brain (Montreal Neurological Institute, MNI, Quebec). ICs with a best-fit equivalent current dipole that accounted for less than 85% of the variance seen at the scalp were excluded from further analysis (Gwin et al., 2011).

We clustered the remaining ICs from all ten subjects using a k-means clustering algorithm on vectors describing similarities in dipole location, scalp topography, and spectra (Gwin et al., 2011). If clusters contained ICs from five or fewer subjects or if their location and/or average scalp map were indicative of eye movement or muscle activity (Jung et al., 2000a;Jung et al., 2000b), we excluded them from further analysis. For each electrocortical cluster and condition, we created an event-locked plot of spectral power fluctuation (Makeig, 1993;Gwin et al., 2011). Our data epochs began at full extension for one arm or leg (active or viewed) and ended at subsequent full extension for the same arm or leg. For each epoch, we computed single trial spectrograms. To ensure that each extension event occurred at the same latency in every trial, we linearly warped each single trial spectrogram. We averaged these spectrograms over trials for each IC and over ICs for each cluster. For each cluster and condition, we subtracted the average log spectrum across all time points from the log spectrum for each individual time point, to easily visualize spectral changes

from baseline. These plots of spectral fluctuation are called event-related spectral perturbation (ERSP) plots. Bootstrapping methods available in EEGLAB (Delorme and Makeig, 2004) determined regions of significant difference from baseline for the ERSP plots ($p<0.05$).

Connectivity Analysis

We also performed effective connectivity analysis on the epochs of data described above. Using the EEGLAB-compatible SIFT toolbox (Delorme et al., 2011), we created a custom data analysis pipeline. The preprocessing pipeline involved first downsampling the data to 128 Hz and piecewise linearly detrending using a 330 ms window every 82.5 ms. Next, we used the Hannan-Quinn, Swartz Baysian, and Akaike Information Criteria to determine the appropriate model order within a 200 ms sliding windows every 54.7 ms. A Vieira-Morf lattice algorithm available in SIFT fit the multivariate autoregressive (MVAR) model. Examining the eigenvalues of the MVAR coefficient matrix allowed us to determine if the model was stable. We checked the whiteness of the model by multiple measures including the Ljung-Box test, the Box-Pierce test, the McLeod-Li test, and the Autocorrelation Function (ACF) test. The smallest model order that lead to stability and whiteness was the desired outcome. A model order between 1 and 3 satisfied these criteria for our data for all subjects and all conditions. With these MVAR models, we calculated connectivity using directed transfer function (Kaminski and Blinowska, 1991). Directed transfer function is generally robust to both noise and indirect connections. To test the significance of the connectivity fluctuations, we used bootstrap significance testing with 200 resamples.

Furthermore, we wished to determine which cluster pairs and conditions had the greatest effective connectivity. We found the maximum connectivity value for each cluster pair at each

condition. We determined which cluster pair/condition combinations had maximum connectivity values at least a standard deviation greater than the mean for all cluster pair/condition combinations. These cluster pair/condition combinations are referred to as having "supratheshold connectivity."

We also wanted to quantify the rate at which the average connectivity in the cortical network changed over time. For each condition, we took fast Fourier transform of the connectivity values across time for each frequency. Because our measure of interest was the relative power at different frequencies, we used a zero-padded window of 128 samples, and took the magnitude of the FFT value to determine the power spectrum for each frequency value from 0 to 18 Hz. We then took the mean of the resultant power spectrum over frequencies and component pairs to get an overall measure of the frequencies at which connectivity fluctuated for each condition.

Results

There were seven clusters of electrocortical sources that had at least five subjects represented (Figure 2). Three clusters were located in the right, left, and middle premotor and supplementary motor area. (Brodmann Area 6) (Figure 3). There were also clusters in the right anterior cingulate (Brodmann area 32), the middle anterior cingulate (Brodmann Area 24), the middle posterior cingulate (Brodmann area 31), and the middle parietal lobe (Brodmann area 7). (Figure 4).

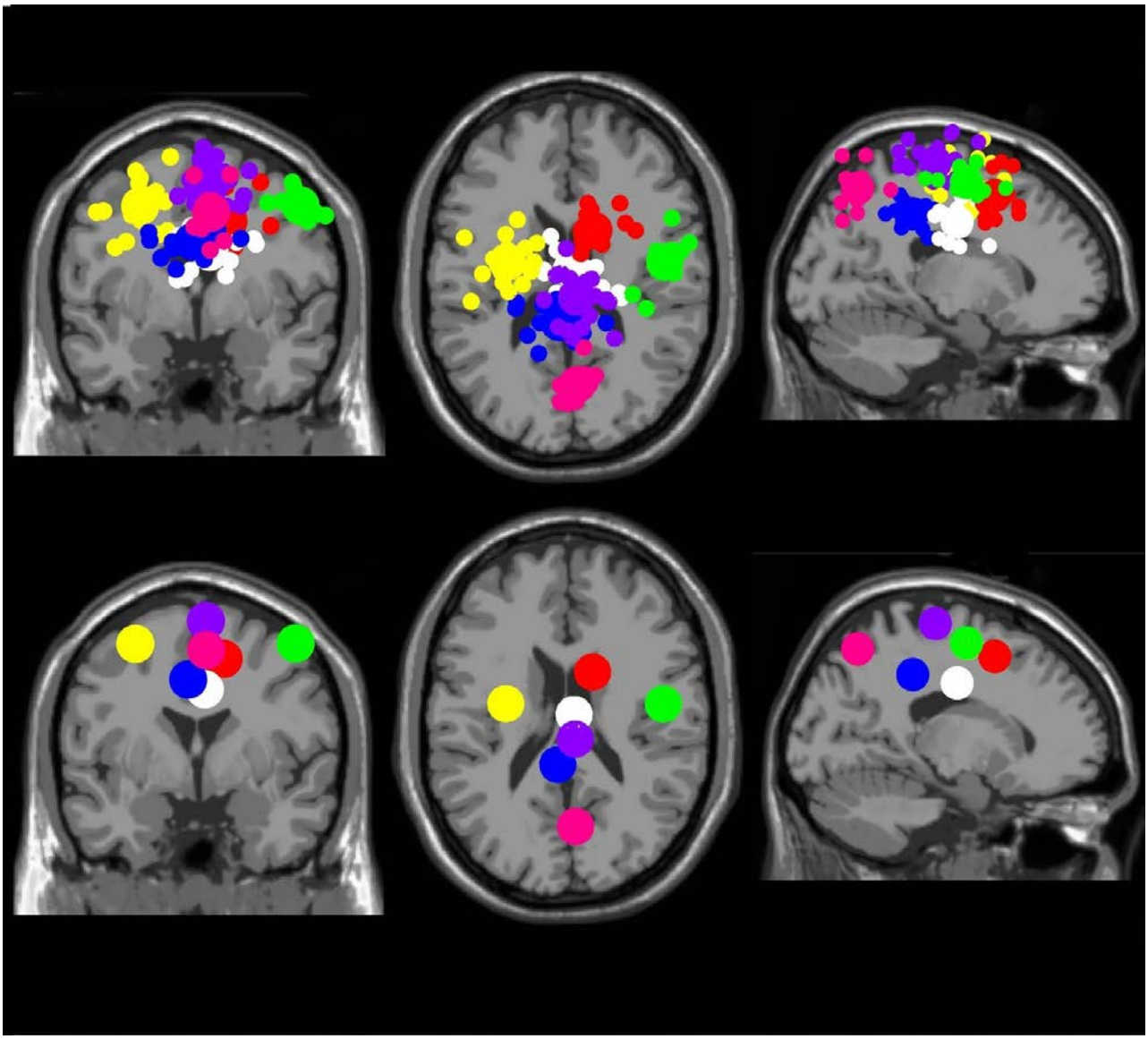

Figure 4-2. Electrocortical clusters. Clusters containing electrocortical sources from at least 5 of 10 subjects. Yellow is left premotor and supplementary motor cortex, purple is middle premotor and supplementary motor cortex, green is right premotor and supplementary motor cortex, red is right anterior cingulate, white is middle anterior cingulate, blue is middle posterior cingulate, and pink is middle parietal cortex. From left to right, the top three images show the independent component dipoles for each cluster from a coronal, horizontal, and sagittal perspective, respectively. The bottom three images show the centroid locations for each cluster from the same three perspectives.

Table 4-1. Centroid location and IC breakdown for each cluster containing electrocortical sources from at least 5 of 10 subjects.

Functional Area	Brodmann Area of Centroid	Subjects (#)	ICs (#)
Right Premotor and Supplementary Motor Cortex	6	5	9
Middle Premotor and Supplementary Motor Cortex	6	9	22
Left Premotor and Supplementary Motor Cortex	6	7	17
Middle Anterior Cingulate	24	6	14
Right Anterior Cingulate	32	7	19
Middle Posterior Cingulate	31	8	17
Middle Parietal Cortex	7	7	11

In the premotor and supplementary motor cortex, spectral fluctuations occurred during the active conditions in the theta (4-8 Hz), alpha (8-13 Hz), beta (13-30 Hz), and gamma (30 Hz and above) bands (Figure 3). In the middle premotor and supplementary motor area, all active conditions elicited bilateral activity. Theta and low alpha band desynchronization occurred during

approximately the middle 50% of the extension phase for either arm in the arms only condition, for either leg in the legs only condition, and for either arm-leg pair in the arms and legs condition. In the right and left premotor and supplementary motor cortex, these alpha and theta spectral power fluctuations showed some lateralization. Prominent desynchronization occurred in right premotor and supplementary motor cortex during approximately the middle 50% of the extension phase when the left leg was extending in both the arms and legs condition and the legs only condition. Prominent desynchronization occurred in left premotor and supplementary motor cortex during approximately the middle 50% of the extension phase when the left arm was extending in the arms only condition and when the right leg was extending in the legs only condition. There were some similar spectral fluctuations during the self viewed arms condition, particularly in the middle premotor and supplementary motor cortex in the theta and low alpha band. However, overall, we did not detect robust or consistent fluctuations across similar pairs of conditions (i.e.,arms vs arms viewed). For the spectral fluctuation plots for all the viewed conditions, see Supplementary Figure 1.

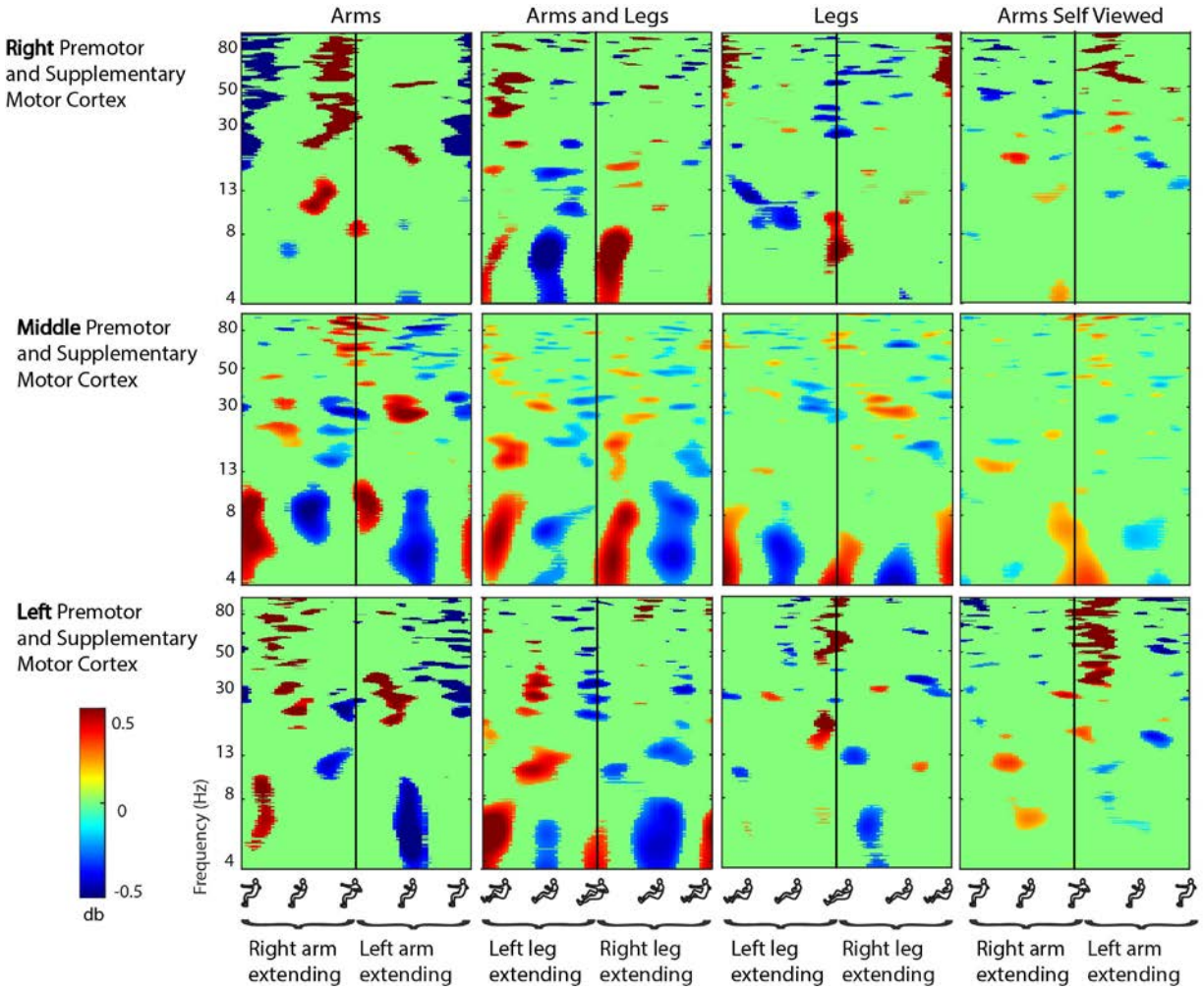

Figure 4-3. Motor Cortex ERSPs. Event-related spectral perturbation (ERSP) plots showing change in spectral power during rhythmic arm and leg movement in the right, middle, and left premotor and supplementary motor cortex. From left to right, subjects moved with their arms only, both their arms and legs, their legs only, and viewed video playback of themselves moving with just their arms. Each row represents a cortical area, and each column represents a condition. For all plots, red represents a power increase from baseline, and blue represents a power decrease from baseline. We set non-significant differences to 0 dB (green). All ERSPs start and end with the same limb fully extended. The figure outlines on the x axis indicate the phase of movement, and the written labels indicate when each limb was extending. Note: for the arms and legs condition, the left leg and right arm extended together, and vice versa.

In the cingulate and parietal areas, spectral fluctuations occurred during active movement in the theta (4-8 Hz), alpha (8-13 Hz), beta (13-30 Hz), and gamma (30 Hz and above) bands (Figure 4). These fluctuations were much greater for both active arms conditions than for the active legs

condition. In the majority of areas, theta and low alpha band desynchronization occurred during approximately the middle 50% of the extension phase when either arm was extending in the arms only condition and when either arm-leg pair was extending in the arms and legs condition. Theta and low alpha synchronization occurred at the transition points for the two active arms conditions. Again, we did not detect highly similar spectral fluctuations for the active arms and self viewed arms conditions. For the spectral fluctuation plots for all the viewed conditions, see Supplementary Figure 1.

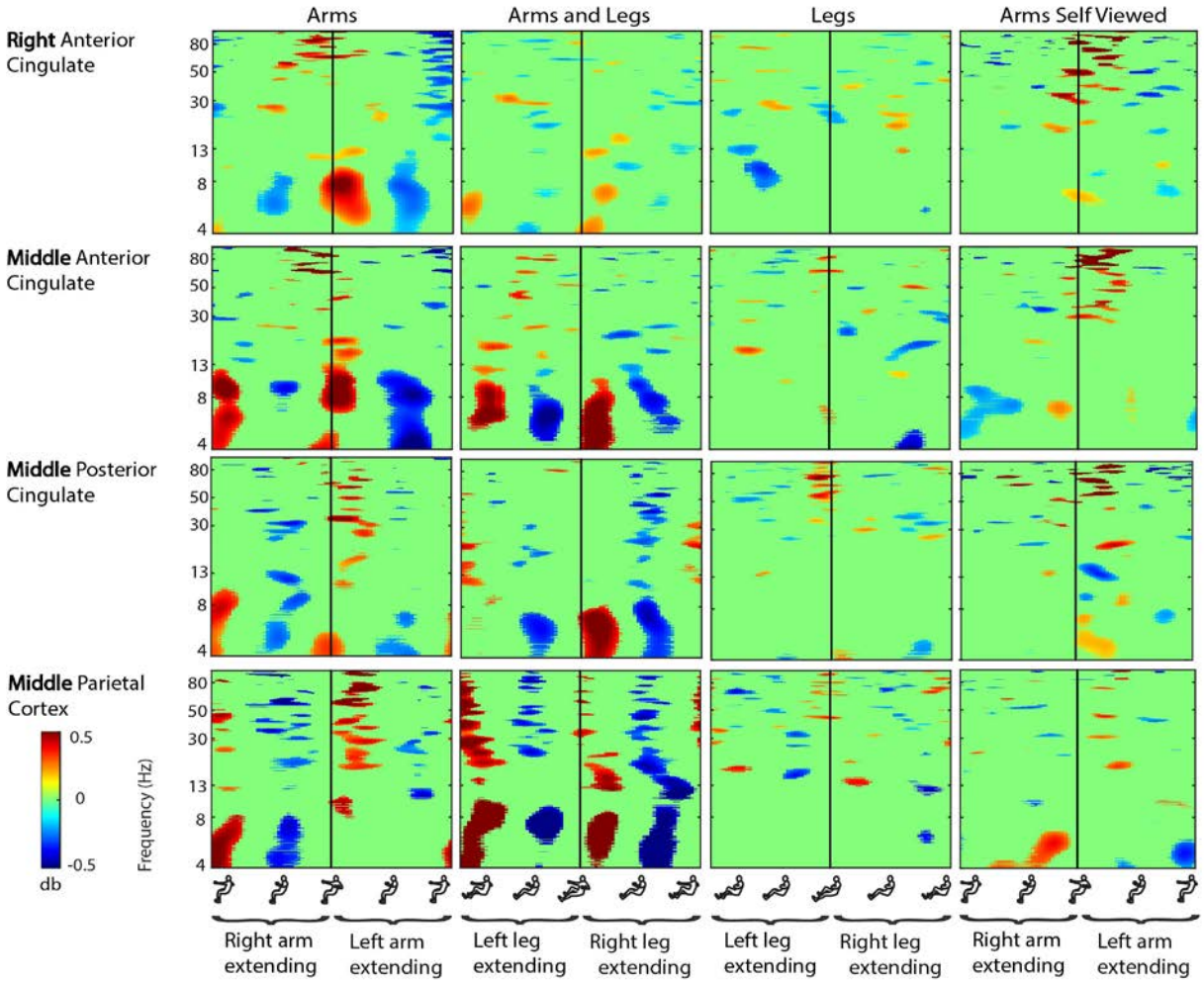

Figure 4-4. Cingulate Cortex ERSPs. Event-related spectral perturbation (ERSP) plots showing change in spectral power during rhythmic upper and lower limb movement in the right anterior cingulate, the middle anterior cingulate, the middle posterior cingulate, and the middle parietal cortex. From left to right, subjects moved with their arms only, both their arms and legs, their legs only, and viewed video playback of themselves moving with just their arms. Each row represents a cortical area, and each column represents a condition. For all plots, red represents a power increase from baseline, and blue represents a power decrease from baseline. We set non-significant differences to 0 dB (green). All ERSPs start and end with the same limb fully extended. The figure outlines on the x axis indicate the phase of movement, and the written labels indicate when each limb was extending. Note: for the arms and legs condition, the left leg and right arm extended together, and vice versa.

Connectivity Results

For all conditions, pairs of cortical areas exhibited suprathreshold connectivity values (maximum connectivity values more than a standard deviation greater than the mean). Examining the connectivity patterns across all conditions (Table 2), a general picture of a movement-related neural network emerges. During every active and viewed movement condition, suprathreshold connectivity occurred between the middle anterior cingulate and the right premotor and supplementary motor cortex. For the majority of conditions, suprathreshold connectivity also occurred between several cortical areas (the middle premotor and supplementary motor cortex, the left premotor and supplementary motor cortex, and the middle posterior cingulate) and the right premotor and supplementary motor cortex, between the right premotor and supplementary motor cortex and the middle posterior cingulate, and between the right anterior cingulate and the middle posterior cingulate (Figure 5).

There were also some differences between the conditions. The most suprathreshold connectivity values between pairs of cortical areas occurred during the self-viewed movement conditions (25 pairs). The least suprathreshold connectivity values between pairs of cortical areas occurred

during the active movement conditions (15 pairs). The number of cortical pairs exhibiting suprathreshold connectivity was intermediate for the other-viewed movement conditions (18 pairs). See Table 2 for all cortical pairs exhibiting suprathreshold connectivity for each condition.

Table 4-2: Suprathreshold connectivity between pairs of cortical areas for the active movement the self-viewed movement, and the other-viewed movement conditions.

	Right Premotor and Supplementary Motor	Middle Premotor and Supplementary Motor	Left Premotor and Supplementary Motor	Middle Anterior Cingulate	Right Anterior Cingulate	Middle Posterior Cingulate	Middle Parietal
Right Premotor and Supplementary Motor		+A +AL +AL +AL +L +L +S	+A +A +L +L +L +S	+A +A +A +AL +AL +AL +L +L +L +S	+A +AL +AL +L	+A +A +AL +AL +AL +L +L +S	+AL +AL +L +L
Middle Premotor and Supplementary Motor	+A +AL +L +L			+L +S		+AL	
Left Premotor and Supplementary Motor							
Middle Anterior Cingulate							
Right Anterior Cingulate	+AL +L					+AL	
Middle Posterior Cingulate	+A +A +A +AL +AL +L +L +S			+S	+A +A +AL +AL +AL +L +L +S		
Middle Parietal				+L			

+ = supratheshold connectivity during active movement conditions
+ = suprathreshold connectivity during self-viewed movement conditions
+ = suprathreshold connectivity during other-viewed movement conditions
+ = suprathreshold connectivity during viewed stepper condition
A = Arms, AL = Arms and Legs, L = Legs, S=Stepper

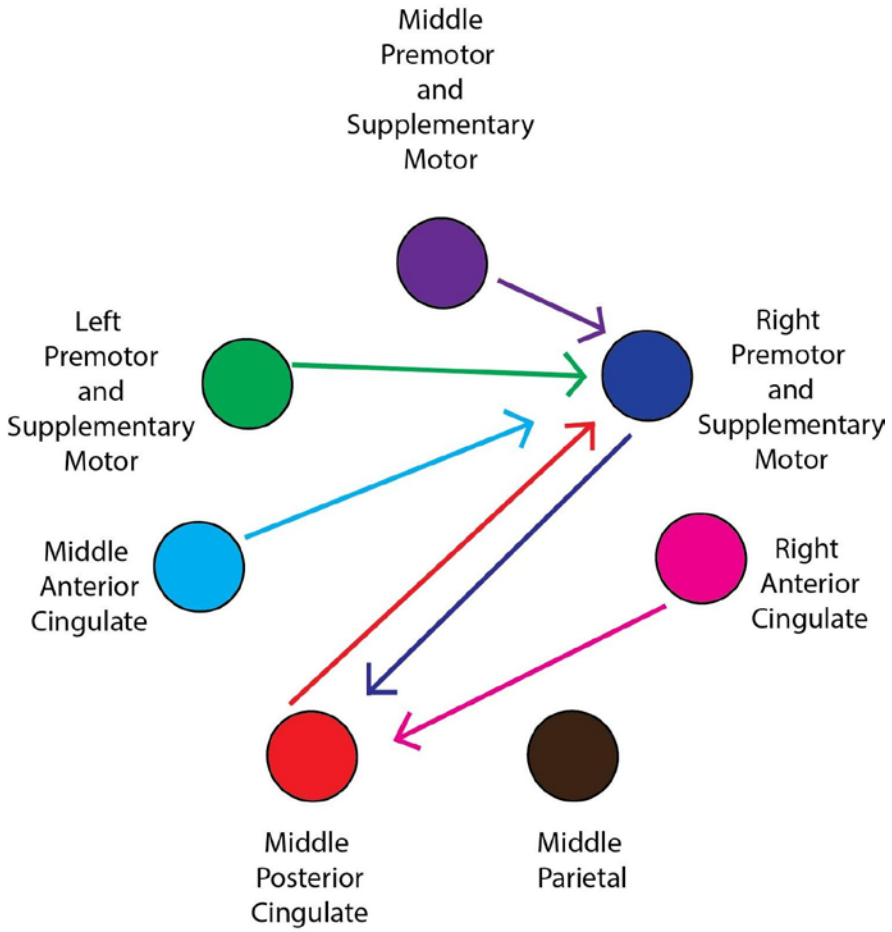

Figure 4-5. General Network Connectivity. Schematic of the cortical network active during active and viewed movement. Arrows between cortical areas indicate suprathreshold connectivities for at least half (5/10) of the conditions.

Connectivity grids showing the strength of directed transfer function connectivity for all frequencies and time points within a stride revealed that significant connectivity fluctuations occurred between many cortical areas for all active and viewed conditions (Figures 6-9). For connectivity grids for all the additional viewed conditions, see Supplementary Figures 2-7.

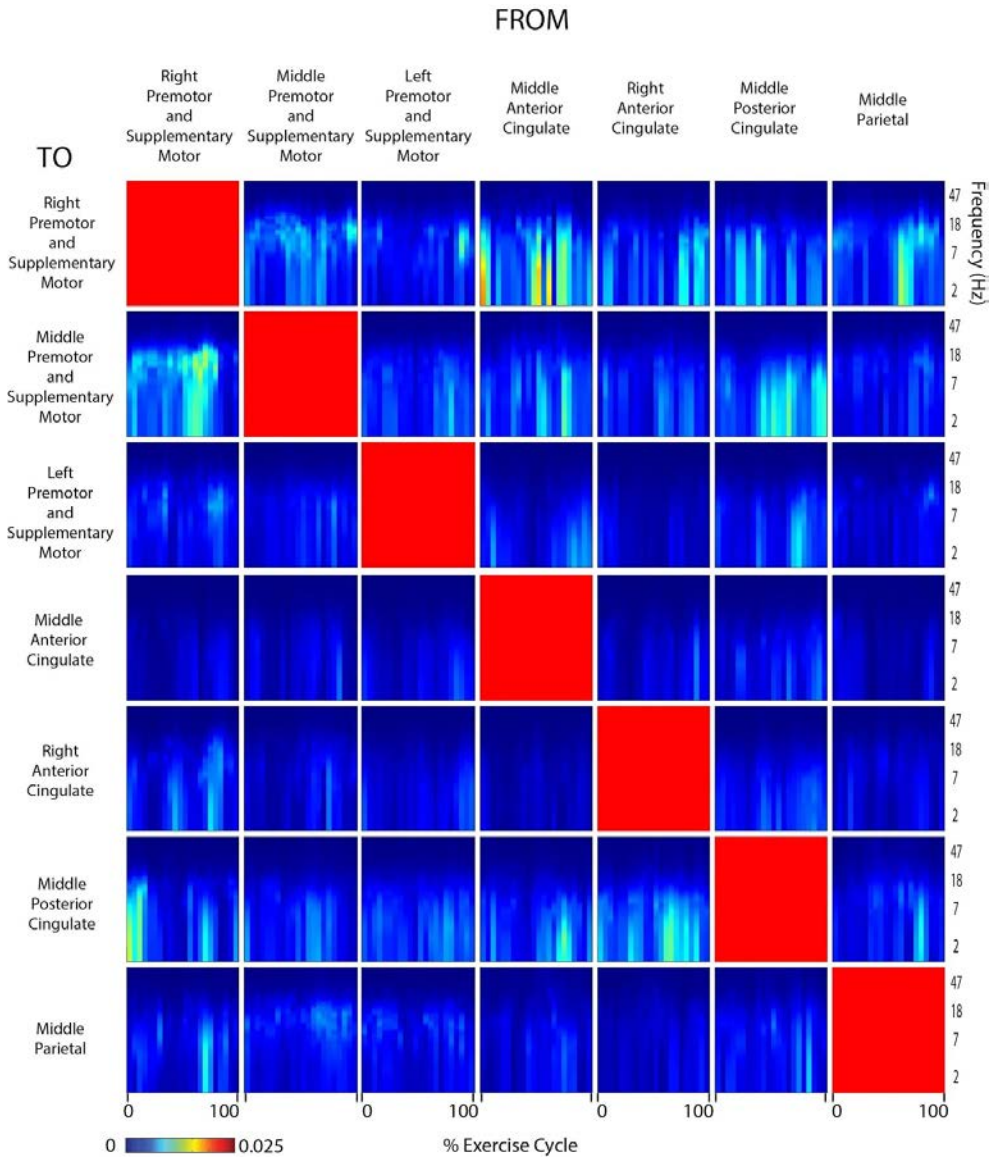

Figure 4-6. Connectivity Active Arms. Diagram showing directed transfer function connectivity values between pairs of cortical areas while the subject performed ACTIVE rhythmic movement using only the ARMS. Each individual plot starts and ends with the right arm fully extended. The numbers on the x-axis indicate the % of the movement cycle. We set non-significant differences to 0 (blue).

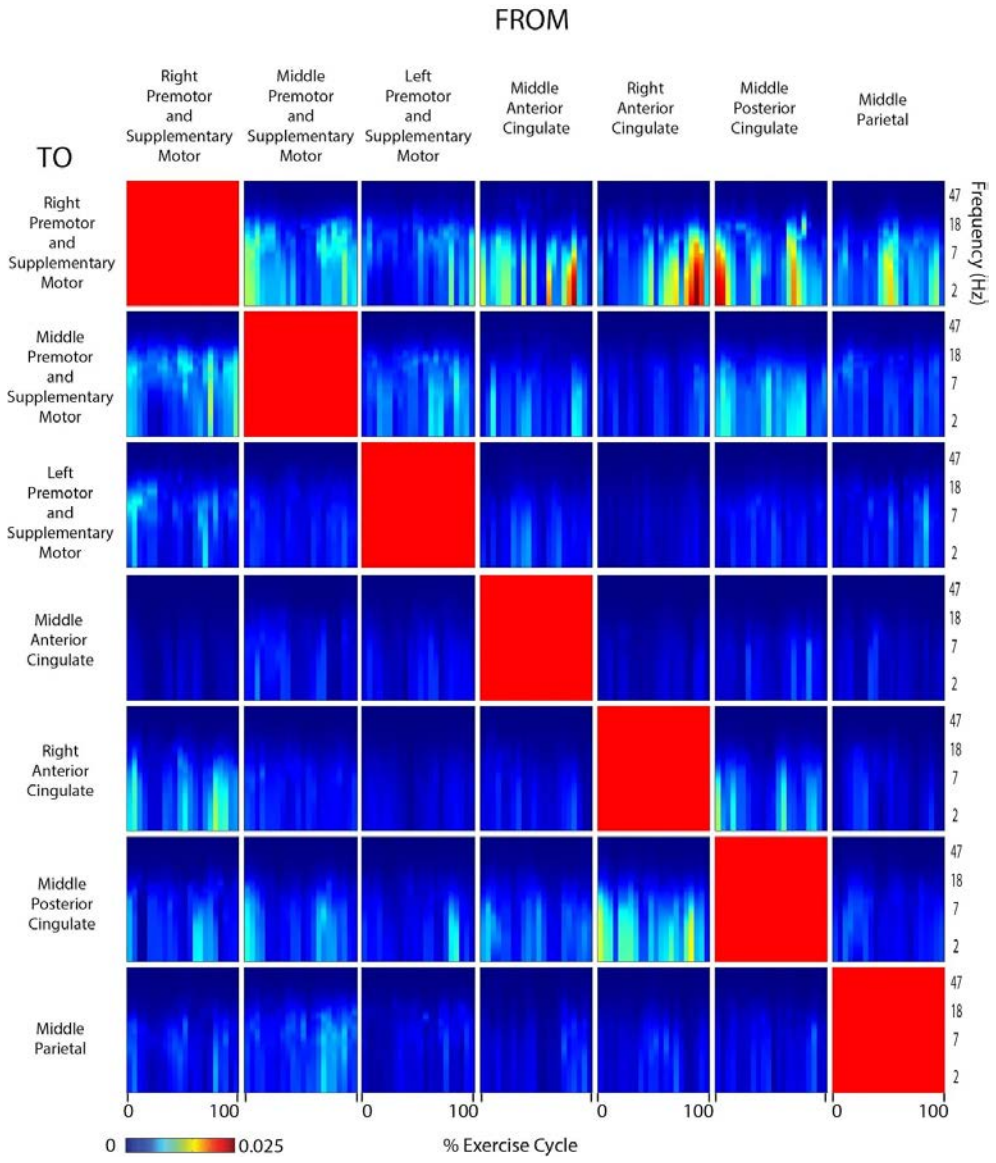

Figure 4-7. Connectivity Active Arms and Legs. Diagram showing directed transfer function connectivity values between pairs of cortical areas while the subject performed ACTIVE rhythmic movement using the ARMS AND LEGS. Each individual plot starts and ends with the left leg fully extended. The numbers on the x-axis indicate the % of the movement cycle. We set non-significant differences to 0 (blue).

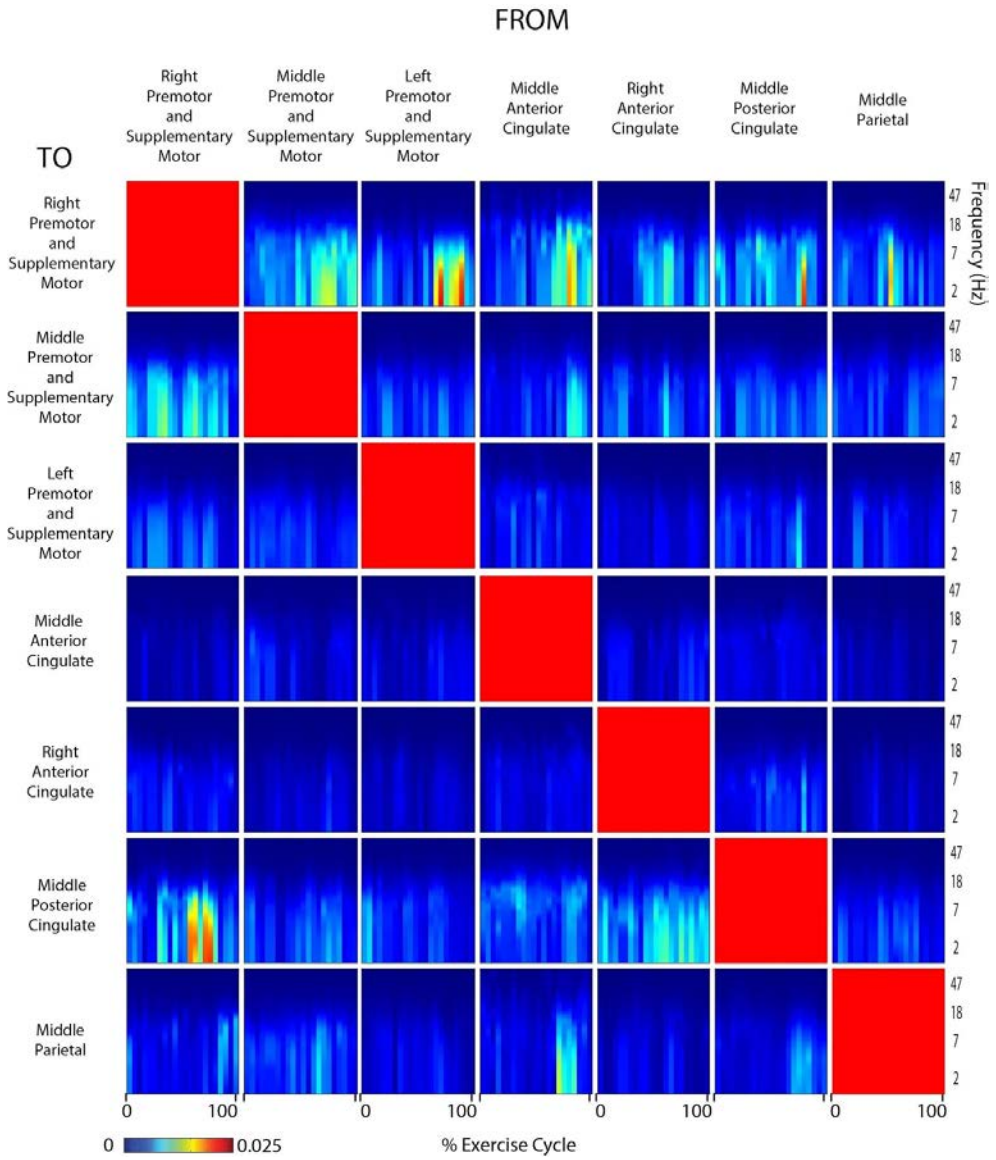

Figure 4-8. Connectivity Active Legs. Diagram showing directed transfer function connectivity values between pairs of cortical areas while the subject performed ACTIVE rhythmic movement using only the LEGS. Each individual plot starts and ends with the left leg fully extended. The numbers on the x-axis indicate the % of the movement cycle. We set non-significant differences to 0 (blue).

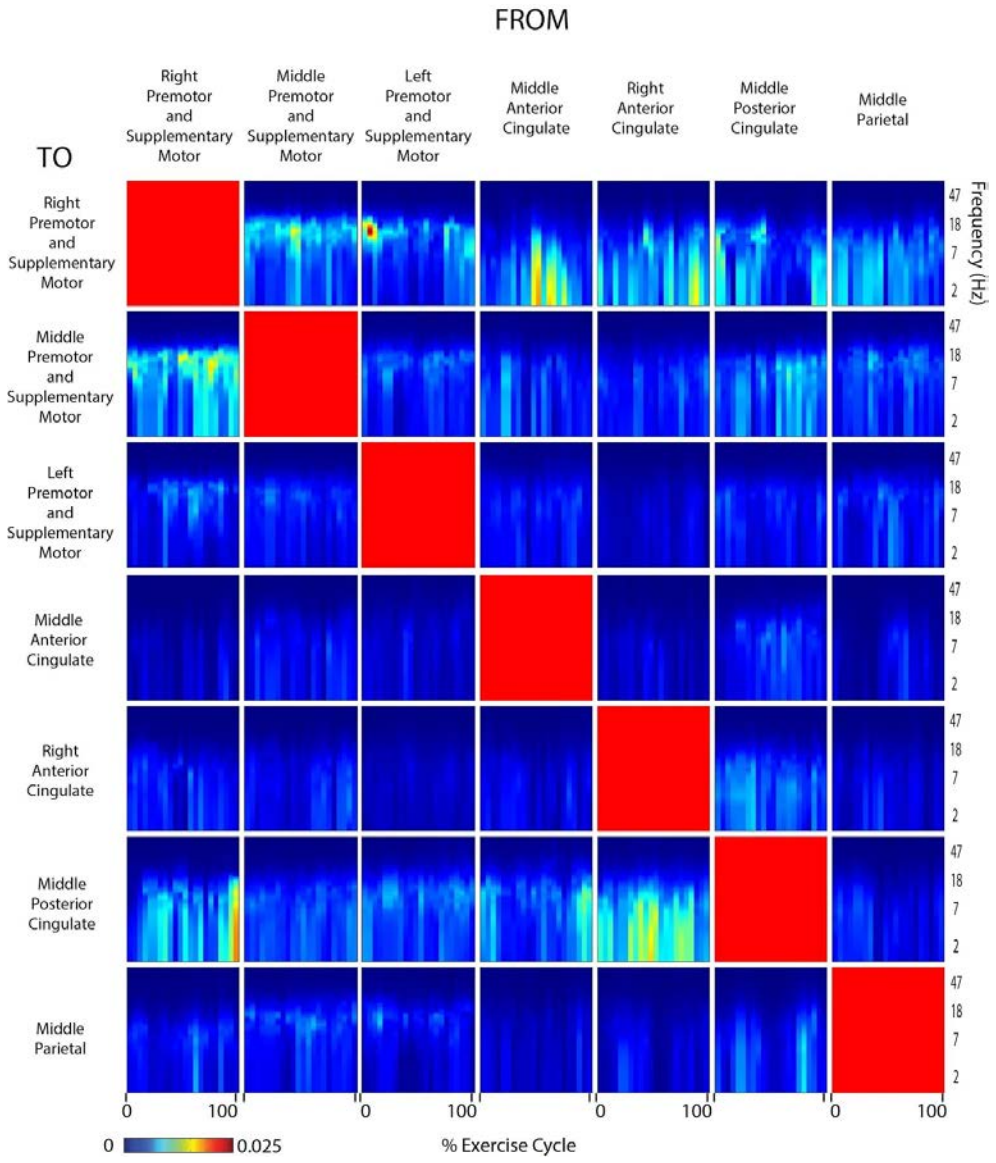

Figure 4-9. Connectivity Viewed Arms Self. Diagram showing directed transfer function connectivity values between pairs of cortical areas while the subjects VIEWED a video of themselves exercising with only the ARMS. Each individual plot starts and ends with the viewed right arm fully extended. The numbers on the x-axis indicate the % of the movement cycle. We set non-significant differences to 0 (blue).

The fast Fourier transform analysis showed that the connectivity strengths in our cortical network fluctuated at a predictable rate for both the active movement and the viewed movement conditions. Connectivity fluctuated rapidly, with the greatest peaks occurring below 3 Hz for all

conditions. Peaks occurred at the harmonics of the movement frequency for both the active movement and the viewed movement conditions. For all conditions, a peak in connectivity fluctuation occurred at 0.5, 1, 1.5, and 2 times the movement frequency (1.17 Hz). Of particular interest is the fact that the peaks in connectivity fluctuation occurred at precisely the same frequencies for the active movement and the viewed movement conditions (Figure 10).

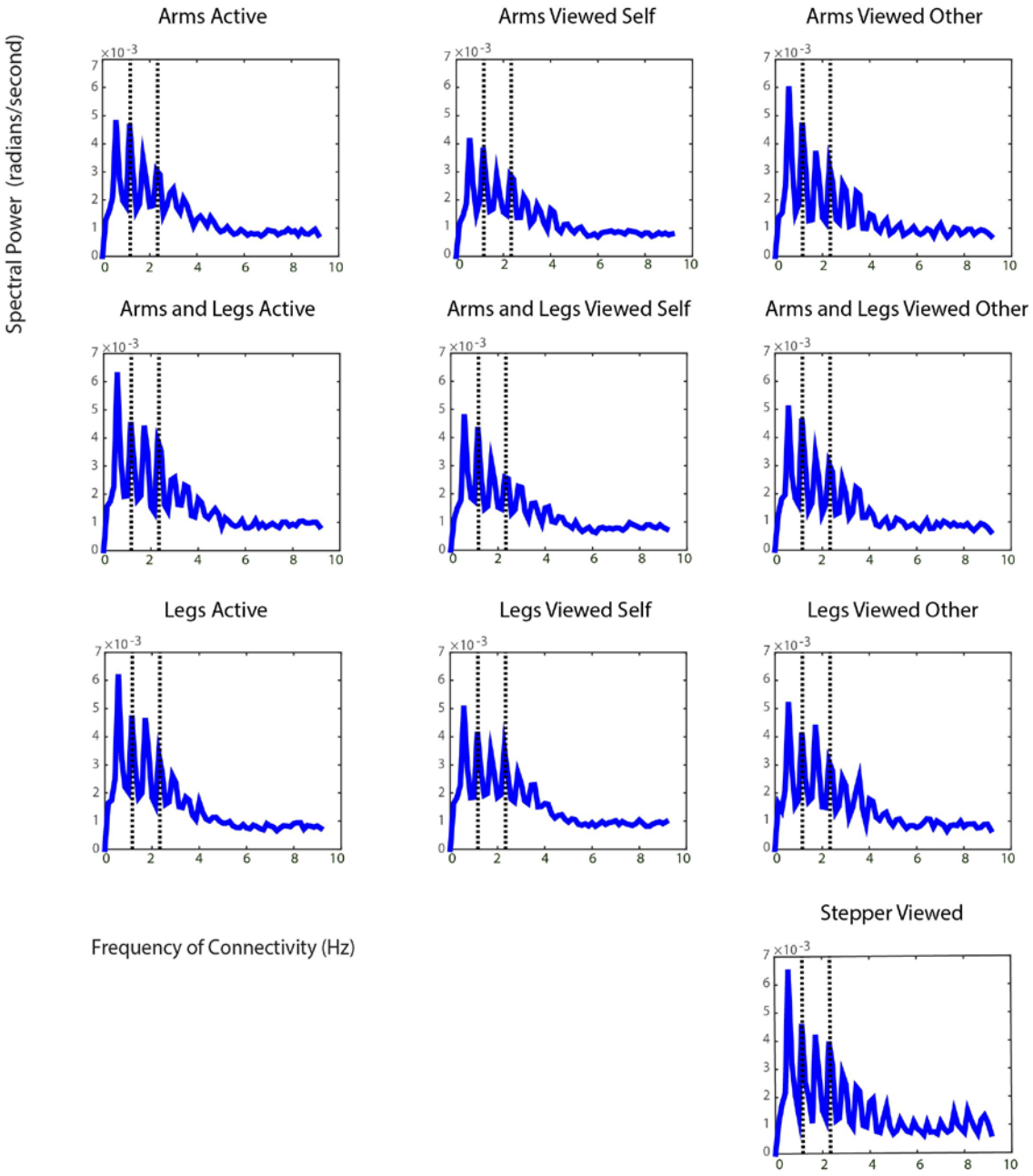

Figure 4-10. Fast Fourier Transform Results. Fast Fourier transform of the average connectivity over time across all IC pairs. The left column shows the values for the three active movement conditions, the middle column shows the values for the three self-viewed movement conditions, the right column shows the values for the four other-viewed movement conditions. The dotted lines show the subjects' stepping frequency and the second harmonic of that frequency.

Discussion

A widely distributed cortical network exhibits fluctuations in spectral power and effective connectivity during active and viewed rhythmic limb movements. This network includes the premotor and supplementary motor cortex, the anterior and posterior cingulate, and the parietal cortex. In the cingulate areas and the parietal cortex, the spectral fluctuations were significantly smaller or nearly absent during the legs only movement condition compared to either arm movement condition. This evidence suggests that rhythmic arm movements induce more cortical spectral activity than rhythmic leg movements. Consistent spectral fluctuations were not evident during the viewed conditions. However, effective connectivity analysis revealed that the strength and direction of information flow was similar between active and viewed movement conditions. There was no strong difference in effective connectivity between the self viewed and other viewed movement conditions. For all the active and viewed conditions, the right premotor and supplementary motor cortex drove the network.

In the premotor and supplementary motor areas, spectral power fluctuations occurred most prominently during active rhythmic movements and less so during viewed movements. We found that the premotor and supplementary motor areas exhibited theta and alpha desynchronization when the contralateral limb was extending and synchronization when the limbs were switching directions. The presence of desynchronization may reflect increased cortical activation for

movement production or sensorimotor processing (Pfurtscheller and Klimesch, 1991;Pfurtscheller et al., 1996;Pfurtscheller and Lopes da Silva, 1999). The presence of synchronization at the transition points may reflect recruitment of the muscles needed to transition from flexion to extension (Jain et al., 2013). There were some similar spectral shifts during the viewed conditions. However they were generally smaller, as in the middle premotor and supplementary motor area during the self viewed arm condition, but for the most part they were absent. This differs from previous EEG studies where spectral fluctuations were evident during viewed movement (Cochin et al., 1998;Cochin et al., 1999;Calmels et al., 2006;Avanzini et al., 2012;Cevallos et al., 2015), and it may be a limitation of our study.

In the cingulate areas and the parietal area spectral fluctuations also occurred during the active conditions. Similar to the premotor and supplementary motor areas, theta and alpha desynchronization occurred when the contralateral limb was extending, and synchronization occurred when the limbs were switching directions. Interestingly the spectral fluctuations in these areas were mainly apparent when the subjects moved their arms, and were much smaller or completely absent when the subjects moved just their legs. This provides evidence that rhythmic leg movements induce less cortical activity than rhythmic arm movements, especially in the cingulate and parietal areas.

There various reasons why the cingulate and parietal areas might have been less cyclically active during rhythmic leg movement compared to rhythmic arm movement in our study. The anterior cingulate area is primarily involved in error detection and correction (Bush et al., 2000;O'Connell et al., 2007;Walton et al., 2007). Past studies from our laboratory have shown activation changes in the anterior cingulate during human walking (Gwin et al., 2011;Sipp et al., 2013), however these

changes may have been primarily related to balance control during walking. Movement on a recumbent stepper does not involve a balance component, which may explain the limited cingulate activity during the active legs condition in the present study. The exact role of the posterior cingulate in rhythmic motion is not known, but it may be involved in the transition between rest and movement (Treserras et al., 2009). It may be that, once initiated, rhythmic leg movement is a continuous task controlled by spinal networks, whereas rhythmic arm movement is a discrete, cortically-mediated task. This would explain the increased posterior cingulate activity during rhythmic arm movement compared to rhythmic leg movement, if the posterior cingulate controls the transition between movement and rest for discrete movements. The middle parietal cortex is known to be involved in visuospatial processing (Harris et al., 2000). There are few occasions in everyday life when humans move the arms rhythmically without also moving the legs. Given the novelty of moving the arms rhythmically on their own, greater visuospatial processing may be required.

In our study, the right premotor and supplementary motor cortex was the central hub of information flow. This right hemisphere dominance for our recumbent stepping task could be related to differences in hemisphere function for motor tasks. It has been theorized that the right hemisphere specializes in impedance control mechanisms for stabilizing the limbs and body in response to unpredictable mechanical conditions (Sainburg, 2014). This explanation fits with the mechanical conditions of our study, given that the recumbent stepper was a one-degree of freedom device with a preset kinematic movement pattern. Sainburg has also suggested that the left hemisphere is much more focused on predicting the effects of body and environment dynamics during movement (Sainburg, 2014). A previous study from our lab on human balance beam walking found a stronger electrocortical response in the left motor cortex compared to the right motor cortex when subjects

lost their balance (Sipp et al., 2013). Having the left motor cortex dominant during a challenging balance task fits with Sainburg's hypothesis about lateralization. In our study, the subjects did not need to maintain their balance and there was no negative consequences for joint kinematic errors. The motion pattern was predominantly prescribed by the motion of the handles and pedals.

Another possible explanation of why the right hemisphere was the center of connectivity is related to its role in spatial processing. It is well-established that the right hemisphere is the more spatially oriented of the two hemispheres (Joseph, 1988). The strongest evidence of this comes from patients who have suffered strokes on the right side of the brain. Hemineglect, or failure to perceive the contralesional side of the world, is typically more pronounced in patients with right hemisphere strokes than similar left hemisphere strokes (Bowen et al., 1999;Heilman et al., 2000). This suggests that the right hemisphere is centrally involved in constructing our perception of the space around us. Furthermore, the right hemisphere may control shifts in attention while viewing a scene. Studies with fMRI have reported right-lateralized ventral fronto-parietal activity during shifts in visual attention (Arrington et al., 2000;Corbetta et al., 2000). Seven of the ten conditions in this study involved a predominantly visual task with frequent shifts in attention from the left to right side of the viewed scene and vice versa. All of this may have accounted for the right hemisphere's prominent role in coordinating the communication of the interacting brain areas.

The results from our fast Fourier transform analysis of the connectivity data highlight similarities in the neural processing of the active movement and viewed movement conditions. The fluctuations in overall connectivity occurred at frequencies related to the movement. Specifically these fluctuations were prominent at 0.5, 1, 1.5, and 2 times the movement frequency. This

observation strongly supports the relevance of the connectivity analysis providing insight into the true brain activity during the conditions. The prominent frequencies for greater connectivity fluctuations were similar for both active movement and viewed movement. In the viewed movement, there was virtually no head motion to influence the EEG recordings. There has been considerable recent debate about the possibility of motion artifact corrupting EEG signals during human movement (Castermans et al., 2014;Kline et al., 2015). There was very little head movement during the active stepping condition, but virtually no head movement during the viewed conditions. The fast Fourier transform analysis of the connectivity found very similar outcomes for all the conditions. The similarity between conditions indicates that the communication within the cortical network was related to the pace of the active or viewed movement.

Overall, the results of this study add new information to our understanding of human motor control. The results of our spectral analysis suggest that rhythmic arm movements are under greater descending cortical control, especially by the cingulate and parietal areas, than rhythmic leg movement. Furthermore, effective connectivity in a cortical network that is driven by the right premotor and supplementary motor cortex fluctuates at harmonics of the movement frequency during both active and viewed movement. These results suggest that a similarly interconnected neural network is in operation during both active and viewed movement. They illustrate that effective connectivity analysis can provide insight into brain network activity beyond what can be gained from traditional spectral analysis.

Supplementary Figures

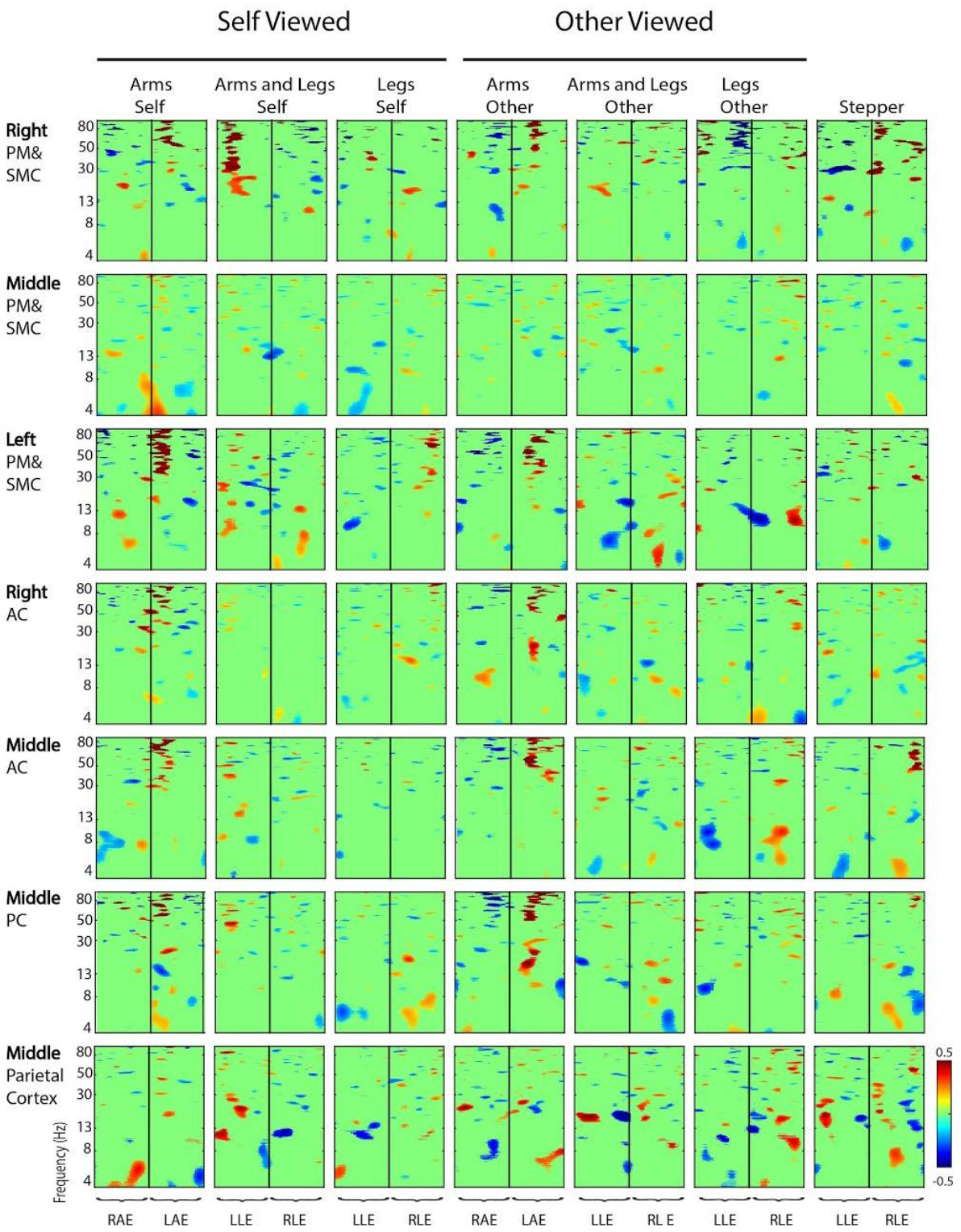

Supplementary Figure 4-1. All Viewed Movement ERSPs. Event-related spectral perturbation (ERSP) plots showing change in spectral power during viewed rhythmic arm and leg exercise in all electrocortical clusters. From left to right, in the first three columns subjects viewed themselves exercising with their arms only, with their arms and legs, and with their legs only. In

the next three columns, they viewed another person exercising with her arms only, with her arms and legs, and with her legs only. In the last column (far right) subjects viewed the recumbent stepper moving on its own, with no one seated on it. Each row represents a cortical area (PM&SMC=Premotor and Supplementary Motor Cortex, AC=Anterior Cingulate, and PC=Posterior Cingulate), and each column represents an exercise condition. For all plots, red represents a power increase from baseline, and blue represents a power decrease from baseline. We set non-significant differences to 0 dB (green). All ERSPs start and end with the same limb fully extended. The written labels indicate when each limb was extending. RAE=Right Arm Extending, LAE=Left Arm Extending, LLE=Left Leg Extending, RLE=Right Leg Extending. Note: for the arms and legs condition, the left leg and right arm extended together, and vice versa. For the stepper condition, the labels indicate the limb that would have been extending, had a person been seated in the stepper.

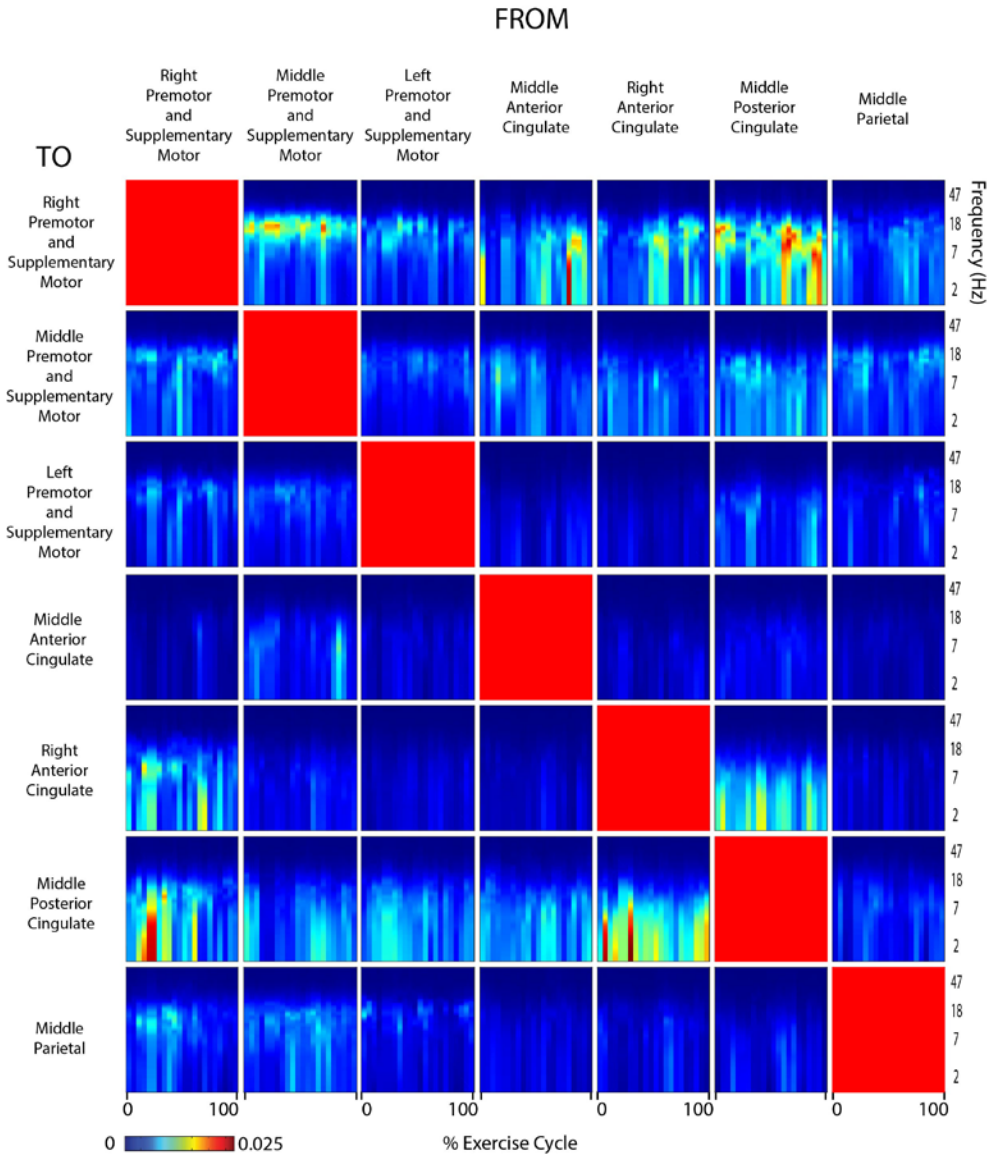

Supplementary Figure 4-2. Connectivity Self Viewed Arms and Legs. Diagram showing directed transfer function connectivity values between pairs of cortical areas while the subjects VIEWED a video of THEMSELVES exercising with their ARMS and LEGS. Each individual plot starts and ends with the viewed left leg fully extended. The numbers on the x-axis indicate the % of the movement cycle. We set non-significant differences to 0 (blue).

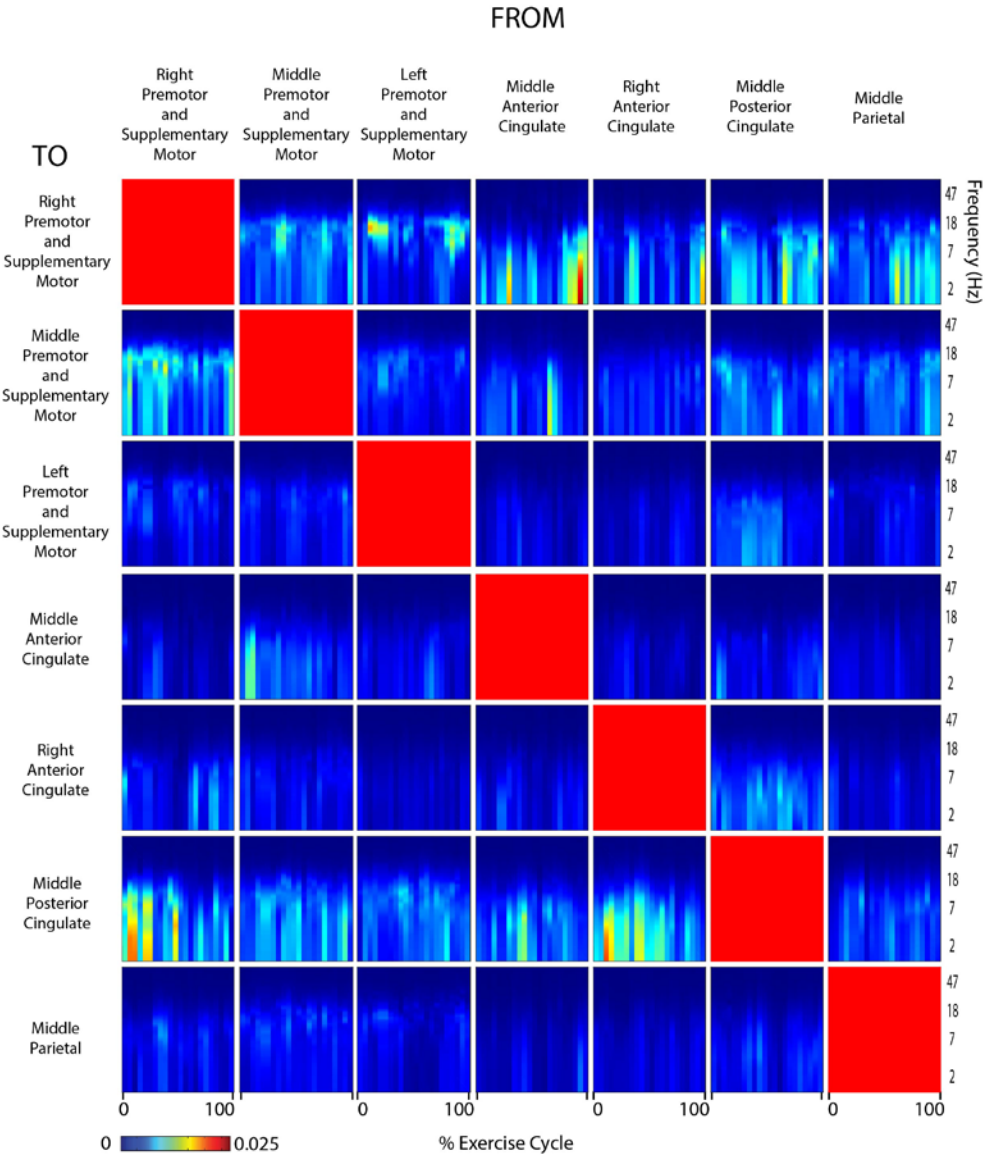

Supplementary Figure 4-3. Connectivity Self Viewed Legs. Diagram showing directed transfer function connectivity values between pairs of cortical areas while the subjects VIEWED a video of THEMSELVES exercising with only the LEGS. Each individual plot starts and ends with the viewed left leg fully extended. The numbers on the x-axis indicate the % of the movement cycle. We set non-significant differences to 0 (blue).

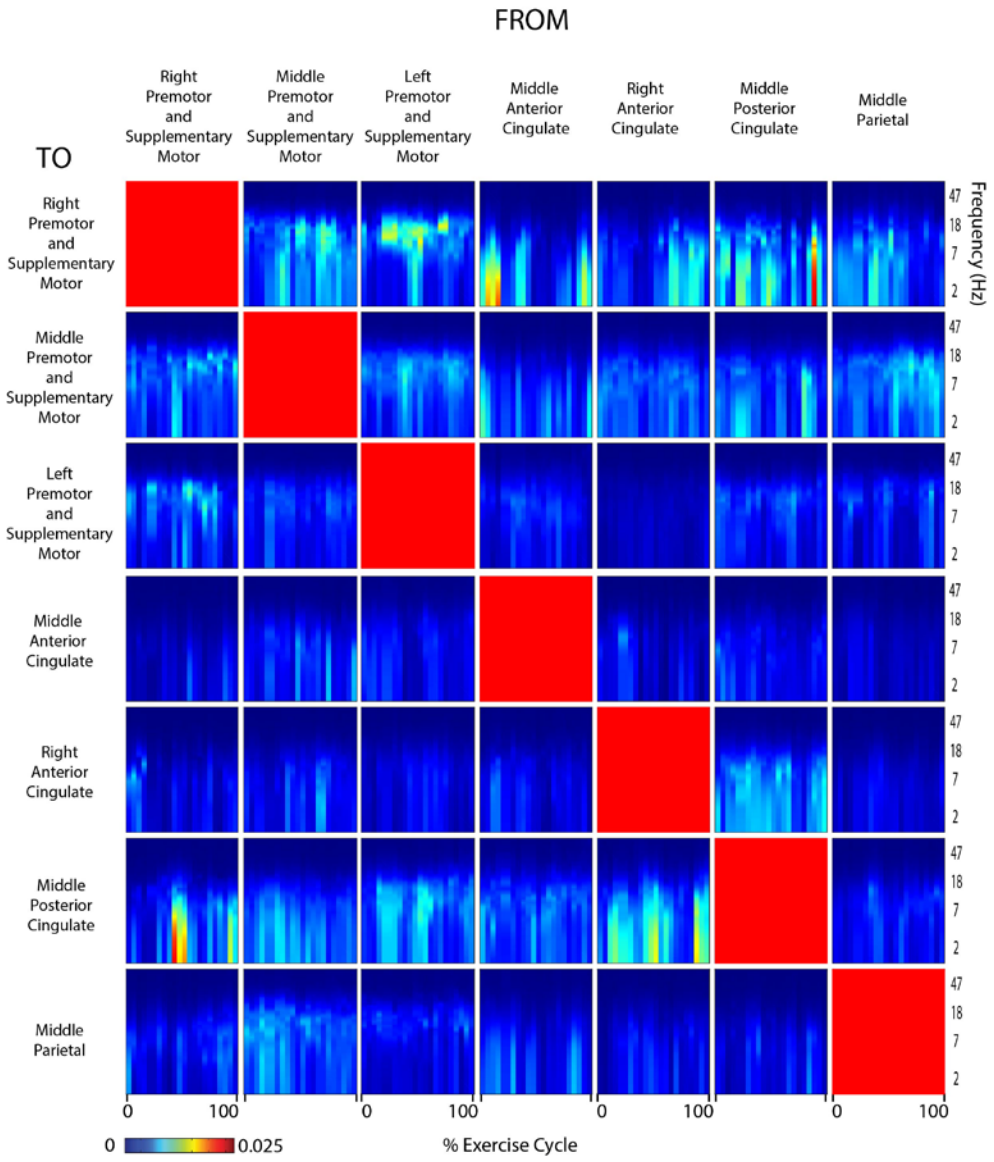

Supplementary Figure 4-4: Connectivity Other Viewed Arms. Diagram showing directed transfer function connectivity values between pairs of cortical areas for five second while the subjects VIEWED a video of ANOTHER PERSON exercising with only the ARMS. Each individual plot starts and ends with the viewed right arm fully extended. The numbers on the x-axis indicate the % of the movement cycle. We set non-significant differences to 0 (blue).

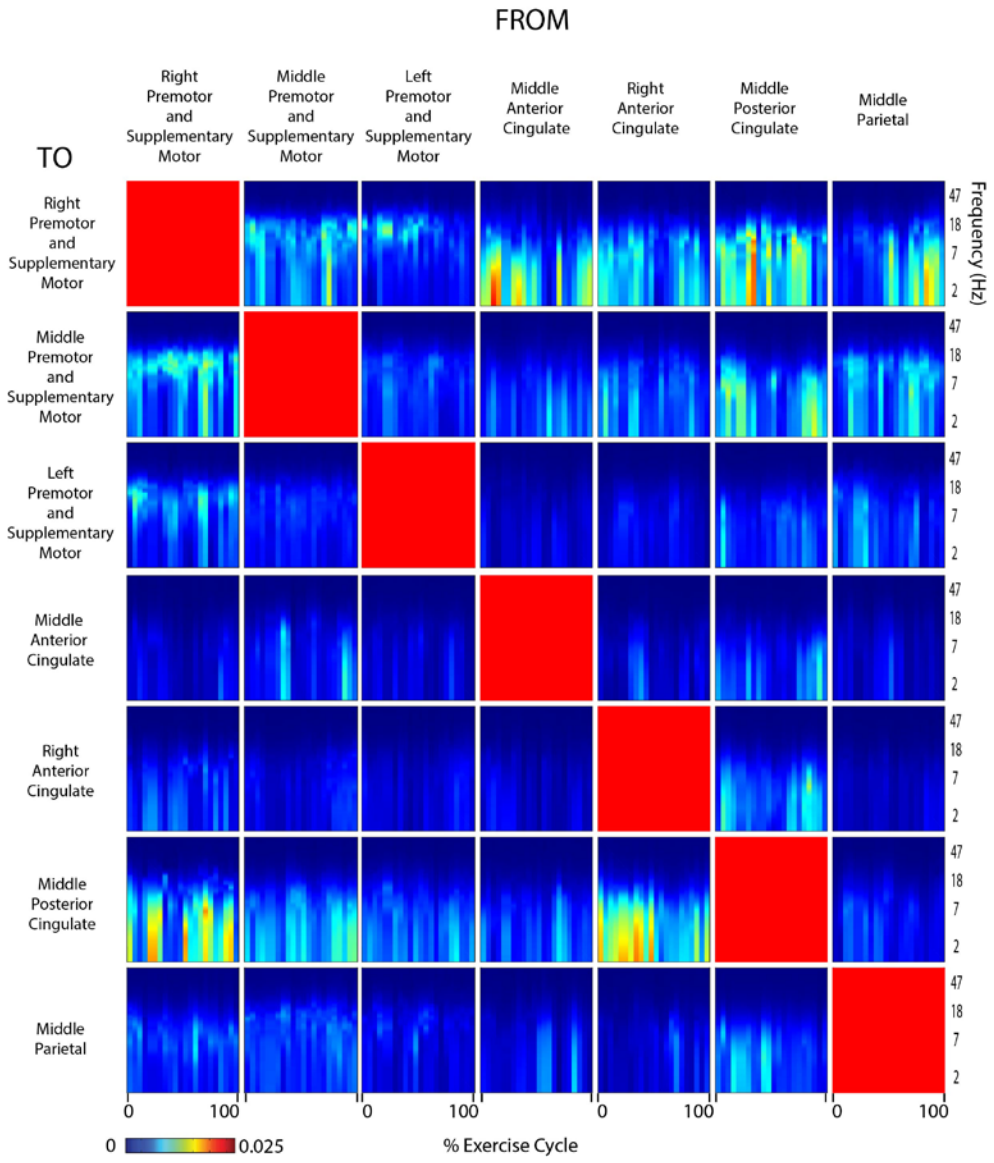

Supplementary Figure 4-5. Connectivity Other Viewed Arms and Legs. Diagram showing directed transfer function connectivity values between pairs of cortical areas while the subjects VIEWED a video of ANOTHER PERSON exercising with their ARMS and LEGS. Each individual plot starts and ends with the viewed left leg fully extended. The numbers on the x-axis indicate the % of the movement cycle. We set non-significant differences to 0 (blue).

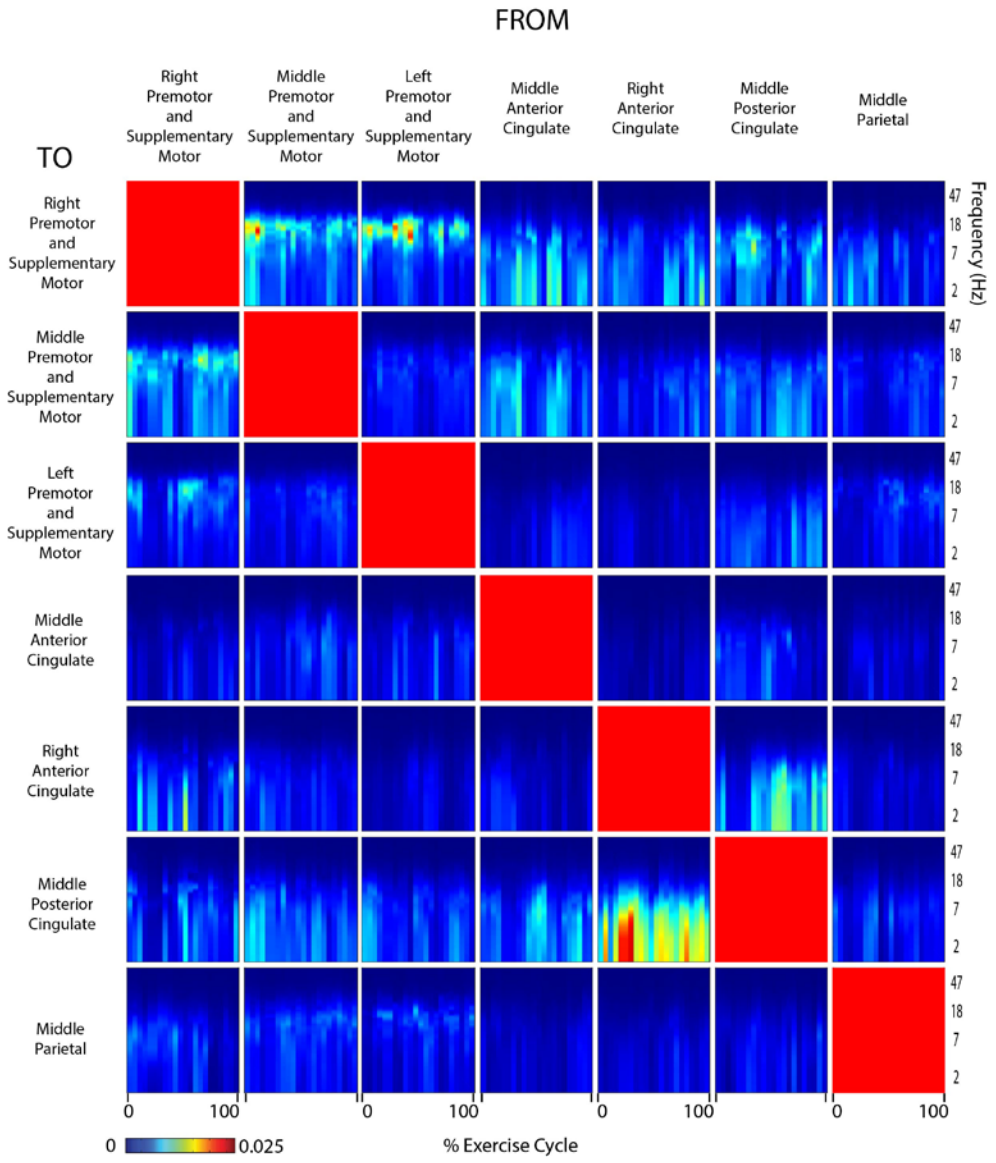

Supplementary Figure 4-6. Connectivity Other Viewed Legs. Diagram showing directed transfer function connectivity values between pairs of cortical areas while the subjects VIEWED a video of ANOTHER PERSON exercising with only the LEGS. Each individual plot starts and ends with the viewed left leg fully extended. The numbers on the x-axis indicate the % of the movement cycle. We set non-significant differences to 0 (blue).

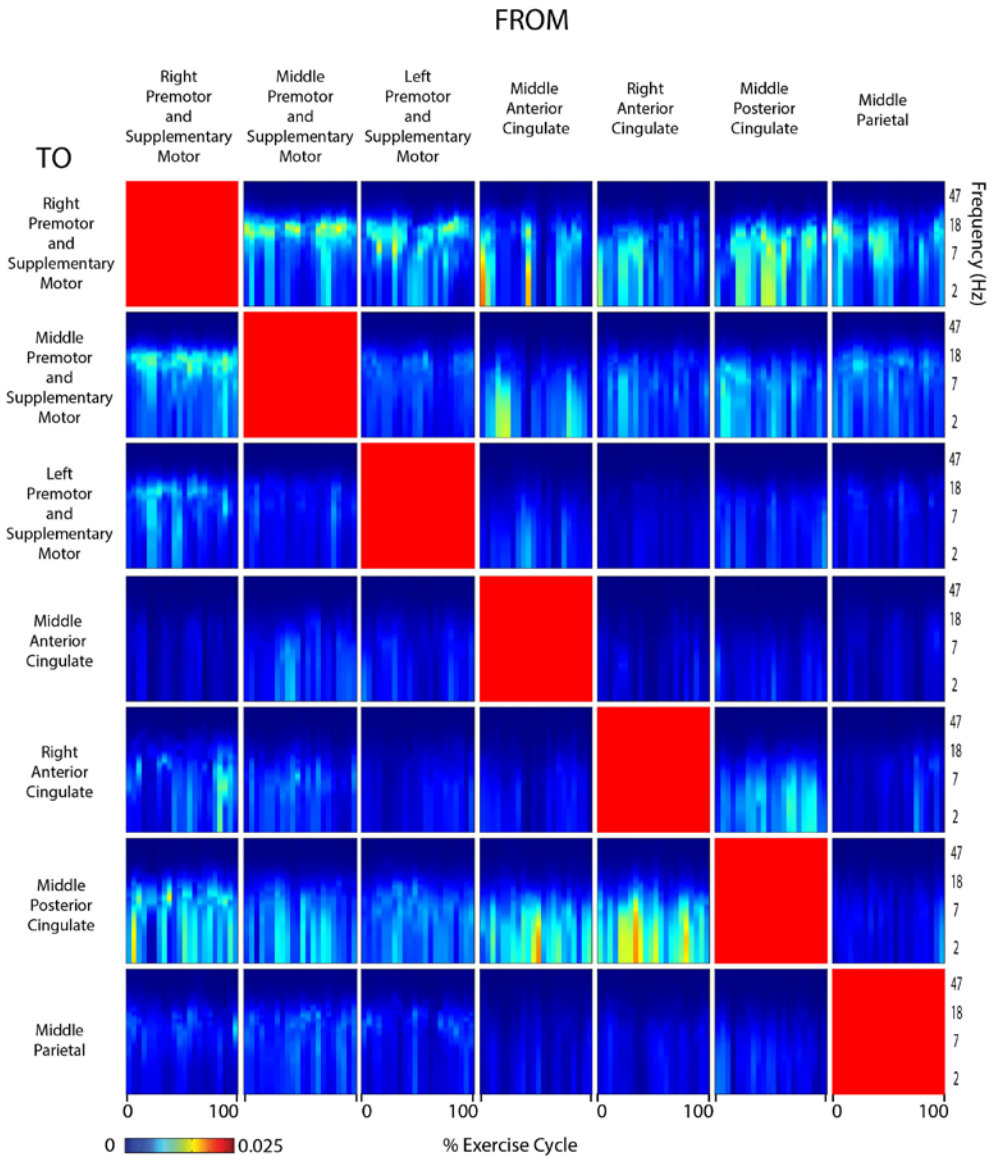

Supplementary Figure 4-7. Connectivity Viewed Stepper. Diagram showing directed transfer function connectivity values between pairs of cortical areas while the subjects VIEWED a video of the RECUMBENT STEPPER moving on its own, with no one seated in it. Each individual plot starts and ends with where the left leg would have been fully extended, had a person been seated in it. We set non-significant differences to 0 (blue).

Chapter 5: Discussion and Conclusion

The main purpose of this dissertation was to use high-density electroencephalography (EEG) and independent component analysis (ICA) to gain a deeper understanding of how the human brain coordinates movement. The specific goals of the projects contained herein were to: 1) Examine how multi-tasking walking and a complex cognitive task affects task performance and gait parameters across speed, 2) isolate and characterize just the gait-related movement artifact captured by EEG at a range of walking speeds and test methods of mitigating this artifact, and 3) quantify the relative amounts of cortical activation and cortical effective connectivity induced by active and viewed rhythmic exercise with varying levels of upper and lower limb effort.

The main finding of study 1 was that walking did not affect the performance of a spatial cognitive task in young, healthy individuals. The subjects showed no change in response accuracy or reaction time for the Brooks spatial memory task across the range of speeds tested (0.0 m/s to 1.6 m/s). We detected strong electrocortical spectral fluctuations in the somatosensory association cortex around the time of memory encoding. These spectral fluctuations were also unchanged across walking speeds. The addition of the Brooks task to walking caused the subjects to adopt a significantly greater step width across all speeds. Wider steps have been associated with more stable gait (Bauby and Kuo, 2000; McAndrew Young and Dingwell, 2012) and may indicate high cognitive load. The results of this study are significant, because they indicate that young, healthy subjects have the cognitive capacities to perform challenging spatial tasks, even at high walking speeds, with no

decrease in task performance. This finding contradicts a popular view that walking while thinking can decrease thinking ability (Kahneman 2011) and supports the recent trends of walking meetings and treadmill desks.

In study 2, the movement artifact patterns recorded by EEG electrodes on the novel interface showed strong gait-locked spectral fluctuations. These spectral fluctuations increased in amplitude and occurred in higher frequency bands as walking speed increased. Some, but not all, of the average artifact plots show decreased spectral power during the swing phase and increased spectral power during double support. This suggests that previous studies reporting spectral power increases during double support and spectral power decreases during swing (Gwin et al., 2011, Cheron et al., 2012, Severens et al., 2012) may have reported a combination of artifact and true neural activity. The results of these studies need to be interpreted with caution.

Furthermore, the movement artifact in our study varied across subject, speed, and electrode location. The artifact was not similar to the spectral fluctuations captured by an accelerometer placed on the head, indicating that accelerometry cannot fully capture the movement artifact that pollutes EEG electrodes during walking. We applied some standard cleaning methods (wavelets, moving average subtraction, and a combination of both) to the artifact data, however these methods were insufficient to remove all artifact. These findings are important because they highlight and quantify limitations in current EEG techniques and data cleaning methods.

The first main finding of study 3 was that cortical spectral fluctuations occurred in the motor and cingulate cortical areas when young, healthy subjects performed rhythmic exercise with 1) both their arms and legs, and 2) just their legs, and 3) just their arms. Desynchronization often occurred

in the alpha band when the contralateral limb was extending and was consistent with event-related desynchronization (Pfurtscheller and Lopes da Silva 1999; Pfurtscheller et al. 1996). However, cortical spectral fluctuations, especially in the alpha and beta band, were much larger during the arms exercise conditions than during the legs only exercise condition. This suggests that rhythmic arm exercise is much more dependent on descending cortical commands than rhythmic leg exercise. Contrary to our hypothesis, we did not detect robust spectral fluctuations, except in the gamma band, during the viewed motion conditions. Overall, these results are important because they suggest that adding upper limb effort to a lower limb rehabilitation task may increase cortical engagement and trigger neuroplasticity.

The second main finding of study 3 was that cortical effective connectivity fluctuations occur in a similar brain network during active and viewed full-body movement. During most active and viewed conditions, the right premotor and supplementary motor cortex was the hub of information flow, receiving connections from the other two premotor and supplementary motor areas (middle and left) and from the middle anterior and posterior cingulate areas. This suggest a right hemisphere dominance for the control of full-body movement tasks with no balance requirements. During all active and viewed movement conditions, the overall connectivity between cortical areas fluctuated at 0.5, 1, 1.5, and 2 times the exercise frequency. This provides further evidence that cortical communication during actual and viewed motion is related to the pace of the movement. This finding adds to our understanding of how the cortex controls active full-body movement and processes viewed full-body movement.

The studies contained in this thesis had several limitations, and more work needs to be done to advance this line of work. Study 1 only focused on young, healthy subjects and only tested one

cognitive task. To truly understand the interplay between walking speed and multi-tasking, many groups of individuals (young, elderly, subjects with neurological impairments, etc.) should be tested while walking with a diverse range of cognitive tasks of varying difficulty levels. Another limitation of study 1 is that there is no way to know if the wider stance adopted when the subjects walked with the cognitive task was indicative of true cognitive load or if it was related to the way the subjects responded to the cognitive task. The subjects typed the Brooks grids into the handheld keypad approximately 5-7 times per walking trial. They may have adopted a wider stance in order to better stabilize themselves while they walked and typed on the keypad. To eliminate this ambiguity, a future study could again have subjects walk with and without the Brooks task, but during the walking only trial subjects could be cued to type 9 random numbers into their keypad 5-7 times per trial.

Study 2 was limited by the fact that the wig/conductive gel interface did not precisely match the impedance of actual human scalp. A more exact match may have produced better results. The findings of study 2 could also be extended by creating an EEG system with coupled electrode pairs, one of which would measure just movement artifact and one of which would measure brain signal plus movement artifact. In the future, this could allow the subtraction of movement artifact from EEG data in real time.

For study 3, we were not able to detect the robust spectral fluctuations that we hypothesized would occur in the viewed motion conditions. This may be because we gave our subjects a fixation point to prevent overt head movements, which did not allow their eyes to freely scan the scene during the viewed conditions. Also, we could not gage the subjects' level of effort, so we had no way to know if they kept their attention focused on the viewed task. Future studies with no gaze

constraints and a way to gage subject effort may produce different results for the viewed conditions. Another limitation for study 3 is the fact that the increased anterior cingulate recruitment seen during the arms condition may have been due to larger shifts in the subjects' center of mass when moving with the arms versus moving with the legs on the recumbent stepper. Because of this confounding factor, we cannot say with precision that rhythmic arm movement induces more anterior cingulate activity than rhythmic leg movement.

Despite some drawbacks, the studies contained in this thesis advance our knowledge about how the human cortex functions during full-body motion. Young, healthy subjects are able to walk and perform a complex spatial cognitive task at many speeds with no change in task performance or task-related electrocortical spectral fluctuations. Spectral fluctuations induced by movement artifact can occur in the same frequency bands as true electrocortical spectral fluctuations, so studies of EEG and walking need to be interpreted with caution. The cortex is much more cyclically active during rhythmic arm movement than rhythmic leg movement, suggesting that human rhythmic arm motion is under stronger cortical control than rhythmic leg motion. Finally, effective connectivity in a network driven by the right premotor and supplementary motor cortex fluctuates at harmonics of the movement frequency during active and viewed full-body movement.

References

Adeli, H., Zhou, Z., and Dadmehr, N. (2003). Analysis of EEG records in an epileptic patient using wavelet transform. *J Neurosci Methods* 123**,** 69-87.

Al-Yahya, E., Dawes, H., Collett, J., Howells, K., Izadi, H., Wade, D.T., and Cockburn, J. (2009). Gait adaptations to simultaneous cognitive and mechanical constraints. *Exp Brain Res* 199**,** 39-48. doi: 10.1007/s00221-009-1968-1.

Al-Yahya, E., Dawes, H., Smith, L., Dennis, A., Howells, K., and Cockburn, J. (2011). Cognitive motor interference while walking: a systematic review and meta-analysis. *Neurosci Biobehav Rev* 35**,** 715-728. doi: 10.1016/j.neubiorev.2010.08.008.

Alderman, B.L., Olson, R.L., and Mattina, D.M. (2014). Cognitive function during low-intensity walking: a test of the treadmill workstation. *J Phys Act Health* 11**,** 752-758. doi: 10.1123/jpah.2012-0097.

Anguera, J.A., Reuter-Lorenz, P.A., Willingham, D.T., and Seidler, R.D. (2010). Contributions of Spatial Working Memory to Visuomotor Learning. *Journal of Cognitive Neuroscience* 22**,** 1917-1930. doi: DOI 10.1162/jocn.2009.21351.

Arrington, C.M., Carr, T.H., Mayer, A.R., and Rao, S.M. (2000). Neural mechanisms of visual attention: object-based selection of a region in space. *J Cogn Neurosci* 12 Suppl 2**,** 106-117. doi: 10.1162/089892900563975.

Avanzini, P., Fabbri-Destro, M., Dalla Volta, R., Daprati, E., Rizzolatti, G., and Cantalupo, G. (2012). The dynamics of sensorimotor cortical oscillations during the observation of hand movements: an EEG study. *PLoS One* 7**,** e37534. doi: 10.1371/journal.pone.0037534.

Bastiaansen, M.C.M., Posthuma, D., Groot, P.F.C., and De Geus, E.J.C. (2002). Event-related alpha and theta responses in a visuo-spatial working memory task. *Clinical Neurophysiology* 113**,** 1882-1893. doi: Pii S1388-2457(02)00303-6

Doi 10.1016/S1388-2457(02)00303-6.

Bauby, C.E., and Kuo, A.D. (2000). Active control of lateral balance in human walking. *Journal of Biomechanics* 33**,** 1433-1440. doi: Doi 10.1016/S0021-9290(00)00101-9.

Beauchet, O., Dubost, V., Stierlam, F., Blanchon, M.A., Mourey, F., Pfitzenmeyer, P., Gonthier, R., and Kressig, R.W. (2002). Study of the influence of a specific cognitive task on spatial-temporal walking parameters in fragile elderly patients. *Presse Medicale* 31**,** 1117-1122.

Behrman, A.L., Lawless-Dixon, A.R., Davis, S.B., Bowden, M.G., Nair, P., Phadke, C., Hannold, E.M., Plummer, P., and Harkema, S.J. (2005). Locomotor training progression and outcomes after incomplete spinal cord injury. *Physical Therapy* 85**,** 1356-1371.

Beres-Jones, J.A., and Harkema, S.J. (2004). The human spinal cord interprets velocity-dependent afferent input during stepping. *Brain* 127**,** 2232-2246. doi: 10.1093/brain/awh252.

Biswal, B., Yetkin, F.Z., Haughton, V.M., and Hyde, J.S. (1995). Functional Connectivity in the Motor Cortex of Resting Human Brain Using Echo-Planar Mri. *Magnetic Resonance in Medicine* 34**,** 537-541. doi: DOI 10.1002/mrm.1910340409.

Bowen, A., Mckenna, K., and Tallis, R.C. (1999). Reasons for variability in the reported rate of occurrence of unilateral spatial neglect after stroke. *Stroke* 30**,** 1196-1202.

Brooks, L.R. (1967). The suppression of visualization by reading. *Q J Exp Psychol* 19**,** 289-299. doi: 10.1080/14640746708400105.

Brown, T.G. (1914). On the nature of the fundamental activity of the nervous centres; together with an analysis of the conditioning of rhythmic activity in progression, and a theory of the evolution of function in the nervous system. *J Physiol* 48**,** 18-46.

Buccino, G. (2014). Action observation treatment: a novel tool in neurorehabilitation. *Philos Trans R Soc Lond B Biol Sci* 369**,** 20130185. doi: 10.1098/rstb.2013.0185.

Buccino, G., Arisi, D., Gough, P., Aprile, D., Ferri, C., Serotti, L., Tiberti, A., and Fazzi, E. (2012). Improving upper limb motor functions through action observation treatment: a pilot study in children with cerebral palsy. *Developmental Medicine and Child Neurology* 54**,** 822-828. doi: DOI 10.1111/j.1469-8749.2012.04334.x.

Buccino, G., Binkofski, F., Fink, G.R., Fadiga, L., Fogassi, L., Gallese, V., Seitz, R.J., Zilles, K., Rizzolatti, G., and Freund, H.J. (2001). Action observation activates premotor and parietal areas in a somatotopic manner: an fMRI study. *Eur J Neurosci* 13**,** 400-404.

Burke, J.F., Zaghloul, K.A., Jacobs, J., Williams, R.B., Sperling, M.R., Sharan, A.D., and Kahana, M.J. (2013). Synchronous and asynchronous theta and gamma activity during episodic memory formation. *J Neurosci* 33**,** 292-304. doi: 10.1523/JNEUROSCI.2057-12.2013.

Bush, G., Luu, P., and Posner, M.I. (2000). Cognitive and emotional influences in anterior cingulate cortex. *Trends Cogn Sci* 4**,** 215-222.

Cabeza, R., Mcintosh, A.R., Tulving, E., Nyberg, L., and Grady, C.L. (1997). Age-related differences in effective neural connectivity during encoding and recall. *Neuroreport* 8**,** 3479-3483. doi: Doi 10.1097/00001756-199711100-00013.

Calmels, C., Holmes, P., Jarry, G., Leveque, J.M., Hars, M., and Stam, C.J. (2006). Cortical activity prior to, and during, observation and execution of sequential finger movements. *Brain Topogr* 19**,** 77-88. doi: 10.1007/s10548-006-0014-x.

Camicioli, R., Bouchard, T., and Licis, L. (2006). Dual-tasks and walking fast: relationship to extra-pyramidal signs in advanced Alzheimer disease. *J Neurol Sci* 248**,** 205-209. doi: 10.1016/j.jns.2006.05.013.

Carlesimo, G.A., Perri, R., Turriziani, P., Tomaiuolo, F., and Caltagirone, C. (2001). Remembering What But Not Where: Independence of Spatial and Visual Working Memory in the Human Brain. *Cortex* 37**,** 519-534. doi: 10.1016/s0010-9452(08)70591-4.

Castermans, T., Duvinage, M., Cheron, G., and Dutoit, T. (2014). About the cortical origin of the low-delta and high-gamma rhythms observed in EEG signals during treadmill walking. *Neurosci Lett* 561**,** 166-170. doi: 10.1016/j.neulet.2013.12.059.

Cevallos, C., Zarka, D., Hoellinger, T., Leroy, A., Dan, B., and Cheron, G. (2015). Oscillations in the human brain during walking execution, imagination and observation. *Neuropsychologia*. doi: 10.1016/j.neuropsychologia.2015.06.039.

Cheron, G., Duvinage, M., De Saedeleer, C., Castermans, T., Bengoetxea, A., Petieau, M., Seetharaman, K., Hoellinger, T., Dan, B., Dutoit, T., Sylos Labini, F., Lacquaniti, F., and Ivanenko, Y. (2012). From spinal central pattern generators to cortical network: integrated BCI for walking rehabilitation. *Neural Plast* 2012**,** 375148. doi: 10.1155/2012/375148.

Chowdhury, M.E., Mullinger, K.J., Glover, P., and Bowtell, R. (2014). Reference layer artefact subtraction (RLAS): a novel method of minimizing EEG artefacts during simultaneous fMRI. *Neuroimage* 84**,** 307-319. doi: 10.1016/j.neuroimage.2013.08.039.

Cochin, S., Barthelemy, C., Lejeune, B., Roux, S., and Martineau, J. (1998). Perception of motion and qEEG activity in human adults. *Electroencephalogr Clin Neurophysiol* 107**,** 287-295.

Cochin, S., Barthelemy, C., Roux, S., and Martineau, J. (1999). Observation and execution of movement: similarities demonstrated by quantified electroencephalography. *Eur J Neurosci* 11**,** 1839-1842.

Collins, S., Ruina, A., Tedrake, R., and Wisse, M. (2005). Efficient bipedal robots based on passive-dynamic walkers. *Science* 307**,** 1082-1085. doi: 10.1126/science.1107799.

Corbetta, M., Kincade, J.M., Ollinger, J.M., Mcavoy, M.P., and Shulman, G.L. (2000). Voluntary orienting is dissociated from target detection in human posterior parietal cortex (vol 3, pg 292, 2000). *Nature Neuroscience* 3**,** 521-521. doi: Doi 10.1038/74905.

Daubechies, I. (1988). Orthonormal Bases of Compactly Supported Wavelets. *Communications on Pure and Applied Mathematics* 41**,** 909-996. doi: DOI 10.1002/cpa.3160410705.

Delorme, A., and Makeig, S. (2004). EEGLAB: an open source toolbox for analysis of single-trial EEG dynamics including independent component analysis. *J Neurosci Methods* 134**,** 9-21. doi: 10.1016/j.jneumeth.2003.10.009.

Delorme, A., Palmer, J., Onton, J., Oostenveld, R., and Makeig, S. (2012). Independent EEG sources are dipolar. *PLoS One* 7**,** e30135. doi: 10.1371/journal.pone.0030135.

Di Pellegrino, G., Fadiga, L., Fogassi, L., Gallese, V., and Rizzolatti, G. (1992). Understanding motor events: a neurophysiological study. *Exp Brain Res* 91**,** 176-180.

Dobkin, B.H., Harkema, S., Requejo, P., and Edgerton, V.R. (1995). Modulation of locomotor-like EMG activity in subjects with complete and incomplete spinal cord injury. *J Neurol Rehabil* 9**,** 183-190.

Dubost, V., Kressig, R.W., Gonthier, R., Herrmann, F.R., Aminian, K., Najafi, B., and Beauchet, O. (2006). Relationships between dual-task related changes in stride velocity and stride time variability in healthy older adults. *Hum Mov Sci* 25**,** 372-382. doi: 10.1016/j.humov.2006.03.004.

Duysens, J., and Van De Crommert, H.W. (1998). Neural control of locomotion; The central pattern generator from cats to humans. *Gait Posture* 7**,** 131-141.

Ertelt, D., Small, S., Solodkin, A., Dettmers, C., Mcnamara, A., Binkofski, F., and Buccino, G. (2007). Action observation has a positive impact on rehabilitation of motor deficits after stroke. *Neuroimage* 36**,** T164-T173. doi: DOI 10.1016/j.neuroimage.2007.03.043.

Ferris, D.P., Gordon, K.E., Beres-Jones, J.A., and Harkema, S.J. (2004). Muscle activation during unilateral stepping occurs in the nonstepping limb of humans with clinically complete spinal cord injury. *Spinal Cord* 42**,** 14-23. doi: DOI 10.1038/sj.sc.3101542.

Fish, R.M., Geddes, L.A., and Babbs, C.F. (2003). *Medical and bioengineering aspects of electrical injuries.* Tucson, AZ: Lawyers & Judges Pub. Co.

Flaherty, A.W. (2011). Brain Illness and Creativity: Mechanisms and Treatment Risks. *Canadian Journal of Psychiatry-Revue Canadienne De Psychiatrie* 56**,** 132-143.

Friese, U., Koster, M., Hassler, U., Martens, U., Trujillo-Barreto, N., and Gruber, T. (2012). Successful memory encoding is associated with increased cross-frequency coupling between frontal theta and posterior gamma oscillations in human scalp-recorded EEG. *Neuroimage* 66C**,** 642-647. doi: 10.1016/j.neuroimage.2012.11.002.

Gallese, V., Keysers, C., and Rizzolatti, G. (2004). A unifying view of the basis of social cognition. *Trends Cogn Sci* 8**,** 396-403. doi: 10.1016/j.tics.2004.07.002.

Genovese, C.R., Lazar, N.A., and Nichols, T. (2002). Thresholding of statistical maps in functional neuroimaging using the false discovery rate. *Neuroimage* 15**,** 870-878. doi: 10.1006/nimg.2001.1037.

Grabiner, M.D., and Troy, K.L. (2005). Attention demanding tasks during treadmill walking reduce step width variability in young adults. *J Neuroeng Rehabil* 2**,** 25. doi: 10.1186/1743-0003-2-25.

Gramann, K., Gwin, J.T., Bigdely-Shamlo, N., Ferris, D.P., and Makeig, S. (2010). Visual evoked responses during standing and walking. *Front Hum Neurosci* 4**,** 202. doi: 10.3389/fnhum.2010.00202.

Gramann, K., Gwin, J.T., Ferris, D.P., Oie, K., Jung, T.P., Lin, C.T., Liao, L.D., and Makeig, S. (2011). Cognition in action: imaging brain/body dynamics in mobile humans. *Rev Neurosci* 22**,** 593-608. doi: 10.1515/RNS.2011.047.

Granacher, U., Bridenbaugh, S.A., Muehlbauer, T., Wehrle, A., and Kressig, R.W. (2011). Age-related effects on postural control under multi-task conditions. *Gerontology* 57**,** 247-255. doi: 10.1159/000322196.

Greicius, M.D., Krasnow, B., Reiss, A.L., and Menon, V. (2003). Functional connectivity in the resting brain: a network analysis of the default mode hypothesis. *Proc Natl Acad Sci U S A* 100**,** 253-258. doi: 10.1073/pnas.0135058100.

Grezes, J., Armony, J.L., Rowe, J., and Passingham, R.E. (2003). Activations related to "mirror" and "canonical" neurones in the human brain: an fMRI study. *Neuroimage* 18**,** 928-937.

Grillner, S. (1975). Locomotion in Vertebrates - Central Mechanisms and Reflex Interaction. *Physiological Reviews* 55**,** 247-304.

Grillner, S., Deliagina, T., Ekeberg, O., El Manira, A., Hill, R.H., Lansner, A., Orlovsky, G.N., and Wallen, P. (1995). Neural networks that co-ordinate locomotion and body orientation in lamprey. *Trends Neurosci* 18**,** 270-279.

Grubaugh, J., and Rhea, C.K. (2014). Gait performance is not influenced by working memory when walking at a self-selected pace. *Exp Brain Res* 232**,** 515-525. doi: 10.1007/s00221-013-3759-y.

Gwin, J.T., Gramann, K., Makeig, S., and Ferris, D.P. (2010). Removal of movement artifact from high-density EEG recorded during walking and running. *J Neurophysiol* 103**,** 3526-3534. doi: 10.1152/jn.00105.2010.

Gwin, J.T., Gramann, K., Makeig, S., and Ferris, D.P. (2011). Electrocortical activity is coupled to gait cycle phase during treadmill walking. *Neuroimage* 54**,** 1289-1296. doi: 10.1016/j.neuroimage.2010.08.066.

Harada, T., Miyai, I., Suzuki, M., and Kubota, K. (2009). Gait capacity affects cortical activation patterns related to speed control in the elderly. *Exp Brain Res* 193**,** 445-454. doi: 10.1007/s00221-008-1643-y.

Hardman, A.E., and Morris, J.N. (1998). Walking to health. *Br J Sports Med* 32**,** 184.

Harris, I.M., Egan, G.F., Sonkkila, C., Tochon-Danguy, H.J., Paxinos, G., and Watson, J.D. (2000). Selective right parietal lobe activation during mental rotation: a parametric PET study. *Brain* 123 (Pt 1)**,** 65-73.

Heilman, K.M., Valenstein, E., and Watson, R.T. (2000). Neglect and related disorders. *Semin Neurol* 20**,** 463-470. doi: 10.1055/s-2000-13179.

Hollman, J.H., Youdas, J.W., and Lanzino, D.J. (2011). Gender differences in dual task gait performance in older adults. *Am J Mens Health* 5**,** 11-17. doi: 10.1177/1557988309357232.

Iacoboni, M., Woods, R.P., Brass, M., Bekkering, H., Mazziotta, J.C., and Rizzolatti, G. (1999). Cortical mechanisms of human imitation. *Science* 286**,** 2526-2528. doi: DOI 10.1126/science.286.5449.2526.

Irani, F., Platek, S.M., Bunce, S., Ruocco, A.C., and Chute, D. (2007). Functional near infrared spectroscopy (fNIRS): an emerging neuroimaging technology with important applications for the study of brain disorders. *Clin Neuropsychol* 21**,** 9-37. doi: 10.1080/13854040600910018.

Isaev, G.G., Gerasimenko, Y.P., Selionov, V.A., and Kartashova, N.A. (2004). Respiratory responses to voluntary and reflexly-induced stepping movements in normal subjects and spinal patients. *J Physiol Pharmacol* 55 Suppl 3**,** 77-82.

Itthipuripat, S., Wessel, J.R., and Aron, A.R. (2013). Frontal theta is a signature of successful working memory manipulation. *Exp Brain Res* 224**,** 255-262. doi: 10.1007/s00221-012-3305-3.

Jahn, K., Deutschländer, A., Stephan, T., Kalla, R., Hüfner, K., Wagner, J., Strupp, M., and Brandt, T. (2008). Supraspinal locomotor control in quadrupeds and humans. 171**,** 353-362. doi: 10.1016/s0079-6123(08)00652-3.

Jain, S., Gourab, K., Schindler-Ivens, S., and Schmit, B.D. (2013). EEG during pedaling: evidence for cortical control of locomotor tasks. *Clin Neurophysiol* 124**,** 379-390. doi: 10.1016/j.clinph.2012.08.021.

John, D., Bassett, D., Thompson, D., Fairbrother, J., and Baldwin, D. (2009). Effect of Using a Treadmill Workstation on Performance of Simulated Office Work Tasks. *Journal of Physical Activity & Health* 6**,** 617-624.

Joseph, R. (1988). The Right Cerebral Hemisphere - Emotion, Music, Visual-Spatial Skills, Body-Image, Dreams, and Awareness. *Journal of Clinical Psychology* 44**,** 630-673. doi: Doi 10.1002/1097-4679(198809)44:5<630::Aid-Jclp2270440502>3.0.Co;2-V.

Jung, T.P., Makeig, S., Humphries, C., Lee, T.W., Mckeown, M.J., Iragui, V., and Sejnowski, T.J. (2000a). Removing electroencephalographic artifacts by blind source separation. *Psychophysiology* 37**,** 163-178.

Jung, T.P., Makeig, S., Westerfield, M., Townsend, J., Courchesne, E., and Sejnowski, T.J. (2000b). Removal of eye activity artifacts from visual event-related potentials in normal and clinical subjects. *Clin Neurophysiol* 111**,** 1745-1758.

Juvin, L., Simmers, J., and Morin, D. (2005). Propriospinal circuitry underlying interlimb coordination in mammalian quadrupedal locomotion. *J Neurosci* 25**,** 6025-6035. doi: 10.1523/JNEUROSCI.0696-05.2005.

Kahneman, D. (2013). *Thinking, fast and slow.* New York: Farrar, Straus and Giroux.

Kaminski, M.J., and Blinowska, K.J. (1991). A New Method of the Description of the Information-Flow in the Brain Structures. *Biological Cybernetics* 65**,** 203-210. doi: Doi 10.1007/Bf00198091.

Kelly, V.E., Eusterbrock, A.J., and Shumway-Cook, A. (2012a). The effects of instructions on dual-task walking and cognitive task performance in people with Parkinson's disease. *Parkinsons Dis* 2012**,** 671261. doi: 10.1155/2012/671261.

Kelly, V.E., Eusterbrock, A.J., and Shumway-Cook, A. (2012b). A review of dual-task walking deficits in people with Parkinson's disease: motor and cognitive contributions, mechanisms, and clinical implications. *Parkinsons Dis* 2012**,** 918719. doi: 10.1155/2012/918719.

Kerr, B., Condon, S.M., and Mcdonald, L.A. (1985). Cognitive spatial processing and the regulation of posture. *J Exp Psychol Hum Percept Perform* 11**,** 617-622.

Kiran, S., Meier, E.L., Kapse, K.J., and Glynn, P.A. (2015). Changes in task-based effective connectivity in language networks following rehabilitation in post-stroke patients with aphasia. *Frontiers in Human Neuroscience* 9. doi: Artn 316

Doi 10.3389/Fnhum.2015.00316.

Kline, J.E., Huang, H.J., Snyder, K.L., and Ferris, D.P. (2015). Isolating gait-related movement artifacts in electroencephalography during human walking. *J Neural Eng* 12**,** 046022. doi: 10.1088/1741-2560/12/4/046022.

Kline, J.E., Poggensee, K., and Ferris, D.P. (2014). Your brain on speed: cognitive performance of a spatial working memory task is not affected by walking speed. *Front Hum Neurosci* 8**,** 288. doi: 10.3389/fnhum.2014.00288.

Kuo, A.D. (2007). The six determinants of gait and the inverted pendulum analogy: A dynamic walking perspective. *Hum Mov Sci* 26**,** 617-656. doi: 10.1016/j.humov.2007.04.003.

Lau, T.M., Gwin, J.T., Mcdowell, K.G., and Ferris, D.P. (2012). Weighted phase lag index stability as an artifact resistant measure to detect cognitive EEG activity during locomotion. *J Neuroeng Rehabil* 9**,** 47. doi: 10.1186/1743-0003-9-47.

Lenartowicz, A., Delorme, A., Walshaw, P.D., Cho, A.L., Bilder, R.M., Mcgough, J.J., Mccracken, J.T., Makeig, S., and Loo, S.K. (2014). Electroencephalography correlates of spatial working memory deficits in attention-deficit/hyperactivity disorder: vigilance, encoding, and maintenance. *J Neurosci* 34**,** 1171-1182. doi: 10.1523/JNEUROSCI.1765-13.2014.

Lindenberger, U., Marsiske, M., and Baltes, P.B. (2000). Memorizing while walking: Increase in dual-task costs from young adulthood to old age. *Psychology and Aging* 15**,** 417-436. doi: Doi 10.1037//0882-7974.15.3.417.

Maegele, M., Muller, S., Wernig, A., Edgerton, V.R., and Harkema, S.J. (2002). Recruitment of spinal motor pools during voluntary movements versus stepping after human spinal cord injury. *J Neurotrauma* 19**,** 1217-1229. doi: 10.1089/08977150260338010.

Makeig, S. (1993). Auditory event-related dynamics of the EEG spectrum and effects of exposure to tones. *Electroencephalogr Clin Neurophysiol* 86**,** 283-293.

Makeig, S., Bell, A.J., Jung, T.P., and Sejnowski, T.J. (1996). Independent component analysis of electroencephalographic data. *Advances in Neural Information Processing Systems 8* 8**,** 145-151.

Makeig, S., Debener, S., Onton, J., and Delorme, A. (2004a). Mining event-related brain dynamics. *Trends Cogn Sci* 8**,** 204-210. doi: 10.1016/j.tics.2004.03.008.

Makeig, S., Delorme, A., Westerfield, M., Jung, T.P., Townsend, J., Courchesne, E., and Sejnowski, T.J. (2004b). Electroencephalographic brain dynamics following manually responded visual targets. *PLoS Biol* 2**,** e176. doi: 10.1371/journal.pbio.0020176.

Makeig, S., and Jung, T.P. (1996). Tonic, phasic, and transient EEG correlates of auditory awareness in drowsiness. *Brain Res Cogn Brain Res* 4**,** 15-25.

Manthey, S., Schubotz, R.I., and Von Cramon, D.Y. (2003). Premotor cortex in observing erroneous action: an fMRI study. *Brain Res Cogn Brain Res* 15**,** 296-307.

Marder, E., and Calabrese, R.L. (1996). Principles of rhythmic motor pattern generation. *Physiol Rev* 76**,** 687-717.

Mcandrew Young, P.M., and Dingwell, J.B. (2012). Voluntary changes in step width and step length during human walking affect dynamic margins of stability. *Gait Posture* 36**,** 219-224. doi: 10.1016/j.gaitpost.2012.02.020.

Mcgeer, T. (1993). Dynamics and control of bipedal locomotion. *J Theor Biol* 163**,** 277-314. doi: 10.1006/jtbi.1993.1121.

Melzer, I., and Oddsson, L.I. (2004). The effect of a cognitive task on voluntary step execution in healthy elderly and young individuals. *J Am Geriatr Soc* 52**,** 1255-1262. doi: 10.1111/j.1532-5415.2004.52353.x.

Miyai, I., Tanabe, H.C., Sase, I., Eda, H., Oda, I., Konishi, I., Tsunazawa, Y., Suzuki, T., Yanagida, T., and Kubota, K. (2001). Cortical mapping of gait in humans: a near-infrared spectroscopic topography study. *Neuroimage* 14**,** 1186-1192. doi: 10.1006/nimg.2001.0905.

Mullen, T., Acar, Z.A., Worrell, G., and Makeig, S. (2011). Modeling cortical source dynamics and interactions during seizure. *Conf Proc IEEE Eng Med Biol Soc* 2011**,** 1411-1414. doi: 10.1109/IEMBS.2011.6090332.

Mullen, T., Kothe, C., Chi, Y.M., Ojeda, A., Kerth, T., Makeig, S., Cauwenberghs, G., and Jung, T.P. (2013). Real-time modeling and 3D visualization of source dynamics and connectivity using wearable EEG. *Conf Proc IEEE Eng Med Biol Soc* 2013**,** 2184-2187. doi: 10.1109/EMBC.2013.6609968.

Nadkarni, N.K., Zabjek, K., Lee, B., Mcilroy, W.E., and Black, S.E. (2010). Effect of working memory and spatial attention tasks on gait in healthy young and older adults. *Motor Control* 14**,** 195-210.

O'connell, R.G., Dockree, P.M., Bellgrove, M.A., Kelly, S.P., Hester, R., Garavan, H., Robertson, I.H., and Foxe, J.J. (2007). The role of cingulate cortex in the detection of errors with and without awareness: a high-density electrical mapping study. *Eur J Neurosci* 25**,** 2571-2579. doi: 10.1111/j.1460-9568.2007.05477.x.

O'regan, S., Faul, S., and Marnane, W. (2013). Automatic detection of EEG artefacts arising from head movements using EEG and gyroscope signals. *Med Eng Phys* 35**,** 867-874; discussion 867. doi: 10.1016/j.medengphy.2012.08.017.

O'regan, S., and Marnane, W. (2013). Multimodal detection of head-movement artefacts in EEG. *J Neurosci Methods* 218**,** 110-120. doi: 10.1016/j.jneumeth.2013.04.017.

Oberman, L.M., Pineda, J.A., and Ramachandran, V.S. (2007). The human mirror neuron system: a link between action observation and social skills. *Soc Cogn Affect Neurosci* 2**,** 62-66. doi: 10.1093/scan/nsl022.

Oostenveld, R., and Oostendorp, T.F. (2002). Validating the boundary element method for forward and inverse EEG computations in the presence of a hole in the skull. *Hum Brain Mapp* 17**,** 179-192. doi: 10.1002/hbm.10061.

Palmer, J.A., Kreutz-Delgado, K., and Makeig, S. (2006). Super-Gaussian mixture source model for ICA. *Independent Component Analysis and Blind Signal Separation, Proceedings* 3889**,** 854-861.

Palmer, J.A., Makeig, S., Kreutz-Delgado, K., and Rao, B.D. (2008). Newton method for the ICA mixture model. *2008 Ieee International Conference on Acoustics, Speech and Signal Processing, Vols 1-12***,** 1805-1808. doi: Doi 10.1109/Icassp.2008.4517982.

Panyakaew, P., and Bhidayasiri, R. (2013). The spectrum of preclinical gait disorders in early Parkinson's disease: subclinical gait abnormalities and compensatory mechanisms revealed with dual tasking. *J Neural Transm* 120**,** 1665-1672. doi: 10.1007/s00702-013-1051-8.

Patel, P., Lamar, M., and Bhatt, T. (2014). Effect of type of cognitive task and walking speed on cognitive-motor interference during dual-task walking. *Neuroscience* 260**,** 140-148. doi: 10.1016/j.neuroscience.2013.12.016.

Pfurtscheller, G., and Klimesch, W. (1991). Event-related desynchronization during motor behavior and visual information processing. *Electroencephalogr Clin Neurophysiol Suppl* 42**,** 58-65.

Pfurtscheller, G., and Lopes Da Silva, F.H. (1999). Event-related EEG/MEG synchronization and desynchronization: basic principles. *Clin Neurophysiol* 110**,** 1842-1857.

Pfurtscheller, G., Stancak, A., Jr., and Neuper, C. (1996). Event-related synchronization (ERS) in the alpha band--an electrophysiological correlate of cortical idling: a review. *Int J Psychophysiol* 24**,** 39-46.

Presacco, A., Goodman, R., Forrester, L., and Contreras-Vidal, J.L. (2011). Neural decoding of treadmill walking from noninvasive electroencephalographic signals. *J Neurophysiol* 106**,** 1875-1887. doi: 10.1152/jn.00104.2011.

Prinz, W. (1997). Perception and action planning. *European Journal of Cognitive Psychology* 9**,** 129-154. doi: Doi 10.1080/713752551.

Rippe, J.M., Ward, A., Porcari, J.P., and Freedson, P.S. (1988). Walking for Health and Fitness. *Jama-Journal of the American Medical Association* 259**,** 2720-2724. doi: DOI 10.1001/jama.259.18.2720.

Rosenbaum, R.S., Furey, M.L., Horwitz, B., and Grady, C.L. (2010). Altered connectivity among emotion-related brain regions during short-term memory in Alzheimer's disease. *Neurobiology of Aging* 31**,** 780-786. doi: DOI 10.1016/j.neurobiolaging.2008.06.002.

Rossignol, S., Dubuc, R., and Gossard, J.P. (2006). Dynamic sensorimotor interactions in locomotion. *Physiol Rev* 86**,** 89-154. doi: 10.1152/physrev.00028.2005.

Sainburg, R.L. (2014). Convergent models of handedness and brain lateralization. *Frontiers in Psychology* 5. doi: Artn 1092

Doi 10.3389/Fpsyg.2014.01092.

Sakamoto, M., Tazoe, T., Nakajima, T., Endoh, T., and Komiyama, T. (2014). Leg automaticity is stronger than arm automaticity during simultaneous arm and leg cycling. *Neuroscience Letters* 564**,** 62-66. doi: DOI 10.1016/j.neulet.2014.02.009.

Sakamoto, M., Tazoe, T., Nakajima, T., Endoh, T., Shiozawa, S., and Komiyama, T. (2007). Voluntary changes in leg cadence modulate arm cadence during simultaneous arm and leg cycling. *Experimental Brain Research* 176**,** 188-192. doi: DOI 10.1007/s00221-006-0742-x.

Schaefer, S., Lovden, M., Wieckhorst, B., and Lindenberger, U. (2010). Cognitive performance is improved while walking: Differences in cognitive-sensorimotor couplings between children and young adults. *European Journal of Developmental Psychology* 7**,** 371-389. doi: Pii 912510315

Doi 10.1080/17405620802535666.

Schaefer, S., and Schumacher, V. (2011). The Interplay between Cognitive and Motor Functioning in Healthy Older Adults: Findings from Dual-Task Studies and Suggestions for Intervention. *Gerontology* 57**,** 239-246. doi: Doi 10.1159/000322197.

Seeber, M., Scherer, R., Wagner, J., Solis-Escalante, T., and Muller-Putz, G.R. (2014). EEG beta suppression and low gamma modulation are different elements of human upright walking. *Front Hum Neurosci* 8**,** 485. doi: 10.3389/fnhum.2014.00485.

Seeber, M., Scherer, R., Wagner, J., Solis-Escalante, T., and Muller-Putz, G.R. (2015). High and low gamma EEG oscillations in central sensorimotor areas are conversely modulated during the human gait cycle. *Neuroimage* 112**,** 318-326. doi: 10.1016/j.neuroimage.2015.03.045.

Severens, M., Nienhuis, B., Desain, P., and Duysens, J. (2012). Feasibility of measuring event related desynchronization with electroencephalography during walking. *Conf Proc IEEE Eng Med Biol Soc* 2012**,** 2764-2767. doi: 10.1109/EMBC.2012.6346537.

Sheridan, P.L., Solomont, J., Kowall, N., and Hausdorff, J.M. (2003). Influence of executive function on locomotor function: divided attention increases gait variability in Alzheimer's disease. *J Am Geriatr Soc* 51**,** 1633-1637.

Simoni, D., Rubbieri, G., Baccini, M., Rinaldi, L., Becheri, D., Forconi, T., Mossello, E., Zanieri, S., Marchionni, N., and Di Bari, M. (2013). Different motor tasks impact differently on cognitive performance of older persons during dual task tests. *Clin Biomech (Bristol, Avon)* 28**,** 692-696. doi: 10.1016/j.clinbiomech.2013.05.011.

Sipp, A.R., Gwin, J.T., Makeig, S., and Ferris, D.P. (2013). Loss of balance during balance beam walking elicits a multifocal theta band electrocortical response. *J Neurophysiol* 110**,** 2050-2060. doi: 10.1152/jn.00744.2012.

Siu, K.C., Lugade, V., Chou, L.S., Van Donkelaar, P., and Woollacott, M.H. (2008). Dual-task interference during obstacle clearance in healthy and balance-impaired older adults. *Aging Clin Exp Res* 20**,** 349-354.

Slepian, M.L., and Ambady, N. (2012). Fluid movement and creativity. *J Exp Psychol Gen* 141**,** 625-629. doi: 10.1037/a0027395.

Smith, E.E., Jonides, J., and Koeppe, R.A. (1996). Dissociating verbal and spatial working memory using PET. *Cerebral Cortex* 6**,** 11-20. doi: DOI 10.1093/cercor/6.1.11.

Srygley, J.M., Mirelman, A., Herman, T., Giladi, N., and Hausdorff, J.M. (2009). When does walking alter thinking? Age and task associated findings. *Brain Res* 1253**,** 92-99. doi: 10.1016/j.brainres.2008.11.067.

Suzuki, M., Miyai, I., Ono, T., Oda, I., Konishi, I., Kochiyama, T., and Kubota, K. (2004). Prefrontal and premotor cortices are involved in adapting walking and running speed on the treadmill: an optical imaging study. *Neuroimage* 23**,** 1020-1026. doi: 10.1016/j.neuroimage.2004.07.002.

Sweeney, K.T., Leamy, D.J., Ward, T.E., and Mcloone, S. (2010). Intelligent artifact classification for ambulatory physiological signals. *Conf Proc IEEE Eng Med Biol Soc* 2010**,** 6349-6352. doi: 10.1109/IEMBS.2010.5627285.

Sweeney, K.T., Mcloone, S.F., and Ward, T.E. (2013). The use of ensemble empirical mode decomposition with canonical correlation analysis as a novel artifact removal technique. *IEEE Trans Biomed Eng* 60**,** 97-105. doi: 10.1109/TBME.2012.2225427.

Szturm, T., Maharjan, P., Marotta, J.J., Shay, B., Shrestha, S., and Sakhalkar, V. (2013). The interacting effect of cognitive and motor task demands on performance of gait, balance and cognition in young adults. *Gait Posture* 38**,** 596-602. doi: 10.1016/j.gaitpost.2013.02.004.

Tomporowski, P.D., and Audiffren, M. (2014). Dual-task performance in young and older adults: speed-accuracy tradeoffs in choice responding while treadmill walking. *J Aging Phys Act* 22**,** 557-563. doi: 10.1123/japa.2012-0241.

Treserras, S., Boulanouar, K., Conchou, F., Simonetta-Moreau, M., Berry, I., Celsis, P., Chollet, F., and Loubinoux, I. (2009). Transition from rest to movement: Brain correlates revealed by functional connectivity. *Neuroimage* 48**,** 207-216. doi: DOI 10.1016/j.neuroimage.2009.06.016.

Venema, D.M., Bartels, E., and Siu, K.C. (2013). Tasks matter: a cross-sectional study of the relationship of cognition and dual-task performance in older adults. *J Geriatr Phys Ther* 36**,** 115-122. doi: 10.1519/JPT.0b013e31827bc36f.

Verrel, J., Lovden, M., Schellenbach, M., Schaefer, S., and Lindenberger, U. (2009). Interacting effects of cognitive load and adult age on the regularity of whole-body motion during treadmill walking. *Psychol Aging* 24**,** 75-81. doi: 10.1037/a0014272.

Villringer, A., and Chance, B. (1997). Non-invasive optical spectroscopy and imaging of human brain function. *Trends Neurosci* 20**,** 435-442.

Wagner, J., Solis-Escalante, T., Grieshofer, P., Neuper, C., Muller-Putz, G., and Scherer, R. (2012). Level of participation in robotic-assisted treadmill walking modulates midline sensorimotor EEG rhythms in able-bodied subjects. *Neuroimage* 63**,** 1203-1211. doi: 10.1016/j.neuroimage.2012.08.019.

Wagner, J., Solis-Escalante, T., Scherer, R., Neuper, C., and Muller-Putz, G. (2014). It's how you get there: walking down a virtual alley activates premotor and parietal areas. *Frontiers in Human Neuroscience* 8. doi: Artn 93

10.3389/Fnhum.2014.00093.

Walton, M.E., Croxson, P.L., Behrens, T.E., Kennerley, S.W., and Rushworth, M.F. (2007). Adaptive decision making and value in the anterior cingulate cortex. *Neuroimage* 36 Suppl 2**,** T142-154. doi: 10.1016/j.neuroimage.2007.03.029.

Wernig, A., and Phys, S.M. (1992). Laufband Locomotion with Body-Weight Support Improved Walking in Persons with Severe Spinal-Cord Injuries. *Paraplegia* 30**,** 229-238.

Yang, J.F., Lamont, E.V., and Pang, M.Y.C. (2005). Split-belt treadmill stepping in infants suggests autonomous pattern generators for the left and right leg in humans. *Journal of Neuroscience* 25**,** 6869-6876. doi: Doi 10.1523/Jneurosci.1765-05.2005.

Yogev-Seligmann, G., Hausdorff, J.M., and Giladi, N. (2008). The role of executive function and attention in gait. *Mov Disord* 23**,** 329-342; quiz 472. doi: 10.1002/mds.21720.

Yogev-Seligmann, G., Rotem-Galili, Y., Mirelman, A., Dickstein, R., Giladi, N., and Hausdorff, J.M. (2010a). How does explicit prioritization alter walking during dual-task performance? Effects of age and sex on gait speed and variability. *Phys Ther* 90**,** 177-186. doi: 10.2522/ptj.20090043.

Yogev-Seligmann, G., Rotem-Galili, Y., Mirelman, A., Dickstein, R., Giladi, N., and Hausdorff, J.M. (2010b). How Does Explicit Prioritization Alter Walking During Dual-Task Performance? Effects of Age and Sex on Gait Speed and Variability. *Physical Therapy* 90**,** 177-186. doi: Doi 10.2522/Ptj.20090043.